Development of new adsorbent by using Ternary mixed hydrous oxide

January, 2025

AHMED MARJJUK

Graduate School of Natural Science and Technology,
Shimane University

List of Figure:

List of Table:

Nomenclature:

SV (h^{-1}): Space velocity per unit time	in Equation (2)
LV (m/h): Linear velocity	in Equation (3)
ΔG (kJ mol^{-1}): Gibbs free energy change	in Equation (14)
ΔH (kJ mol^{-1}): Adsorption enthalpy	in Equation (15)
KD (L g^{-1}): Thermodynamic equilibrium constant	in equation (14)
T (K): Temperature	
V (L): Volume of solution	

Abstract

Water is an essential resource, crucial not only for survival but also for industrial and agricultural processes. However, the treatment of wastewater containing hazardous inorganic anions like fluoride, arsenic, phosphate, and others has become a critical concern due to their stable and toxic nature, leading to severe environmental and health risks. Adsorption has emerged as a promising solution for the removal of these pollutants, especially at low concentrations. Yet, the effective removal of fluoride and arsenic remains challenging, particularly in regions with high natural levels of these contaminants, causing widespread drinking water contamination and significant health impacts.

This research explores the adsorption capacity of mixed hydrous oxide materials, particularly SAM118 and SFM05905, for the removal of fluoride and arsenic from water. SAM118, a Si-Al-Mg oxide material, and SFM05905, a Si-Fe-Mg composite with a higher iron ratio, were synthesized using a neutralization-precipitation method to enhance adsorption performance. SAM118 demonstrated high selectivity for fluoride, while SFM05905 exhibited increased arsenic adsorption, with notable effectiveness for both arsenate (As-V) and arsenite (As-III).

The study's objectives include investigating the adsorption mechanisms of fluoride and arsenic in these materials, analyzing the effect of competing ions and temperature on adsorption efficiency, and assessing adsorption performance in column-based systems with granular adsorbents. The findings reveal the potential of SAM118 and SFM05905 as cost-effective, high-capacity adsorbents for treating contaminated water sources. This research contributes to advancing water purification technologies by offering practical insights into adsorption-based treatment solutions, aiming to improve access to safe drinking water in arsenic- and fluoride-affected regions.

Acknowledgement

I extend my heartfelt appreciation to **Professor Shingo Matsumoto** for his invaluable support with the experimental facility of ICP-MS. I am deeply grateful to **Professors Ryo Sasai** and **Toshio Sato**, along with my lab mates, for their assistance in laboratory experiments.

My sincerest thanks go to my supervisor, **Professor Tomoyuki Kuwabara**, for accepting me under his guidance and for his unwavering encouragement throughout this research. During challenging times, he has been a profound source of inspiration, for which I am deeply indebted. I would also like to express my gratitude to all my past and present lab mates at Shimane University for their generous support.

Special thanks go to **Md. Zubair bin Shahjahan** and **Sheikh Muhammad Shamim** from Bangladesh for their invaluable encouragement, as well as their steadfast moral and emotional support throughout this journey. Their constant motivation has been an immense source of strength.

I am eternally grateful to my parents, my beloved wife, and all my relatives for their unwavering love and support. My wife has been a pillar of strength, a constant source of inspiration, and an enduring motivator who has encouraged me to persevere and give my utmost to my research. This work is lovingly dedicated to my parents, whose unconditional love, unwavering belief, have been the foundation of my motivation and success, both personally and professionally.

Lastly, I draw endless strength and enthusiasm from the innocent smile of my beloved daughter, whose presence inspires me to face challenges with courage and determination. Last but not the least, I offer my deepest gratitude to **Almighty Allah** for His countless blessings, for helping me through this journey, and for enabling me to achieve my goals.

Sincerely yours,
Marjjuk Ahmed

Chapter 1: Introduction

1.1Research Background

Water is an essential life-sustaining resource, vital not only for survival but also for industrial processes and food production. However, the treatment of wastewater containing harmful inorganic anions, such as fluoride, boron, arsenic, phosphate, and selenite, has become a significant concern. The accumulation of stable inorganic pollutants, particularly toxic metal ions like arsenic and fluoride, is a growing environmental issue that poses serious risks to both ecosystems and human health. As arsenic and fluoride are widespread in the environment, their concentrations are increasing rapidly, exacerbating global water pollution. Adsorption has emerged as an effective technique for removing these elements, especially at low concentrations, making it a key aspect of water treatment for contaminated sources. Nonetheless, the removal of fluoride and arsenic remains challenging due to geochemical reactions, biological activity, and naturally high levels of arsenic in groundwater in several countries. This has led to widespread contamination of drinking water, resulting in serious health problems. Arsenic and fluoride primarily enter the human body through ingestion, while the extent of their absorption through inhalation is still uncertain.

Fluoride, a major industrial pollutant, poses significant health risks worldwide. In its ionic form, it contaminates environmental water sources. The World Health Organization (WHO) has set a maximum fluoride concentration of 1.5 ppm in drinking water, yet many countries, including Japan, India, Sri Lanka, China, Turkey, and South Africa, struggle with high fluoride levels in groundwater. Excessive fluoride in drinking water can lead to severe health problems such as dental and skeletal fluorosis (Karagas, et al., 2015), as well as gastroenteritis, muscle weakness, and cardiovascular issues (Farrah, et al., 1987; Meenakshi, et al., 2006). Fluoride occurs naturally in rocks and minerals, and high soil concentrations can leach into groundwater, which is then absorbed by plants and humans. While low concentrations of fluoride (<1 mg/L) can prevent dental issues, concentrations above 1.5 mg/L are harmful. Various technologies have been employed for fluoride removal, including ion exchange (Chubar et al., 2004), adsorption (Bhatnagar, et al., 2011), chemical precipitation (Yu-Bin et al., 2011), and electrocoagulation (Shao et al. 2022), Among these, adsorption is particularly attractive due to the absence of chemical reagents and sludge, along with the ability to regenerate adsorbents. However, adsorbents can be costly, with materials such as carbon-based adsorbents, nano-adsorbents, bio-adsorbents, inorganic materials, and modified or composite adsorbents like activated alumina, ferric hydroxides, aluminum hydroxide, clay, and fly ash commonly used for fluoride removal from water. The performance of these adsorbents for fluoride adsorption from aqueous media is influenced by various factors, including, but not limited to, contact time, particle size, adsorbent surface area, pH, and temperature. Fluoride removal can be achieved through two processes: adsorption and ion exchange.

Arsenic contamination in water is another global health concern due to its high toxicity, especially in its inorganic forms. Chronic exposure to arsenic in water can cause severe health problems (Shao et al., 2022). such as skin lesions (Karagas et al., 2015), lung damage (Karagas et al., 2015), and impairments to the digestive and nervous systems (Chubar et al., 2004). Arsenic is found naturally in high concentrations in groundwater in regions like Southeast Asia and South America. It primarily exists in two oxidation states, arsenite (As-III) and arsenate (As-V), both of which are highly soluble in water and difficult to remove. WHO has lowered the permissible arsenic concentration in drinking water to 10 μg/L, prompting the development of more efficient removal techniques. Adsorption has proven to be a promising solution due to its simplicity, lack of reagents, minimal sludge production, and ease of regenerating adsorbents. Despite these advantages, economic challenges persist, particularly for small-scale systems.

A neutralization-precipitation method at 20 to 25°C has been employed to synthesize ternary mixed hydrous oxides using inexpensive polyvalent metal elements, which are effective for ionic adsorption (Kuwabara et al., 2009). SAM118, a composed material composed of Si: Al: Mg in a 0.1: 0.1: 0.8 molar ratio, has demonstrated high selectivity for fluoride and arsenate ions. Its adsorption isotherm for fluoride follows the Freundlich model, showing potential for fluoride removal in hot springs with various ions (Yanai et al., 2010). However, powdered form of SAM118, presents challenges for practical water treatment, which has led to the granulation of SAM118 for use in column-based treatment.

In previous studies, Si-Fe-Mg-based composite hydrous oxides (SFM) with different Fe/Mg ratios were tested for low-concentration arsenic removal in groundwater (Kuwabara et al., 2015). It was found that increasing the Fe/Mg ratio improved arsenic adsorption while reducing interference from other anions. SFM118, in particular, exhibited a high adsorption capacity for both arsenate (As-V) and arsenite (As-III), with the iron content playing a key role in arsenite (As-III) adsorption. To enhance arsenic removal efficiency, a new material, SFM05905, with a higher iron content, was developed. This study investigates the adsorption isotherms and anion selectivity of powdered SFM05905, alongside its arsenic removal capability in granular form using column methods. The study also evaluates the effect of phosphate (PO_4) on arsenic adsorption in aqueous solutions and examines distinct adsorption behavior associated with different functional groups.

Various natural and synthetic adsorbents have been explored for the removal of harmful ions, such as fluoride and arsenic, from aqueous solutions. Materials like multivalent metal oxides, metal-incorporated activated carbon, and calcium phosphate compounds have shown high adsorption capacities. Among these, granulated ternary mixed hydrous oxides, such as SAM and SFM, offer an effective and low-cost option for ion removal. Traditional water treatment methods such as chemical precipitation, membrane separation, and electrodialysis, may be ineffective for low-concentration ions. In contrast, ternary mixed hydrous oxides, containing elements such as Si, Al, Mg (SAM), and Si, Fe, Mg (SFM) have demonstrated exceptional potential for removing fluoride and arsenic ions, making them highly suitable for water treatment applications.

1.2 Research objectives

The objectives of this research study are aimed at developing and enhancing the performance of mixed hydrous oxide adsorbents for removing fluoride and arsenic from water sources. Specifically, the objectives are:

1. **Fluoride Adsorption Capacity**: To investigate the influence of space velocity on the adsorption equilibrium capacity of fluoride anions using granular Si-Al-Mg mixed

hydrous oxides. This includes exploring the relationship between the material's structure and its adsorption efficiency, especially in the presence of various coexisting ions.

2. **Arsenic Adsorption Behavior**: To explore the effects of phosphate (PO_4) on arsenic adsorption in Si-Fe-Mg mixed hydrous oxides, focusing on anion selectivity and the competition between arsenic and phosphate ions. This will help understand the material's behavior in real-world water conditions, where multiple contaminants coexist.

1.3 Purpose of this research study

The primary purpose of this study is to address the challenges associated with fluoride and arsenic contamination in water by developing and optimizing novel adsorbent materials that can effectively remove these pollutants. The specific goals of this research include:

a) **Development of Granulated SAM118**: To enhance the fluoride removal capacity of SAM118 materials by investigating the influence of granular structure and space velocity on adsorption performance. This will help determine the material's practicality for use in large-scale water treatment systems.

b) **Effect of Space Velocity**: To assess the impact of space velocity on fluoride adsorption capacity in granular Si-Al-Mg mixed hydrous oxides. This will provide insights into optimizing flow rates and designing efficient column-based adsorption systems.

c) **Impact of Coexisting Anions on Fluoride Adsorption**: To evaluate the effect of coexisting ions, particularly in hot spring water, on the fluoride removal efficiency of SAM118. This is crucial for understanding how these adsorbents perform under complex environmental conditions.

d) **Arsenic Adsorption by SFM05905**: To assess the arsenic adsorption capacity of SFM05905 under varying aqueous concentrations, particularly focusing on the removal of both As(III) and As(V).

e) **Effect of Temperature on Arsenic Adsorption**: To investigate the influence of temperature on arsenic adsorption, as temperature fluctuations are common in real-world water treatment scenarios, particularly in regions with geothermal sources like hot springs.

f) **Adsorption Mechanisms of Arsenic Species**: To explore the adsorption mechanisms of arsenic species (As(III) and As(V)), providing a detailed understanding of how these materials interact with different forms of arsenic in solution.

1.4 Significance of the Study

This research holds profound implications for environmental sustainability and public health by addressing the critical challenge of water contamination. Central to this endeavor are the innovative materials SAM118 and SFM05905, whose unique properties make them invaluable in the quest for effective and affordable solutions to fluoride and arsenic pollution.

SAM118, a ternary hydrous oxide composed of silicon (Si), aluminum (Al), and magnesium (Mg) in a 0.1:0.1:0.8 molar ratio, has demonstrated exceptional efficiency in selectively adsorbing fluoride ions. This property, coupled with its adaptability for use in granular form, makes SAM118 an ideal candidate for dynamic, column-based water treatment systems. Its potential for applications in treating fluoride contaminated sources, such as hot springs, highlights its versatility and relevance to real-world scenarios.

SFM05905, a Si-Fe-Mg-based composite hydrous oxide, represents a breakthrough in arsenic removal technologies. Engineered with an optimized Fe/Mg ratio, this material exhibits remarkable adsorption capabilities for both arsenite (As-III) and arsenate (As-V), even in the presence of competing anions such as phosphate. Its robustness, combined with its granular form, enables effective deployment in diverse environmental conditions, including groundwater systems burdened by complex contaminant profiles.

By advancing the design and application of these adsorbents, this study contributes to the development of cutting-edge water treatment technologies that are not only efficient and scalable but also environmentally sustainable. The exploration of their performance under varying conditions—such as temperature fluctuations and the presence of coexisting ions—ensures that these materials are well-suited for a wide array of practical applications.

Ultimately, this research paves the way for large-scale implementation of SAM118 and SFM05905, offering a transformative approach to water purification. These materials hold the promise of delivering clean and safe drinking water to communities worldwide, reinforcing the importance of science and innovation in addressing global environmental challenges.

1.5 Graphical Abstract:

The graphical abstract below depicts the removal efficiency of fluoride and arsenic adsorption.

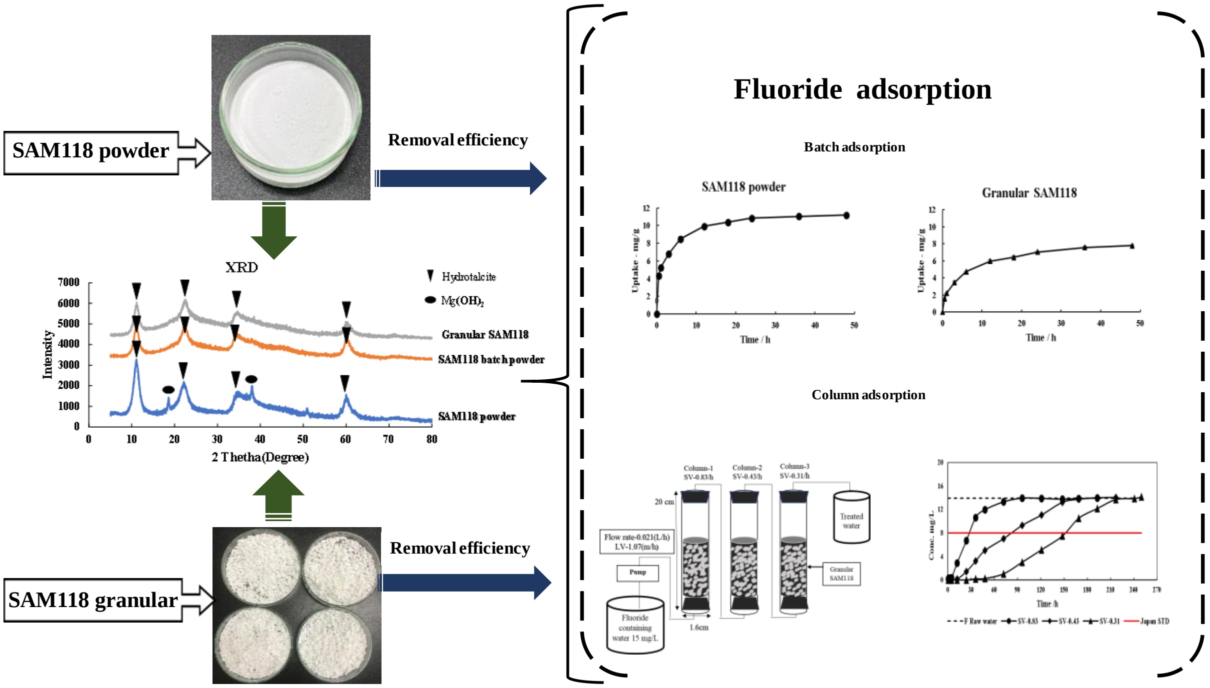

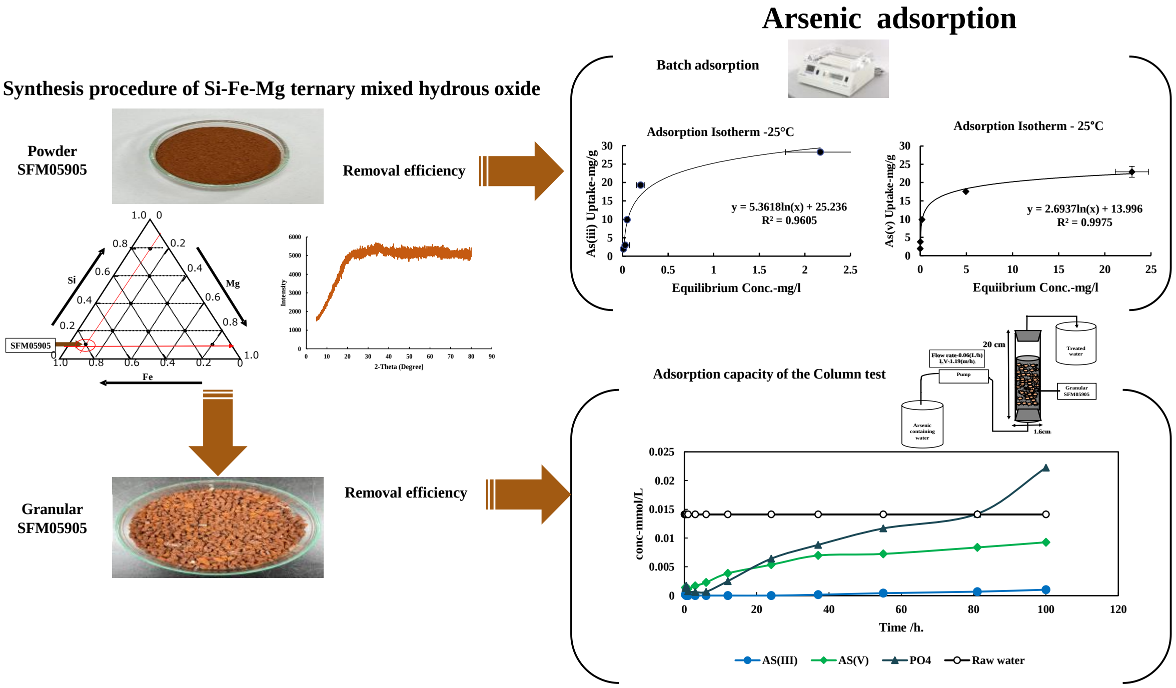

Chapter 2: Evaluation of the fluoride adsorption capacity of Si-Al-Mg (SAM) mixed hydrous oxides

2.1 Introduction:

This section introduces the synthesis of Si-Al-Mg mixed hydrous oxides (SAM) through a precipitation method, emphasizing the need for effective fluoride removal from groundwater and polluted water. Fluoride contamination poses significant health risks, such as dental and skeletal fluorosis, making its removal a critical environmental concern. Conventional methods for fluoride removal, while useful, often face challenges such as high costs and generation of waste (Meenakshi et al., 2006). In contrast, the adsorption method using SAM powder offers a more efficient and cost-effective solution, with the added benefits of ease of regeneration and selective adsorption capabilities. This chapter explores the synthesis, characterization, and potential of SAM powder for effective fluoride removal.

2.2 Experimental Methodology:

2.2.1 *Preparation of SAM118:*

2.2.2 *Materials and reagent:*

The materials and reagents utilized for the synthesis of Si-Al-Mg mixed hydrous oxides (SAM) included Sodium silicate solution No.3 ($Na_2O\ nSiO_2\ xH_2O$, Kishida Chemical, Osaka, Japan). Additionally, aluminum chloride hexahydrate ($AlCl_3{\cdot}6H_2O$), magnesium chloride hexahydrate ($MgCl_2{\cdot}6H_2O$), and hydrochloric acid (HCl) were obtained from Fujifilm Wako Pure Chemical Corp., Osaka, Japan. Ultrapure water, provided by the Milli-Q system from Merck Millipore, Darmstadt, Germany, was employed for the synthesis process as well as for conducting water quality analyses. These high-purity materials ensured accuracy and reliability throughout the synthesis and experimental phases.

2.2.3 Synthesis of SAM118:

The Si-Al-Mg-based sample, SAM118, was synthesized using the neutralization-precipitation method. The process involved dissolving prescribed amounts of sodium silicate ($Na_2O \cdot nSiO_2 \cdot xH_2O$), aluminum chloride hexahydrate ($AlCl_3 \cdot 6H_2O$), and magnesium chloride hexahydrate ($MgCl_2 \cdot 6H_2O$), as listed in Table 1, into an aqueous solution of hydrochloric acid (HCl). The mixed acidic solution and sodium hydroxide (NaOH) solution were simultaneously added to the mixture, carefully maintaining a pH range of 11.5 to 12.0. Once the desired pH was reached, final adjustments were made to achieve a pH of 12.20.

The synthesis conditions, such as temperature, agitation rate, and dripping rate of the mixed acidic solution, were controlled to ensure consistency in the ion adsorption properties of the resulting hydrous oxides. After achieving homogeneity, the precipitate was collected through centrifugation. This precipitate was then dried, pulverized, washed thoroughly with ultrapure water, dried again, and passed through a 100-mesh sieve. The fine powder thus obtained was labeled as SAM118 (shown in Figure 1) and stored for subsequent use. The following section provides a detailed step-by-step outline of the synthesis procedure.

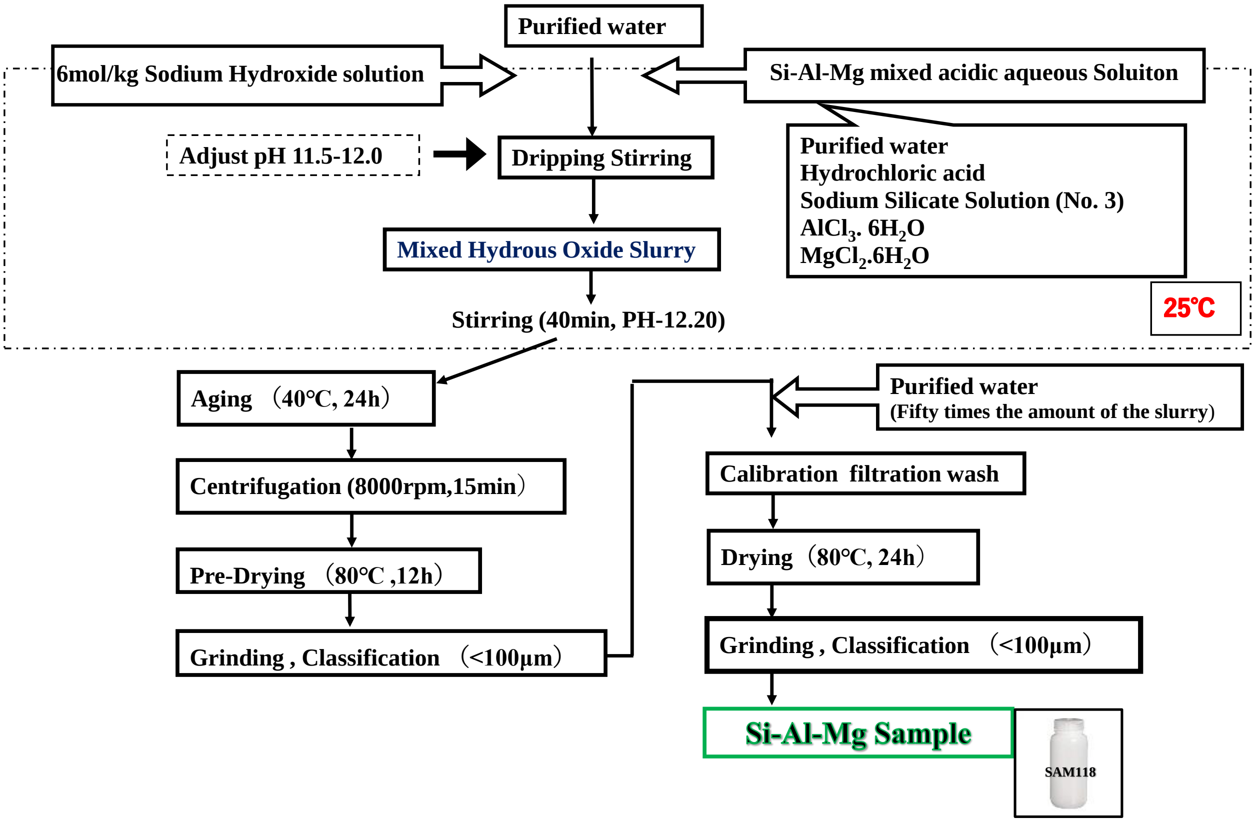

Figure 1: Schematic diagram showing the step-by-step process of synthesizing SAM (Si-Al-Mg mixed hydrous oxide).

The SAM118 samples were synthesized using the neutralization-precipitation method described in section 2.3. The quantities of the reagents used in the synthesis process were determined according to the measurement scale outlined in Table 1. These quantities ensured precise and consistent preparation of the SAM118 sample. After synthesis, the sample was treated as described earlier to ensure its uniformity and suitability for adsorption experiments.

Table 1: Measurement Scale for SAM118 Synthesis.

Reagent ***(SAM118)***	**Quantity (g)** ***(Reference Value)***
Si (No.3 water glass)	(1.0013~) 1.035935 g
Al ($AlCl_3.6H_2O$)	1.206996692 g
Mg ($MgCl_2.6H_2O$)	8.130992 g
Thick hydrochloric acid (35.0-37.0%)	1.875 ml
DIW for reagents dissolution	25 ml
DIW for synthesis.	50 ml

a) Preparation of Mixed Acidic Aqueous Solution:

To prepare the mixed acidic aqueous solution, 10.359 g of sodium silicate (water glass) was dissolved in 200 mL of deionized water (DIW) in a 200 mL beaker, and the mixture was stirred continuously. Thick hydrochloric acid, aluminum chloride hexahydrate, and magnesium chloride hexahydrate were then added in sequence, with each reagent being carefully added to avoid any precipitation. After each addition, the beaker and reagents were rinsed with 50 mL of DIW to ensure all components were incorporated. The solution was monitored for transparency to confirm the absence of colloid formation, and it was continuously stirred after the addition of all reagents to maintain a homogeneous mixed acidic solution. This solution served as the precursor for further synthesis steps.

b) **Preparation of 6 mol-kg^{-1} NaOH aqueous**:

To prepare the NaOH solution, 119.99 g of sodium hydroxide (NaOH) was gradually added to 500 mL of deionized water (DIW) while the mixture was cooled using an ice bath to prevent excessive heat generation during the dissolution process. The NaOH was stirred until fully dissolved, ensuring the solution was clear and homogenous. The prepared 6 $mol \cdot kg^{-1}$ NaOH solution was then transferred into a plastic bottle and stored for later use in the synthesis process.

c) **Preparation of equipment of dropwise:**

In this experiment, 500 mL of deionized water (DIW) was placed in a 3L beaker equipped with a magnetic stirrer to ensure continuous mixing throughout the process. A roller pump (peristaltic pump) was set up for the dropwise addition of both the mixed acidic aqueous solution and NaOH aqueous solution. The NaOH solution's power cord was connected to the LOW/ON setting of the pH controller (pH Stud), and the pump was inserted directly into the outlet of the pH controller to regulate the dropwise addition, ensuring precise pH control during the neutralization-precipitation process.

d) **Dropwise Addition:**

Following the simultaneous dropwise addition of the mixed acidic aqueous solution and the 6 $mol\text{-}kg^{-1}$ NaOH aqueous solution, the pH of the reaction mixture in the beaker was initially maintained around 11.0. The pH was carefully monitored throughout the reaction and adjusted to remain within the range of 12.0 to 12.2. Stirring was continued for an additional 40 minutes at room temperature, while the NaOH solution was steadily added to ensure optimal conditions for the neutralization-precipitation process.

e) **Washing and sieving of slurry:**

The slurry was aged at a temperature of 40°C for 24 hours in a dry heat sterilizer (DVS602, Yamato Scientific Co., Ltd., China). After the aging process, the slurry underwent centrifugal separation (CR21N, Eppendorf Himac Technologies Co., Ltd., Hamburg, Germany), and the supernatant was discarded. The resulting precipitate was transferred into a glass petri dish and dried at 80°C for 12 hours. Once dried, the precipitate was crushed using a blender (As One, WB-1, AC100V, 50/60Hz) and sieved through a mesh with an opening size of 150 µm (100 mesh).

The dried powdery product was then washed using deionized water (DIW). The volume of water used for washing was equal to that of the slurry, and the washing process was repeated 10 times. After washing, the suspension underwent suction filtration, and the solid matter was collected on filter paper (5C, Toyo Roshi Kaisha, LTD., Tokyo, Japan). The collected material was dried again at 80°C for more than 12 hours, pulverized, and sieved once more to yield the final powder sample, SAM118.

f) Preparation of Al and Mg measurement.

To prepare the sample for the measurement of aluminum (Al) and magnesium (Mg), the powdery product, SAM118, was placed in a crucible cup and dried in an oven for 24 hours. Following this, 1.0 g of SAM118 was added to 10 mL of perchloric acid ($HClO_4$) in a beaker and stirred with a glass rod to facilitate dissolution. The mixture was then heated on a hotplate, with careful moisture evaporation achieved by gradually raising the temperature in increments of 100°C to prevent bumping. Once white smoke from the perchloric acid appeared, the beaker was covered with a watch glass and heated for an additional 5 minutes. After cooling the beaker on a wet Kim towel, 5 mL of 6 mol L^{-1} hydrochloric acid (HCl) and 20 mL of warm water were added. The solid residue was crushed with a glass rod, and the watch glass was rinsed with warm water, which was then flushed into the beaker. The mixture was filtered using filter paper (5C, Toyo Roshi Kaisha, LTD., Tokyo, Japan) and washed 10-12 times with warm water to avoid rupture during subsequent heating. The filtrate was refined in a 500 mL beaker, cooled to room temperature, transferred to a 250 mL flask, and shaken with warm water before being filled to volume. The concentrations of Al and Mg were measured using inductively coupled plasma mass spectrometry (ICP-MS) (Agilent 8800, Agilent Technologies, Inc., California, USA), as outlined in Table 2.

g) Preparation of Silicon oxide measurement:

To prepare the crucible cup and filter paper for subsequent silicon oxide analysis, the crucible cup was first dried in an oven at 1100°C for 24 hours. After cooling, the filter paper was placed in the crucible cup, which was then heated in the drying oven at 1100°C for an additional 24 hours. The dried filter paper was incinerated with a gas burner at 1050°C for 1 hour using a muffle furnace (FO410, Yamato Scientific Co., LTD, China). After cooling, the weight of the silicon oxide was measured using a desiccator, as detailed in Table 2.

2.2.4 Measurement of the metal element composition ratio of SAM118:

The metal element composition ratio of the ternary mixed hydrous oxide was analyzed using inductively coupled plasma mass spectrometry (ICP-MS) (Agilent 8800, Agilent Technologies, Inc., California, USA). This analysis was essential to assess the various molar ratios involved in the synthesis of the SAM118 sample (Kuwabara et al., 2009, and Kuwabara et al., 2010). The phase behavior of the mixture, which includes the three elements—silicon (Si), aluminum (Al), and magnesium (Mg)—was represented by a triangular phase diagram, as illustrated in Figure 2. This diagram provides a visual representation of the composition of the SAM118 sample, highlighting the relationships between the different metal elements and their respective proportions within the synthesized material.

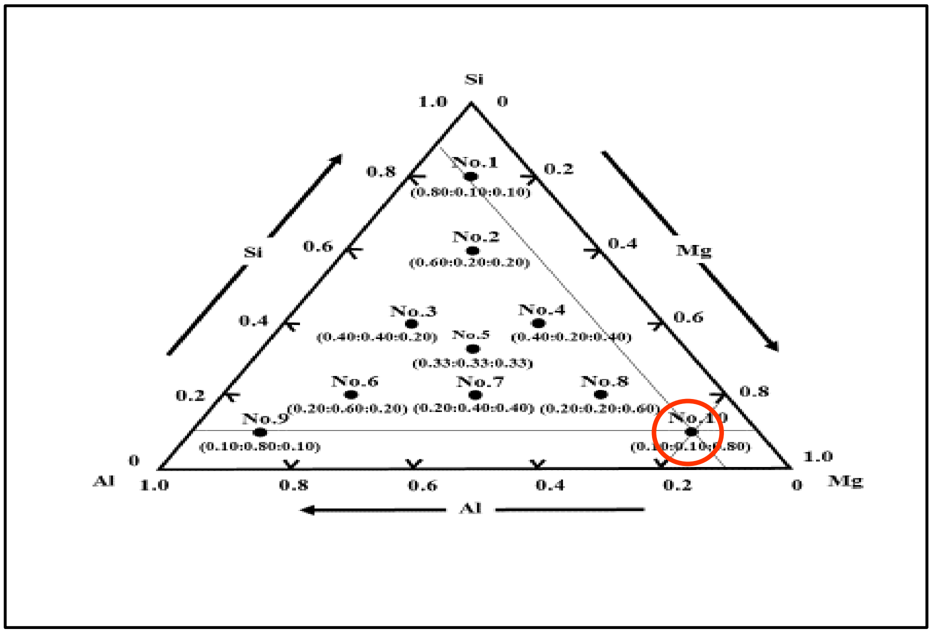

Figure 2: Ternary phase diagram of SAM sample compositions, showcasing sample numbers and categorizing them into groups such as Al-clays and Mg-clays. The Al-clays group encompasses various kaolin minerals, while the Mg-clays category includes minerals such as serpentine, talc, phlogopite, and other magnesium-based minerals. Additionally, the diagram features hydrotalcite as noted by (Onodera et al.,2009), illustrating the compositional relationships among these materials within the SAM sample framework.

2.3 Adsorption test:

The suitability of an adsorbent for practical applications hinges on several key characteristics, including adsorption capacity, selectivity for fluoride ions, regenerability, compatibility, particle and pore size, and cost. The efficiency of fluoride removal through adsorption is influenced by the raw water quality profile, which encompasses factors such as initial fluoride concentration, pH, temperature, contact time, and adsorbent dosage (Farrah et al., 1987; Martínez-Miranda, et al., 2016; Tolkou, et al., 2021). Among various methods, adsorption stands out as the most promising due to its cost-effectiveness, operational simplicity, significant adsorption capacity, potential for reuse, multiple useful cycles, and feasibility of regeneration (Fan et al., 2003). In this study, SAM118, synthesized with varying Si-Al-Mg molar ratios, will be evaluated for its adsorption properties through batch testing, with measurements conducted using ion chromatography. The adsorption process entails water passing through a contact bed, where fluoride ions are removed via ion exchange or surface chemical reactions with the solid bed matrix.

2.3.1 Batch adsorption:

The adsorption process was conducted in batches using a fluoride stock solution prepared at approximately 1000 mg/L with sodium fluoride (NaF, 99%) sourced from Fujifilm Wako Pure Chemical Corporation (Osaka, Japan). This stock solution was then diluted to a concentration of 15 mg L^{-1}. The pH of the solution was subsequently adjusted to 7.0 using 1 mol kg^{-1} hydrochloric acid (HCl) and 1 mol kg^{-1} sodium hydroxide (NaOH) solutions. In the batch experiments, SAM118 was added at a concentration of 0.1% (w/v) to the fluoride solution. The mixture was stirred using a magnetic stirrer, and samples were taken at various time intervals.

Each sample was filtered using a 0.2 µm pore-size membrane filter (HP020AN, Advantec, Tokyo, Japan), and the fluoride concentration was determined using a high-speed liquid ion chromatography system (ICS-1600, Dionex, Ontario, Canada). The pH of the filtrate was measured with a pH meter (LAQUAtwin AS-712, HORIBA, Kyoto, Japan). The adsorption amount of fluoride ions per gram of SAM118 was calculated using the following equation:

$$W_g = V\,(C_0 - C_t)/w \qquad (1)$$

Where:

W_g: Adsorption amount per 1 g of SAM118 (mg g^{-1})

C_0: Initial concentration (mg L^{-1})

C_t: Concentration in sample water after t hours of agitation (mg L^{-1})

V: water volume *of* the sample (L)

w: Added quantity of SAM118 (g)

The study also investigated adsorption isotherms and the equilibrium time for fluoride adsorption using the SAM118 powder adsorbent.

2.4 Characterization of SAM118

2.4.1 Characterization of SAM118 sample (TG-DTA):

The TG-DTA measurement results for SAM118 are presented in Figure 3. The sample was characterized using a thermogravimetric differential thermal analyzer (TG-DTA) to evaluate its thermal properties under a nitrogen atmosphere at a flow rate of 200 mL/min, covering a temperature range of 25 to 1000°C with a heating rate of 10°C/min. As previously reported (Kuwabara et al., 2010), the DTA curve distinctly shows endothermic peaks around 100°C and 400°C. Correspondingly, the TGA curve exhibits a two-step weight loss linked to these peaks. The analysis utilized aluminum oxide (Al_2O_3) powder as a reference material, revealing a linear baseline during the melting process and indicating phase transitions between crystalline forms. These findings illustrate the thermal behavior and stability of the SAM118 sample under elevated temperatures, providing insights into its potential applications.

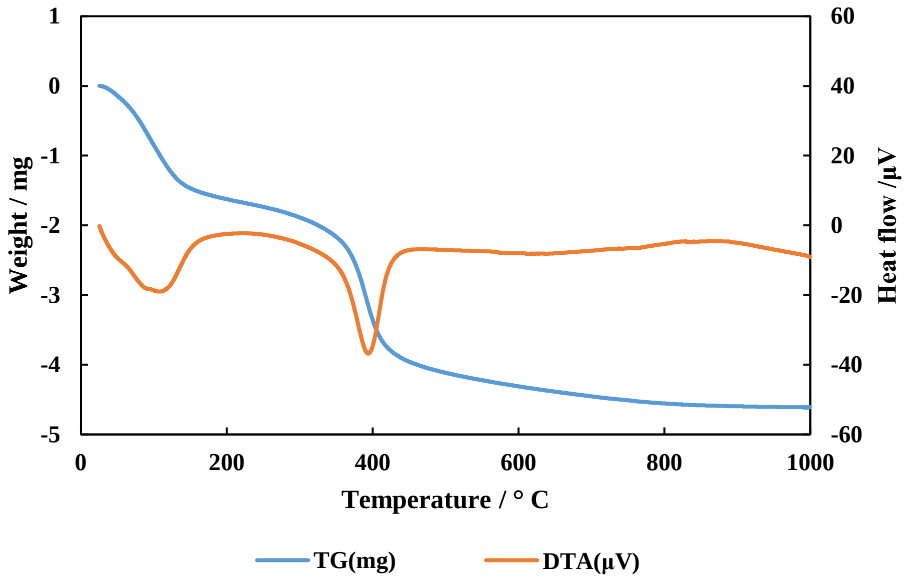

Figure 3: TG-DTA pattern of the synthesized SAM118, illustrating the thermal properties and endothermic behavior of the sample during the heating process.

2.4.2 Characterization of SAM118 sample (XRD):

The SAM118 sample was characterized using powder X-ray diffractometry (XRD) with Cu-Kα radiation, revealing a significant presence of hydrotalcite and magnesium hydroxide [Mg (OH)₂], with silica as the main component phase. The XRD pattern indicated that the SAM118 sample exhibits a hydrotalcite-like structure, characterized by its ion exchange capacity and the incorporation of magnesium hydroxide into its basic framework. The use of layered double hydroxides (LDHs) and hydrotalcite-related materials can mitigate the environmental impact of human activities, and these materials can be synthesized efficiently through various methods. Consequently, the physical and structural properties of SAM118 enhance its applicability in a range of industrial processes, particularly in environmental remediation efforts. The XRD measurement results for the SAM118 sample are illustrated in Figure 4, highlighting its crystalline structure and composition.

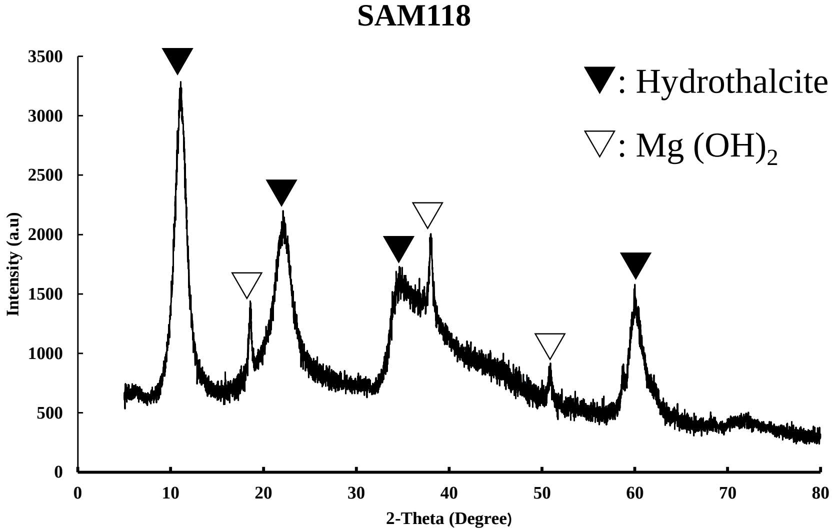

Figure 4: XRD patterns of powder SAM118, showcasing the characteristic peaks associated with hydrotalcite and magnesium hydroxide, highlighting the material's crystalline structure and composition.

2.4.3 Characterization of SAM118 sample (FTIR spectroscopy):

The characterization of the SAM118 compound was performed using Fourier Transform Infrared (FTIR) spectroscopy, revealing significant peaks in both the functional group and fingerprint regions of the spectra. The band at 3392 cm^{-1} corresponds to the hydroxyl (-OH) groups, indicating their presence in the compound. A peak at 1629 cm^{-1} confirms the existence of aromatic cycles within the extracts, while vibrations associated with the C–O bond are observed at 1100 cm^{-1} in the C–H region. The peak at 577 cm^{-1} is attributed to the Fe–O bond. Notably, the absence of carbonyl groups suggests that the reduction of salt precursors to SAM118 did not occur. Furthermore, peaks related to Fe-OH stretching and banding vibrations indicate that iron oxide has transformed into transient complex species, such as Fe-OH, $Fe(OH)_2$, or FeO (OH), on the surface of SAM118. These findings are illustrated in Figure 5.

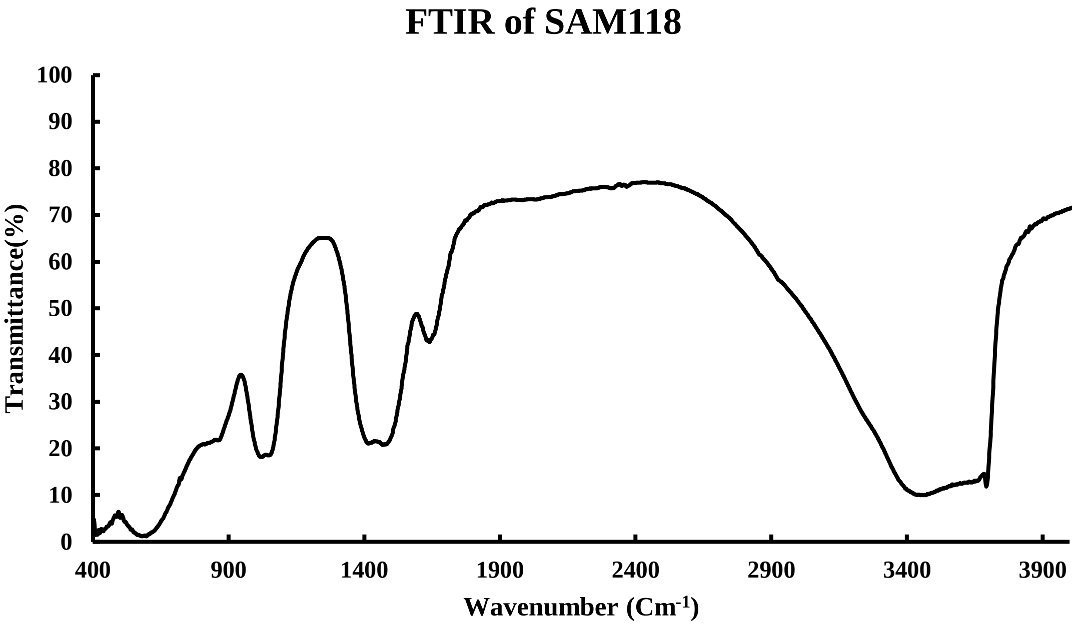

Figure 5: FT-IR spectroscopy of powder SAM118, showing the characteristic peaks corresponding to functional groups and confirming the presence of hydroxyl, aromatic, and Fe-O bonds.

2.5 Result and discussion

This chapter presents and discusses the findings from the evaluation of the fluoride adsorption performance of the SAM118 sample, synthesized with a higher Mg ratio. The results indicate that SAM118 exhibits enhanced fluoride adsorption capacity, primarily due to the anion exchange mechanism facilitated by the presence of layered double hydroxides (LDHs), like hydrotalcite-like compounds. The chapter delves into the elemental composition, structural characterization (XRD), thermal stability (TG-DTA), and adsorption properties, analyzing these results within theoretical frameworks and previous research to underscore SAM118's potential application in water treatment processes.

2.5.1 Metal element composition ratio containing Si-Al-Mg mixed hydrous oxide particles:

In this study, mixed hydrous oxide particles containing Si, Al, and Mg in a molar ratio of 1:1:8 were synthesized through co-precipitation under ambient laboratory conditions. The actual metal element composition for SAM118 was determined to be 0.1 Si: 0.11 Al: 0.79 Mg, as shown in Table 2. The synthesized particles underwent a thorough filtration process, followed by washing with deionized water and drying at 80°C (±5°C). Subsequently, the dried particles were ground and sifted to collect those under 250 µm for experimental use.

The fluoride ion adsorption rate of the Si-Al-Mg mixed hydrous oxide was notably rapid, reaching equilibrium after 24 hours in the fluoride solution. However, SAM118 exhibited some peaks that challenged the expected equilibrium adsorption pattern. These fluctuations may be attributed to the concentration of fluoride ions in the solution, indicating the complex dynamics of the adsorption process and the potential influence of competing ions present in the aqueous environment. Further investigation into the adsorption isotherms and kinetics will provide deeper insights into these observations and their implications for practical applications in water treatment.

Table 2: SAM118 powder molar and composition ratio.

SAM118 powder					
Target Composition ratio	Si (mole/gm)	Al (mole/gm)	Mg (mole/gm)	Obtained Composition ratio	SAM118 Specific gravity(gm/cm^3)
SAM118 = (Si: Al: Mg) = (0.1:01:08)	1.213	1.223	9.068	0.1Si:0.11Al:0.79Mg	2.5

2.5.2 XRD analysis of the SAM118:

The XRD analysis of SAM118 was performed to elucidate its physicochemical properties. The diffractograms presented in Figure 4 indicate that the sample is primarily a hydrotalcite-like compound, containing significant amounts of Mg $(OH)_2$, aligning with findings from previous studies (Kuwabara et al., 2015). These compounds are known to exhibit high anion exchange capacities. The general formula for hydrotalcite-like compounds is represented as $[M(II)_{1-x}M(III)_x(OH)_2]^{x+}(A^{n-}{}_{x/n})\cdot mH_2O$, where M(II) is a bivalent metal ion, M(III) is a trivalent metal ion, and A is the exchangeable anion. In generally, the structural stability of hydrotalcite-like compounds is maintained with x values ranging from 0.20 to 0.33 (Cavani et al., 1991). For SAM118, the calculated x value was found to be 0.11, indicating an excess of Mg relative to Al. Consequently, SAM118 is identified as a mixed phase of hydrotalcite-like compound and Mg $(OH)_2$, with a considerable portion of the latter likely existing in an amorphous state. Notably, although Mg $(OH)_2$ peaks were not detected in the XRD analysis post fluoride adsorption, it is presumed that the compound remains dissolved in the solution.

2.5.3 TG-DTA analysis of the SAM118:

The physicochemical characteristics of SAM118 were further examined using TG-DTA, with the results illustrated in Figure 5. The DTA curve reveals endothermic peaks at approximately 100 °C and 400 °C, which correspond to a two-step weight loss observed in the TGA curve. The TG-DTA profile is consistent with that of hydrotalcite-like compounds, as noted in previous research (Wang et al., 2011), and aligns with the XRD results discussed earlier (Kuwabara et al., 2010). This thermal behavior suggests significant thermal stability and potential for practical applications in adsorption processes.

2.5.4 Fluoride adsorption of powder SAM118:

The fluoride adsorption properties of SAM118 powder were thoroughly investigated, and the results are illustrated in Figure 6. At an initial pH of approximately 10 and a fluoride concentration of 15.0 mg L^{-1}, the SAM118 powder demonstrated a rapid adsorption rate, quickly approaching saturation within 24 hours. Notably, the adsorption process continued even after 48 hours, ultimately yielding a saturated adsorption amount of 11.190 mg g^{-1}. These findings indicate that the microporous structure of the SAM118 cryogel facilitates easy access for the fluoride solution, enhancing the interaction between the solution and the mixed hydrous oxide particles. The high surface area and reactivity of the crystalline structure of SAM118 contribute significantly to its effective fluoride adsorption capacity, highlighting its potential for practical applications in water purification processes.

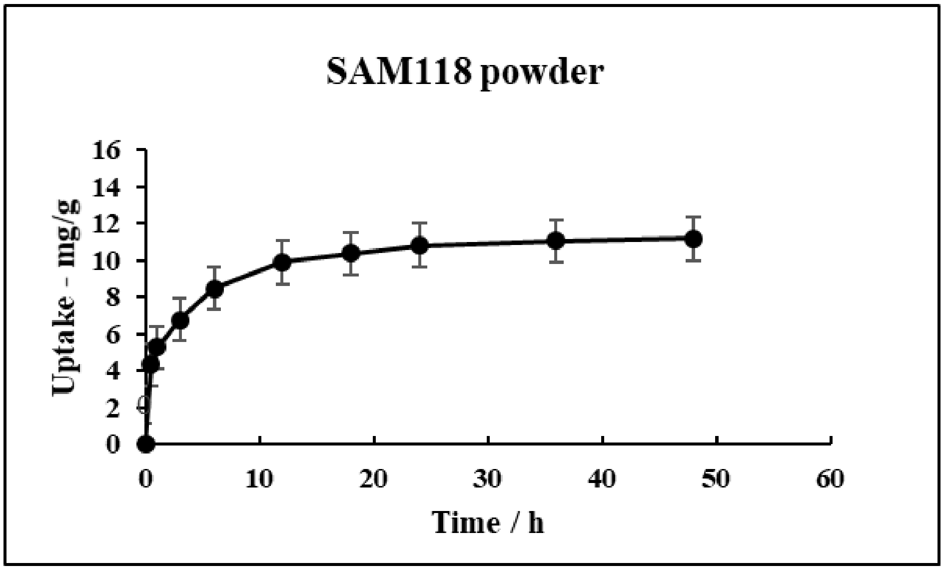

Figure 6: Fluoride Adsorption Kinetics of SAM118 Powder.

2.6. Conclusion

This study thoroughly evaluated the performance of SAM118 powder for fluoride adsorption, establishing it as a new and effective material for fluoride removal. Key findings are summarized as follows:

①. **Adsorption Performance**: SAM118 powder exhibited a rapid adsorption rate, achieving equilibrium within 24 hours and a maximum fluoride adsorption capacity of 11.190 mg g^{-1}. The results emphasize the importance of optimizing the metal element composition ratio to match specific water quality conditions, positioning SAM118 as a highly effective fluoride removal material.

②. **XRD Analysis**: X-ray diffraction analysis confirmed the presence of a significant amount of amorphous substance within SAM118, indicating its complex structural composition, which contributes to its adsorption performance.

③. **TG-DTA Analysis**: Thermogravimetric and differential thermal analysis revealed that SAM118 resembles hydrotalcite-like compounds, supporting its structural stability and potential for real-world applications.

④. **FT-IR Analysis**: Fourier-transform infrared spectroscopy demonstrated that hydroxyl groups on the surface of SAM118 play a critical role in facilitating fluoride adsorption, highlighting the material's functional efficiency.

Overall, SAM118 emerges as a promising candidate for fluoride removal, offering potential for further performance enhancement. Its characteristics suggest that it could serve as a cost-effective adsorbent for both heavy metals and fluoride, particularly in column processes. Structural analyses, including XRD and TG-DTA, confirm its resemblance to hydrotalcite-like compounds, further reinforcing its thermal stability and potential for large-scale use in water treatment systems. Future studies on the adsorption mechanisms and the influence of competing ions will be essential in refining SAM118's efficacy for practical applications.

2.7 References

1. Bhatnagar, A., Kumar, E., & Sillanpää, M. (2011). Fluoride removal from water using adsorbents—A review. *Chemical Engineering Journal*, 171(3), 811-840. http://doi.10.1016/j.cej.2011.05.028

2. Shao Xinxin, Ran Zhenzhen, Ji Shengfu. (2022). Layered double hydroxides catalysts and their acid-base synergistic catalytic reactions. *Industrial Catalysis*. 30(4): 1-7, https://doi.org/10.3969/j.issn.1008-1143.2022.04.001

3. Cavani, F., Trifirò, F., & Vaccari, A. (1991). Hydrotalcite-type anionic clays: Preparation, properties and applications. *Catalysis Today*, 11(2), 173-301. http://dx.doi.org/10.1016/0920-5861(91)80068-K

4. Yu-Bin Wang, Jih-Mirn Jehng, (2011). Hydrotalcite-like compounds containing transition metals as solid base catalysts for transesterification. *Chemical Engineering Journal*, 175(15), 548-554. https://doi.org/10.1016/j.cej.2011.09.126

5. Natália Chubar, Jorge R. Carvalho, M. Joana Neiva Correia, (2004). Heavy metals biosorption on cork biomass: effect of the pre-treatment, *Colloids and Surfaces A: Physicochemical and Engineering Aspects*, 238(1-3), 51-58. https://doi.org/10.1016/j.colsurfa.2004.01.039.

6. X. Fan, D.J. Parker, M.D. Smith (2003). Adsorption kinetics of fluoride on low-cost materials. *Water Research*, 37(20), 4929-4937. https://doi.org/10.1016/j.watres.2003.08.014.

7. Meenakshi, R.C. Maheshwari (2006). Fluoride in drinking water and its removal. *Journal of Hazardous Materials*, 137(1), 456-463. https://doi.org/10.1016/j.jhazmat.2006.02.024.

8. Spencer H, Kramer L, Norris C, Wiatrowski E. (1980). Effect of aluminum hydroxide on fluoride metabolism. *Clinical Pharmacology and Therapeutics*, 28(4):529-535. https://doi.org/ 10.1038/clpt.1980.198 .

9. Karagas, M. R., Gossai, A., Pierce, B., & Ahsan, H. (2015). Drinking water arsenic contamination, skin lesions, and malignancies: a systematic review of the global evidence. *Current Environmental Health Reports*, 2(1), 52-68. https://doi.org/10.1007/s40572-014-0040-x

10. Kuwabara T, Kikutani K, Sato T, Onodera Y. (2009) Adsorption properties of harmful anion to synthetic Si–Al–Mg mixed hydrous oxides. *Journal of Japan Society on Water Environment*, 32. 655-660. [in Japanese with English abstract]. https://doi.org /10.2965/jswe.32.655.

11. Kuwabara T, Kikutani K, Sato T, (2010) Synthesis of Si-Al-Mg composite hydrous oxides and their adsorption properties for harmful ions. *Journal of the Society of Inorganic Materials, Japan*, 17(345) .81−88 [in Japanese with English abstract].

12. Kuwabara, T., Fukui, A., Maeno, M., & Sato, T. (2015). Regeneration properties of fluoride Ion Adsorption Ability with Si-Al-Mg Mixed Hydrous Oxide. *Journal of the Society of Inorganic Materials Japan*, 22, 261-267.

13. J.J. García-Sánchez, M. Solache-Ríos, M.T. Alarcón-Herrera, V. Martínez-Miranda, (2016). Removal of fluoride from well water by modified iron oxides in a column system. *Desalination and Water Treatment*.57(5)2125-2133. https://doi.org/10.1080/19443994.2014.980332.

14. Farrah, H., Slavek, J., & Pickering, W.F. (1987). Fluoride interactions with hydrous aluminum oxides and alumina. *Australian Journal of Soil Research*, 25(1), 55-69. https://doi.org/10.1071/SR9870055.

15. Sarma, Gautam Kumar, Rashid, Md. Harunar (2018). Synthesis of Mg/Al Layered Double Hydroxides for Adsorptive Removal of Fluoride from Water: A Mechanistic and Kinetic Study. *Journal of Chemical & Engineering Data*, 63(8),2957–2965. https://doi.org/10.1021/acs.jced.8b00242.

16. Tolkou, A. K., Manousi, N., Zachariadis, G. A., Katsoyiannis, I. A., & Deliyanni, E. A. (2021). Recently Developed Adsorbing Materials for Fluoride Removal from Water and Fluoride Analytical Determination Techniques: A Review. *Sustainability (MDPI)*, 13(13), 7061. https://doi.org/10.3390/su13137061.

Chapter 3: Granulation of SAM118 and evaluation of fluoride adsorption capacity of granular SAM118

3.1 Introduction:

The use of granular materials has been found to be an efficient method for powder processing in various industrial applications (Kurozumi et al., 2015)**.** However, the increasing utilization of nano powders has raised concerns regarding contamination and processing risks (Mohammad et al., 2003). Granulation presents a viable solution to these challenges, facilitating the formation of micro- or millimeter-sized granules by suspending powders in binders and subjecting them to freeze drying and thermal processing. This method significantly reduces dust formation and enhances the flowability of the resulting granulated powder. In this study, SAM118 was granulated using polyacrylamide as a binder, and its fundamental physical properties were evaluated.

3.2 Experimental Methodology:

3.2.1 *Preparation of granular SAM118:*

The preparation of granular SAM118 was carried out using the method reported by (Kurozumi et al., 2015), (Kurozumi et al., 2016)**,** which detail the incorporation of iron hydroxide oxide onto polyacrylamide cryogel.

3.2.2 *Materials and reagents:*

The reagents used in the preparation of the polyacrylamide granular SAM118 included monomeric acrylamide (AAm) and ammonium peroxydisulfate (APS) obtained from Fuji-film Wako Pure Chemical Corp. (Osaka, Japan), N,N'-methylene bisacrylamide (MBAAm) and N,N,N',N'-tetramethylethylenediamine (TEMED) were sourced from Alfa Aesar (Ward Hill, USA) and Combi-Blocks (San Diego, USA), In addition, SAM118 powder and degassed water were used.

3.2.3 *Preparation of granular SAM118 by using polyacrylamide.:*

Polyacrylamide granular SAM118 was prepared through a systematic method designed to optimize the incorporation of SAM118 into a polymer matrix. Initially, 20 g of SAM118 was dispersed in 200 mL of degassed water to create a uniform suspension. Following this, 8 g of acrylamide (AAm) and 2 g of N,N'-methylene bisacrylamide (MBAAm) were added sequentially, with vigorous stirring for 1.5 hours to ensure complete dissolution. To facilitate the removal of dissolved oxygen, nitrogen gas was passed through the solution for 3 minutes. Subsequently, an ammonium peroxydisulfate (APS) solution, prepared by dissolving 1.0 g of APS in 1.0 mL of degassed water, was added, and the mixture was stirred for an additional 30 minutes to activate the polymerization process. To further initiate this process, 0.24 g of N,N,N',N'-tetramethylethylenediamine (TEMED) was quickly introduced while stirring. Approximately 10 mL of the resulting mixture was then transferred into syringes, which were sealed and frozen at -15 °C for 24 hours to allow for granule formation. Finally, the frozen polyacrylamide (PAAm) containing SAM118 was cut into appropriate sizes of less than 1.0 cm and subsequently dried using a freeze dryer (VD-800R, TAITEC, Koshigaya, Japan), as illustrated in Figure 7. This method effectively produces granular SAM118 with enhanced properties suitable for various applications.

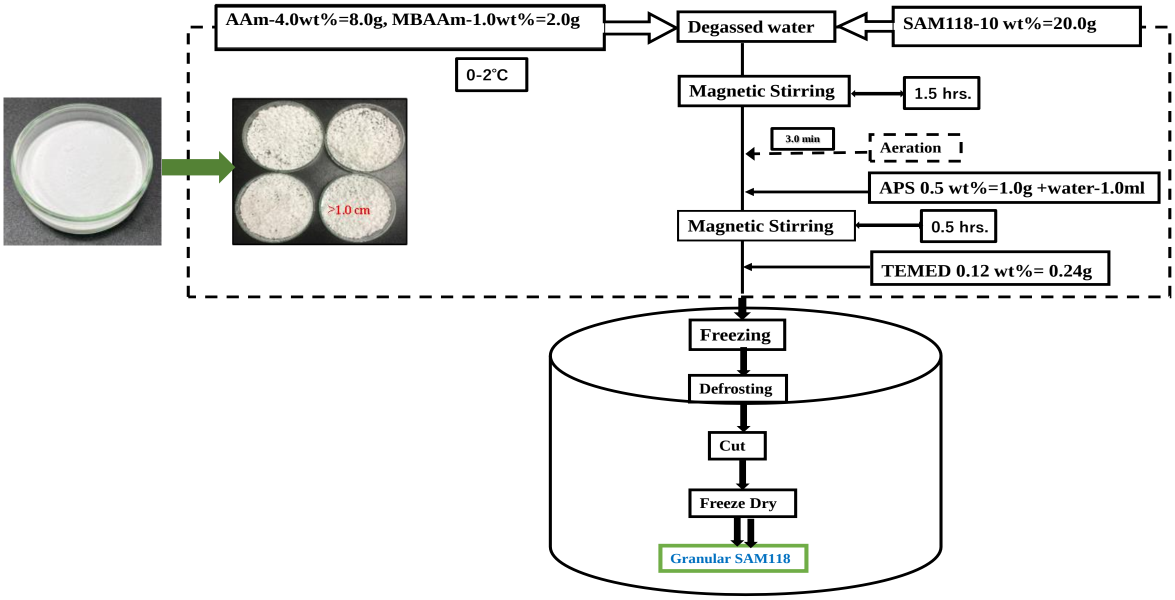

Figure 7: A flow chart illustrating the preparation process for polyacrylamide-containing granular SAM118, alongside a diagram depicting its pore structure.

3.2.4 Measurement process for SAM118 content in cryogels.

The preparation of cryogels containing SAM118 particles involved a series of washing steps to ensure the removal of unreacted materials. Initially, the polyacrylamide (PAA) cryogels were washed thoroughly with degassed water until a neutral pH of 7.0 was achieved. Following this, the cryogels were mechanically squeezed in a syringe to facilitate the extraction of trapped particles. To ensure complete removal, the washing process was repeated until no particles flowed out. After the washing procedure, the cryogels were lyophilized and cut into smaller sizes of less than 1.0 cm. The resulting samples were then stored in the refrigerator to allow for ice formation. The next day, these cryogels were removed from the refrigerator and subsequently dried using a Freeze Dryer (Model # VD-800R), as illustrated in Figure 8.

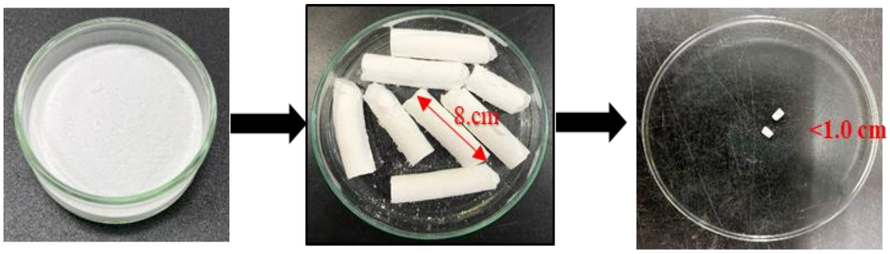

SAM118 Before cut After cut

Figure 8: Cryogel containing SAM118 particles during the freeze-drying process using a Freeze Dryer (Model # VD-800R).

3.3 Adsorption experiment of granular SAM118:

3.3.1 Batch Adsorption of Fluoride with the granular SAM118:

In the fluoride adsorption experiment, Cryogels containing SAM118 particles were utilized via a batch method. The Cryogels were placed into a sample beaker, and an aqueous solution of NaF was added. The mixture was then shaken for a duration of 48 to 60 hours, as illustrated in Figure 9. Following this period, the solution and Cryogels were separated, and the concentration of fluoride in the solution was measured using an ion chromatography system. The adsorption capacity of fluoride on the adsorbents was calculated based on the lyophilized weight of the Cryogels, expressed in mg g^{-1}.

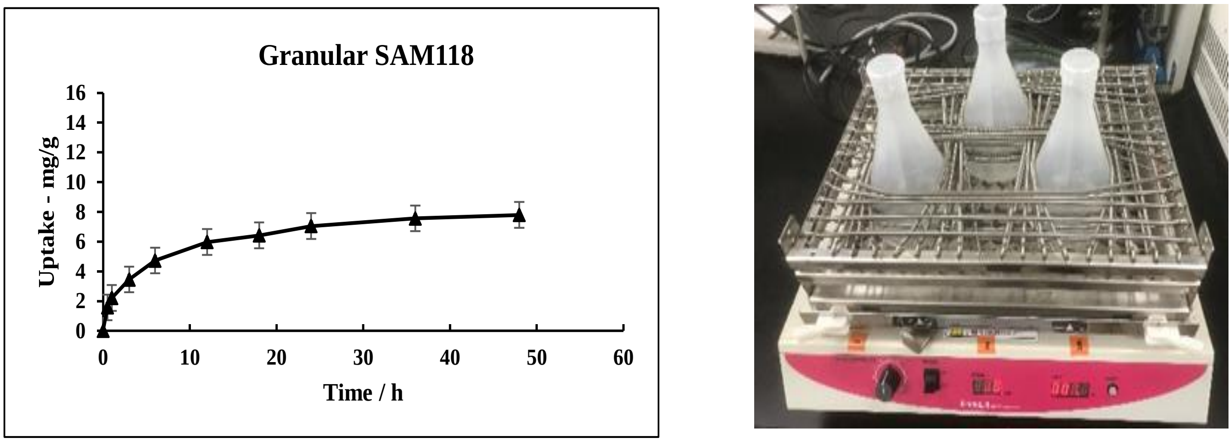

Figure 9: Batch adsorption setup of granular SAM118, illustrating the process of fluoride adsorption using Cryogels containing SAM118 particles in an aqueous NaF solution.

3.3.2 Column Adsorption of fluoride with the granular SAM118.

The continuous flow fluoride adsorption experiment was conducted using an adsorption column method, as depicted in Figure 10. The experimental setup involved polyethylene columns measuring 20.0 cm in length and 1.6 cm in internal diameter, packed with dry granular SAM118. To eliminate air from the granular samples, negative pressure was applied using water. A fluoride solution, either a NaF aqueous solution or actual hot spring water, was adjusted to a concentration of 15 mg $L^{-1}$and introduced into the column via a silicon tube connected to the bottom, ensuring an upward flow. The space velocity (SV) was systematically varied by altering the amount of adsorbent in the column, with specific SV settings of approximately 0.83/h for column-1, 0.43/h for column-2, and 0.31/h for column-3, arranged in series. Additionally, experiments utilizing Matsue Shinjiko Onsen hot spring water were conducted at room temperature (25°C) with a single column operating at an SV of 1.09/h. Treated water was collected from the column's outlet at regular intervals, and both residual fluoride concentrations and pH levels were measured. The breakthrough capacity was determined by identifying the point at which the treated water's fluoride concentration reached Japan's water standard of 8 mg L^{-1}. The Matsue Shinjiko Onsen hot spring water was characterized by predominant elements including Na, Ca, Cl, and SO_4, with key anion concentrations measured as F (16.521 mg L^{-1}), Cl (634 mg L^{-1}), and SO_4 (580 mg L^{-1}), while other anions such as CO_3, Br, and HCO_3

remained below 30 mg/L. The space velocity (SV) quantifies the reciprocal of contact time between treated and raw water per unit time, reflecting how frequently the column's volume processes the fluid, calculated by dividing the flow rate by the column volume. Liquid velocity (LV) denotes the rate at which the fluid traverses the filtration tank's cross-section.

SV(/h) and LV(m/h) were calculated by using the following equation (2) and (3), respectively.

$$SV = \frac{Flow\ rate(L/h)\ \times 1000}{Volume\ of\ adsorbent(cm^3)} \tag{2}$$

$$LV = \frac{Flow\ rate\ (L/h) \times 1000}{Cross\text{-}sectional\ area(cm^2) \times 100} \tag{3}$$

Table 3 Experimental condition of the column test.

Column	**Flow rate (L/h)**	**Linear Velocity (m/h)**	**Space velocity (/h)**	**Packed Granular SAM118 (g)**	**Volume of packed granule SAM118 (cm^3)**	**Length of packed Granular SAM118 (cm)**	
①. NaF Aqueous water-(15mgF L^{-1}, 20-25°C, Column Size-20.0 cm×φ 1.6 cm)						**Dry cond.**	**Wet cond.**
Column-1	0.021	0.11	0.83	2.513	26.12	11	13
Column-2			0.43	2.415 (4.928) *	24.12 (50.24) *	10	12
Column-3			0.31	2.206 (7.134) *	19.09 (69.33) *	8	9.5
②. Hot Spring water -(15mgF L^{-1}, 20-25°C, Column Size-20.0 cm×φ 1.6 cm)							
Column-4	0.024	0.12	1.09	2.4	22.11	9	11

(*For columns 1-2 or columns 1-3, the values in parentheses indicate the total packed weight or volume. *)

Table 4 Composition of Matsue Shinjiko hot spring water.

Anion Component	Concentration (mg-L^{-1})	Concentration (mmol-L^{-1})
F^-	4.2	0.22
Cl^-	540	15.23
Br^-	1.4	0.017
SO_4^{2-}	738	7.68
HCO_3^{2-}	24.3	0.39
CO_3^{2-}	3.0	0.05

(The source: Matsue city tourism development public corporation.)

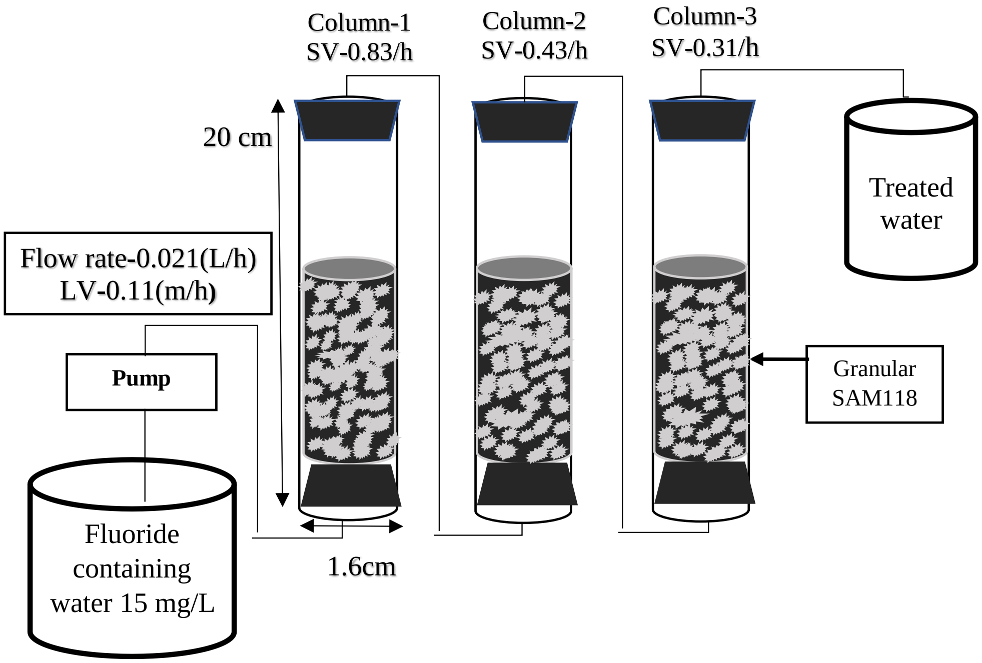

Figure10: Illustrates the granular SAM118 column adsorption setup used in this study.

3.4 SAM118 in Cryogels Content measurement:

To quantify the content of SAM118 in the Cryogels, a heating and melting method utilizing nitric and sulfuric acids was employed, as illustrated in Figure 11. In this procedure, the granular form of SAM118 was dissolved in a mixture of the acids while being heated, with the resultant gel collected using quantitative filter paper (5B, Toyo Roshi Kaisha, LTD., Tokyo, Japan). After thoroughly washing the filter paper, the aluminum concentration in the filtrate was measured to determine the SAM118 content within the granular form. Furthermore, the filtrate underwent analysis using inductively coupled plasma mass spectrometry (ICP-MS) (Agilent 8800, Agilent Technologies, Inc., California, USA) to accurately assess the magnesium and aluminum concentrations. This method provides a reliable means of evaluating the incorporation of SAM118 in the cryogel structure, facilitating further insights into its functional properties.

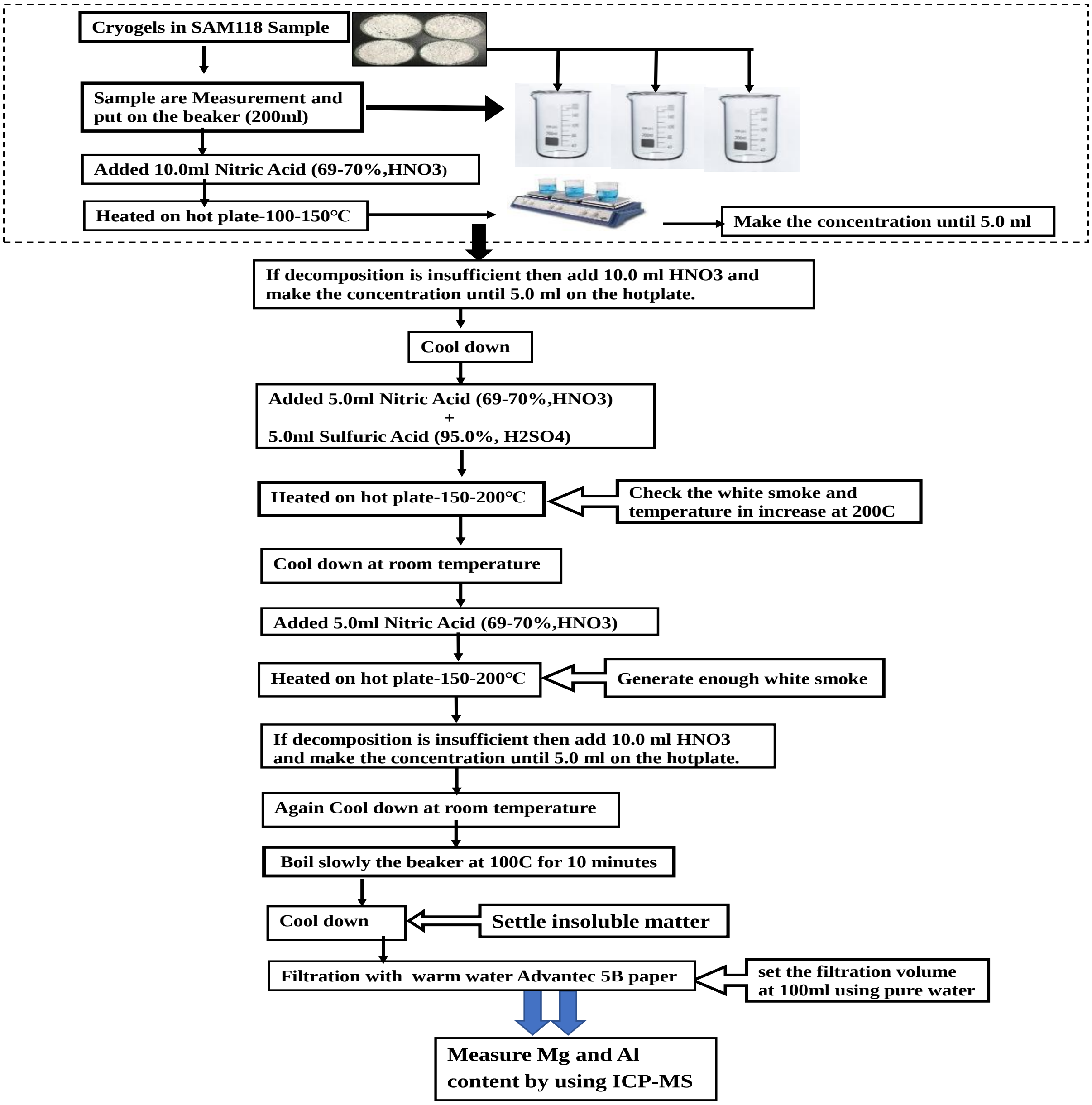

Figure 11: Illustrates the process used for measuring the content of SAM118 in the Cryogels.

3.5 Result and discussion

This chapter presents a comprehensive analysis of the results obtained from the study on granular Si-Al-Mg mixed hydrous oxide particles containing SAM118, emphasizing their fluoride ion adsorption properties. The data presented in this chapter addresses various aspects, including metal element composition, physicochemical properties, adsorption behavior, and the potential application of SAM118 for environmental remediation, particularly fluoride removal. The results from different analyses, such as XRD, TG-DTA, FTIR, and adsorption tests, are critically discussed in this context to elucidate the material's behavior under different conditions.

3.5.1 The metal elements composition ratio containing granular Si-Al-Mg mixed hydrous oxide particles.:

The investigation revealed that the metal element composition molar ratio for SAM118 was 0.099Si:0.100Al:0.801Mg, as summarized in Table 4. This ratio aligns with the initial composition of the reagents used during the synthesis process. To assess the carrying ratio of SAM118 in granular form, the aluminum (Al) content was compared between the granulated and powdered forms. The Al content in the granular SAM118, determined through acid dissolution, was measured at 0.996 mmol g^{-1}, whereas the powder form exhibited an Al content of 1.402 mmol g^{-1}. Consequently, the calculated Al ratio of the granulate to the powder was 71.0%, indicating that the carrying ratio of SAM118 in the granular form was approximately 71.0 wt.%. The detailed content measurements for both forms are as follows:

Table 5. The metal element composition ratio of the powder SAM118 and the carrying ratio of SAM118 in the granular SAM118 form.

		Si	**Al**	**Mg**	**Density (g/cm^3)**	**Carrying ratio of SAM118(%)**	**Particle size**
Powder SAM118	**Content (mmol/g)**	**1.388**	**1.402**	**11.244**	**2.50**	**-**	**＜250µm**
	Obtained composition ratio	**0.099**	**0.100**	**0.801**			
	(Target composition ratio	**0.1**	**0.1**	**0.8)**			
Granular SAM118	**Content (mmol/g)**	**-**	**0.996**	**-**	**2.38**	**71.0**	**About <1 cm^3**

3.5.2 XRD and TG-DTA analysis of the Si-Al-Mg mixed hydrous oxide.:

The physicochemical properties of SAM118 were thoroughly examined using X-ray diffraction (XRD) and thermogravimetric-differential thermal analysis (TG-DTA). The XRD diffractograms presented in Figure 12 reveal the presence of a hydrotalcite-like compound alongside magnesium hydroxide (Mg $(OH)_2$), indicating a high anion exchange capacity, which is beneficial for applications in fluoride removal. The analysis further showed that SAM118 consists of a mixed phase of hydrotalcite-like structures and Mg $(OH)_2$, with the calculated x value being approximately 0.11. This low x value suggests a predominance of magnesium relative to aluminum in the structure.

Notably, after conducting adsorption tests with an initial fluoride concentration of 15 mg L^{-1}, no distinct peak for Mg $(OH)_2$ was observed in the XRD results, implying that this compound likely remained dissolved in the fluoride solution during the experiment. These findings highlight the stability and behavior of SAM118 under fluoride adsorption conditions, providing essential insights into its structural characteristics and potential efficacy as an adsorbent material. The combination of XRD and TG-DTA analyses not only elucidates the composition of SAM118 but also supports its suitability for practical applications in environmental remediation.

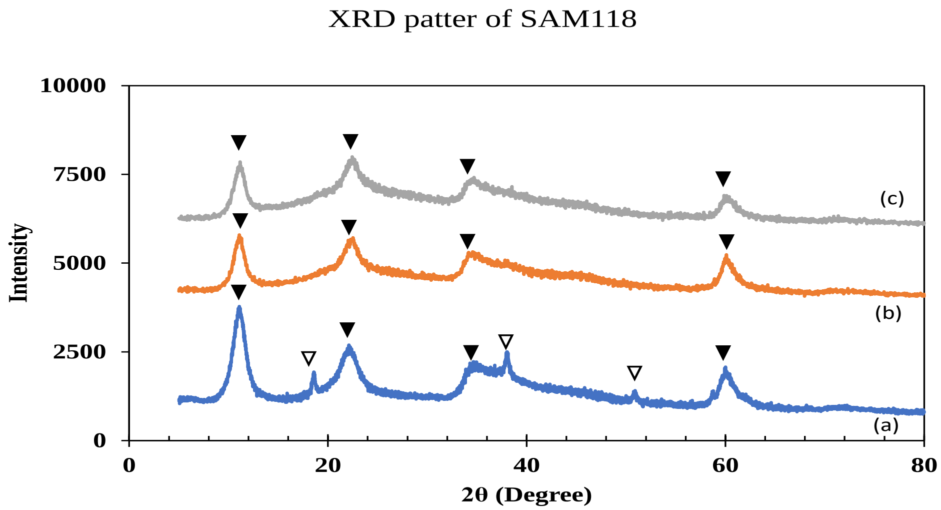

Figure 12: XRD patterns of (a) SAM118, (b) SAM118 after F- adsorption, (c) Granular SAM118 after F-adsorption. ▼: Hydrothalcite ▽: Mg (OH)2

The TG-DTA results, presented in Figure 3, exhibited endothermic peaks at approximately 100℃ and 400℃, corroborating findings from previous studies (Zheng et al., 2010, Kuwabara et al., 2010). The DTA curve displayed clear thermal transitions, while the TGA curve indicated a two-step weight loss associated with these peaks, consistent with the characteristics of hydrotalcite-like compounds. Collectively, these analyses enhance our understanding of SAM118's structural properties and behavior, highlighting its potential effectiveness in applications such as environmental remediation.

3.5.3 FTIR Analysis of SAM118 (powder and Granular) before and after fluoride adsorption.:

FTIR analysis was conducted to investigate structural changes in SAM118 powder and granular SAM118 following fluoride adsorption, with spectra presented in Figure 13. To facilitate accurate comparison, the adsorption amount for granular SAM118 was normalized based on its SAM118 content (71.0 wt%). The results indicated that, when normalized, the adsorption capacity of granular SAM118 closely matched that of powder SAM118, underscoring the material's effectiveness in fluoride removal. To enhance clarity, the Y-axis was adjusted to maintain a 100% transmittance. The manuscript motes that the spectra were overlaid for comparative purposes, ensuring that individual transmittance values remained within expected limits.

The FTIR spectrum of SAM118 powder exhibited characteristic peaks at 538 cm^{-1}, 736 cm^{-1}, 958 cm^{-1}, 1169 cm^{-1}, 1617 cm^{-1}, 1775 cm^{-1}, 2369 cm^{-1}, 2940 cm^{-1}, 3313 cm^{-1}, and 3691 cm^{-1}, corresponding to various vibrational modes of functional groups present in SAM118. Following fluoride adsorption, notable changes in intensity and peak sharpness were observed at similar wavenumbers, suggesting interactions between fluoride ions and the SAM118 structure, which may indicate potential structural modifications.

The FTIR spectrum of granular SAM118 after fluoride adsorption displayed similarities to the powder form, with distinct peaks at corresponding wavenumbers, such as 538 cm^{-1}, 736 cm^{-1}, 958 cm^{-1}, and 3691 cm^{-1}, confirming the presence of fluoride ions and their interaction with the adsorbent material. The normalization of adsorption values based on SAM118 content further substantiated the material's efficacy in both powder and granular forms.

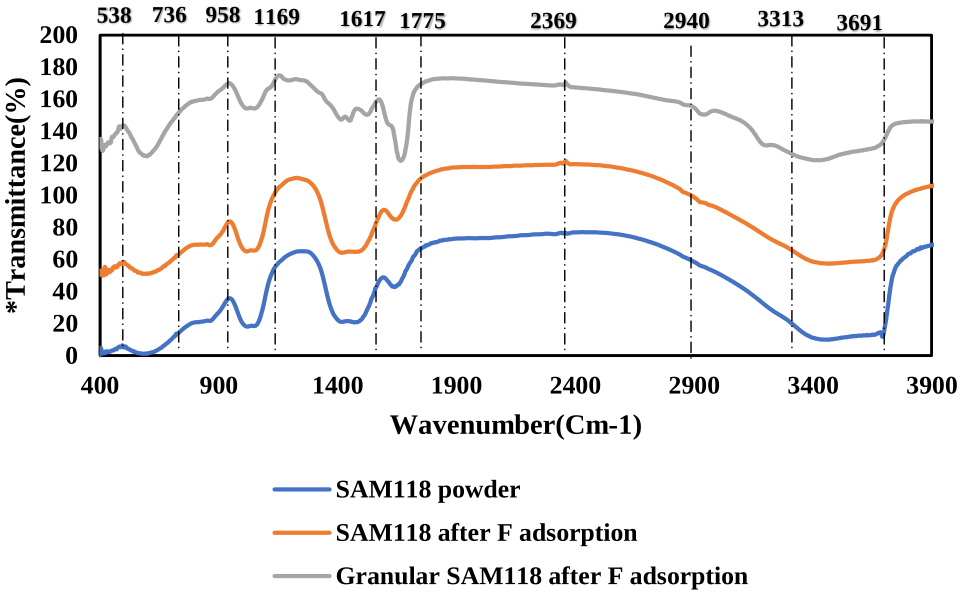

Figure 13: Fourier transform infrared (FTIR) analysis of Powder SAM118 and granular SAM118 before and after adsorption.

[* where the transmittance axis has been rescaled accordingly for accurate visualization]

For comparative analysis, the FTIR spectra of polyacrylamide (PAAm) were also examined, allowing for clearer differentiation between the peaks associated with SAM118 and the polymer matrix. Notable peaks included a broad peak at 3392 cm^{-1}, attributed to hydroxyl (-OH) groups, a band at 1629 cm^{-1} representing C-H aromatic ring stretching vibrations, and peaks at 1100 cm^{-1} associated with C-O bond vibrations, along with a peak at 577 cm^{-1} assigned to the Fe-O bond. These peaks, particularly in the functional group and fingerprint regions, illustrate the structural nature of SAM118 and its efficacy as an adsorbent. The detailed analysis of these spectra sheds light on the adsorption mechanism, providing insights into the interactions between fluoride ions and the functional groups of SAM118.

3.6 Fluoride ion adsorption capacity:

The fluoride ion adsorption capacity of SAM118 powder and granular SAM118 was evaluated and analyzed using adsorption isotherms. The results indicated that SAM118 powder reached adsorption equilibrium within 24 hours, whereas granular SAM118 did not achieve equilibrium even after 48 hours, primarily due to a decreased adsorption rate resulting from granulation. At an initial fluoride concentration of 15 mg L^{-1}, the adsorption amounts were 11.190 mg $g^{-1}$for SAM118 powder and 7.793 mg g^{-1} for granular SAM118. To facilitate a direct comparison, the adsorption amount of granular SAM118 was adjusted to reflect the fluoride adsorption capacity excluding the influence of polyacrylamide (PAAm). It was observed that while PAAm contributed to a reduction in the adsorption rate, it did not significantly impact the overall adsorption capacity.

The adsorption isotherm for fluoride ions closely followed the Freundlich equation, suggesting that the SAM118 mixed hydrous oxide possesses a high affinity for fluoride ions, allowing for effective removal of these harmful ions from aqueous solutions across a broad concentration range, as illustrated in Figure 14. This indicates the potential of SAM118 as a viable adsorbent for fluoride remediation in water treatment applications.

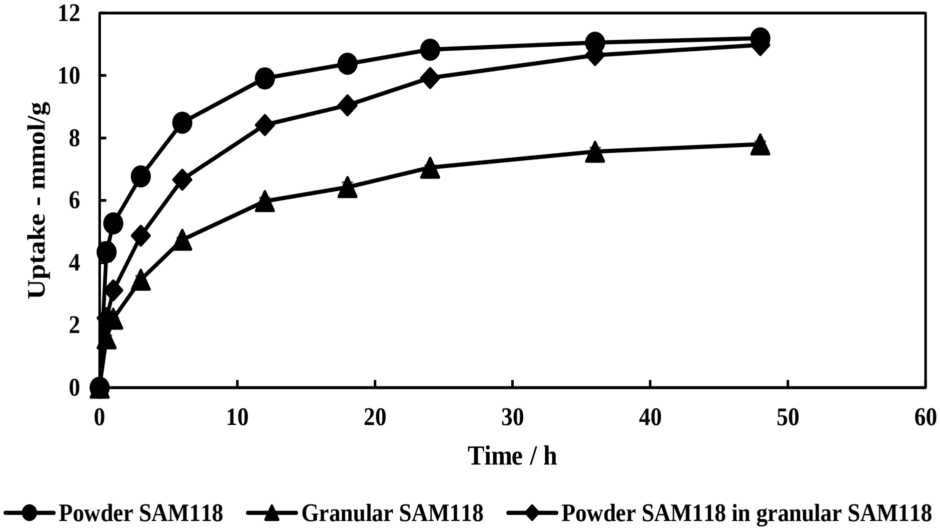

Figure 14: SAM118 powder, granular SAM118 and convert powder SAM118 in granular SAM118 adsorption uptake analysis. ※Error bars show the SD. SAM118 in granular SAM118.

3.7 Fluoride ion adsorption ability by using NaF aqueous water in terms of space velocity (SVs) of the granular SAM118.:

The fluoride ion adsorption breakthrough curves for granular SAM118 at an inflow concentration of 15.0 mg L^{-1} are illustrated in Figure 15(a) and 15(b). The breakthrough termination point was determined based on the Japanese fluorine wastewater standard of 8.0 mg L^{-1}. The results from using the NaF aqueous solution showed that the breakthrough capacities at space velocities (SV) of 0.83/h, 0.43/h, and 0.31/h were 2.5 mg g^{-1}, 3.66 mg g^{-1}, and 5.27 mg g^{-1}, respectively. For higher space velocities of 20.5/h, 10.5/h, and 7.2/h, the corresponding breakthrough capacities were 1.70 mg g^{-1}, 2.358 mg g^{-1}, and 3.127 mg g^{-1}, respectively. Breakthrough capacity, which is defined as the amount of fluoride that granular SAM118 can adsorb before the effluent concentration reaches the specified threshold of 8.0 mg L^{-1}, serves as a critical parameter for evaluating adsorption performance under dynamic conditions. The data demonstrate that a lower flow velocity significantly enhances the adsorption performance of granular SAM118 for fluoride ions.

The data indicates that a lower flow velocity enhanced the best adsorption performance of granular SAM118 for fluoride ions. Notably, the breakthrough capacity of 5.27 mg g^{-1}can be converted to 8.06 mg g^{-1} when adjusted to exclude the influence of polyacrylamide (PAAm) at an SV of 0.31/h. However, this capacity is reduced in comparison to the approximately 15 mg g^{-1} adsorption amount predicted from the adsorption isotherm of SAM118 at an equilibrium fluoride concentration of 15 mg L^{-1}, as reported by (Kuwabara et al. 2010). This discrepancy highlights the complexities involved in dynamic adsorption processes and underscores the potential for further optimization of SAM118's performance in real-world applications.

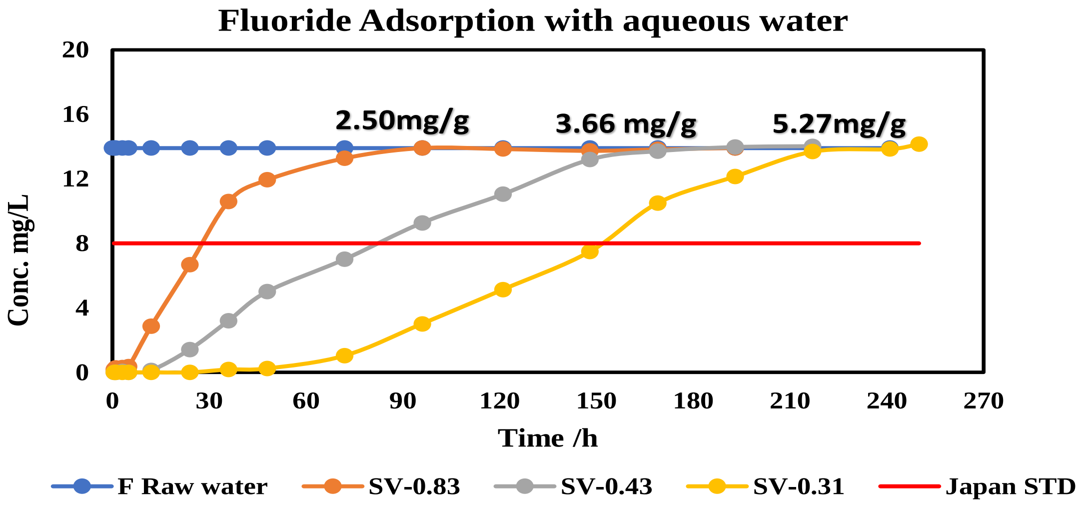

Figure 15(a): Illustrates the breakthrough curves of fluoride ion adsorption using granular SAM118 at different space velocities (SV) with an initial fluoride ion concentration of 15.0 mg L−1.

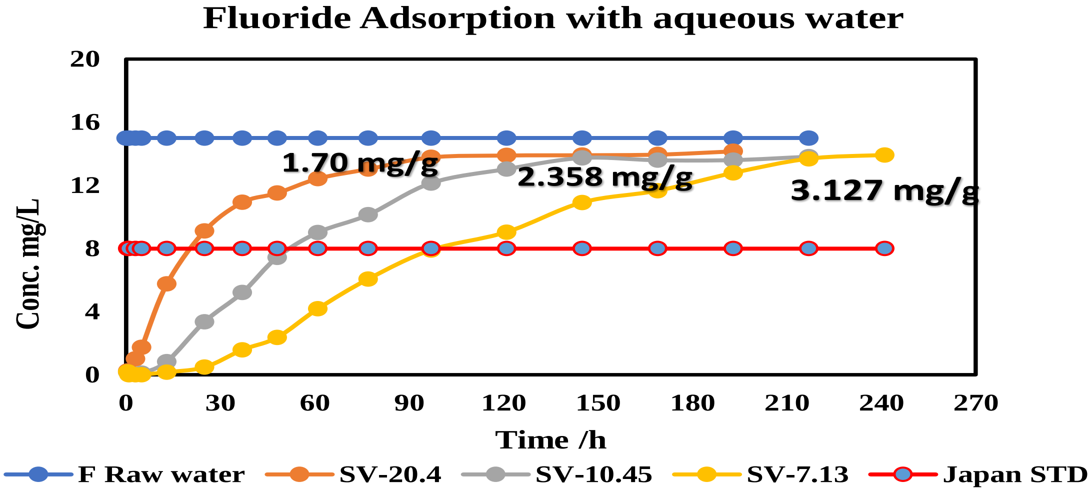

Figure 15(b): Illustrates the breakthrough curves of fluoride ion adsorption using granular SAM118 at high space velocities (SV) with an initial fluoride ion concentration of 15.0 mg L−1.

3.8 Fluoride ion adsorption removal ability by using hot spa water in terms of space velocity (SVs) of the granular SAM118.

The adsorption isotherm for fluoride ions derived from artificial fluoride water cannot be directly compared to the results obtained from the column tests using Matsue Shinjiko Onsen hot spring water. The hot spring water contains a variety of coexisting anions and cations, including sulfates, chlorides, carbonates, and bicarbonates, which influence the adsorption dynamics. Specifically, the sulfate and chloride concentrations were recorded and are detailed in our experimental documentation. In addition, cations such as calcium (Ca^{2+}), magnesium (Mg^{2+}), sodium (Na^{+}), and potassium (K^{+}) contribute to the overall ionic composition of the hot spring water. Notably, the fluoride adsorption capacity in this natural water reached 2.40 mg g^{-1} (or 3.38 mg g^{-1} without PAAm) at a space velocity (SV) of 1.09/h, closely aligning with the breakthrough capacity of 2.5 mg g^{-1} observed at SV 0.83/h in the aqueous solution, as shown in Figure 16. Remarkably, the adsorption capacity in Matsue Shinjiko Onsen hot spring water did not decrease despite the presence of competing anions, largely because the initial fluoride concentration (16.521 mg L^{-1}) was higher than that of the artificial water (13.913 mg L^{-1}).

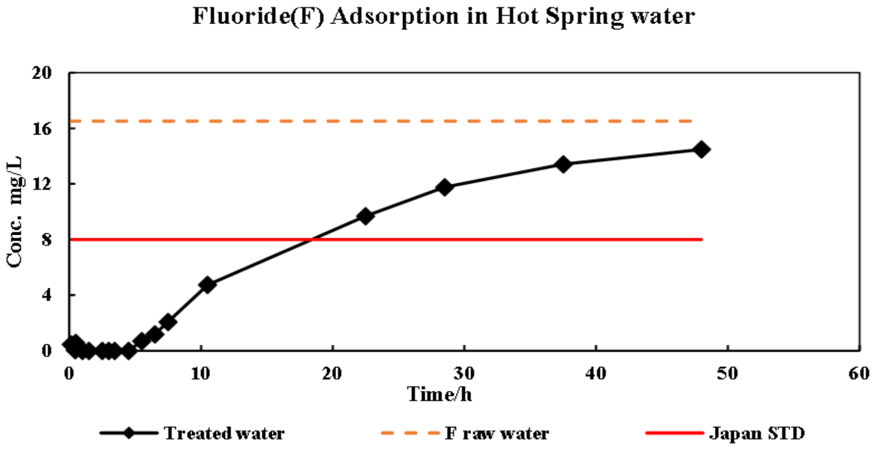

Figure 16: Breakthrough curves for fluoride ion adsorption by granular SAM118 at a space velocity (SV) of 1.09/ h in Matsue Shinjiko Onsen hot spring water.

In our study, we specifically examined the influence of chloride (Cl^-) and sulfate (SO_4^{2-}) on fluoride adsorption in the context of Matsue Shinjiko Onsen hot spring water, where the initial concentrations of these anions were approximately 600 $mg\,L^{-1}$, as determined by ion chromatography. Figure 17 illustrates the concentration changes of fluoride, chloride, and sulfate during the adsorption process. Initially, chloride and sulfate anions are displaced by fluoride, which is preferentially adsorbed. As the system approaches equilibrium, the concentrations of chloride and sulfate in the treated water increase, indicating desorption of these anions, thus providing further insights into the competitive adsorption behavior in complex aqueous environments.

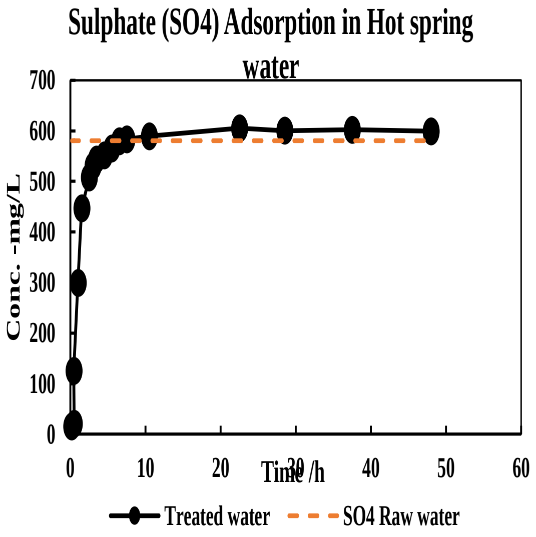

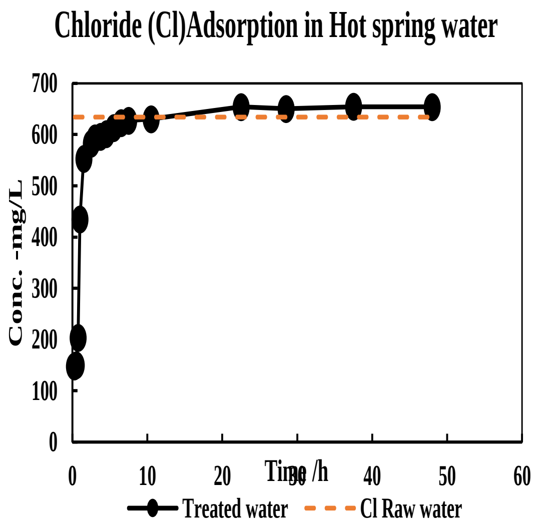

Figure 17: Breakthrough curves for sulfate and chloride ion adsorption by granular SAM118 at a space velocity (SV) of 1.09/ h in Matsue Shinjiko Onsen hot spring water.

3.9 Effect of pH on the adsorption.

The effect of pH on fluoride adsorption by Cryogels was tested in the pH range of 9 to 10, with an initial fluoride concentration of 15 mg/L. The best pH for adsorption was found to be 9.6. Changes in pH within this range had little effect on how much fluoride the Cryogels could remove. This means that while pH plays a role in the adsorption process, making the Cryogels at the right pH can improve their ability to remove fluoride. These results show how important pH is in creating and using adsorbent materials for cleaning fluoride from water.

3.10 Adsorption distribution model of the fluoride removal.

The maximum adsorption capacity of powder SAM118 has been reported to be 1.32 meq g^{-1}, as determined by the adsorption isotherm in a previous study (Kuwabara et al., 2010). The unit " meq g^{-1} " (milliequivalents per gram) quantifies the amount of adsorbed ions per gram of the adsorbent, with one milliequivalent representing one-thousandth of an equivalent—the quantity of substance that reacts with or provides one mole of hydrogen ions (H^+) in a chemical reaction. This measurement is particularly relevant for assessing ion exchange capacities in water treatment processes.

As illustrated in Figure 19, the adsorption capacities of granular SAM118 increased over a 12.5-hour period, specifically showing fluoride adsorption reaching 0.842 meq g^{-1}, while chloride peaked at 0.210 meq g^{-1} and sulfate at 0.165 meq g^{-1} the latter of which was released by the 12.5-hour mark. Notably, the graph also indicates that the adsorption of fluoride remains stable and is not significantly influenced by other anions after 18.4 hours, especially in water meeting Japan's standard of 8 mg L^{-1}. However, after 48.0 hours, a decrease in the adsorption levels of chloride and sulfate may occur, likely due to the presence of competing anions such as CO_3^{2-}, PO_4^{3-}, and NO_2^-, along with potential exchanges with hydroxide (OH^-) anions. Future research should investigate the effects of these additional anions to further enhance the performance of granular SAM118 for treating Matsue Shinjiko Onsen hot spring water. Overall, granular

SAM118 demonstrates significant potential for industrial applications and environmental protection by improving water quality.

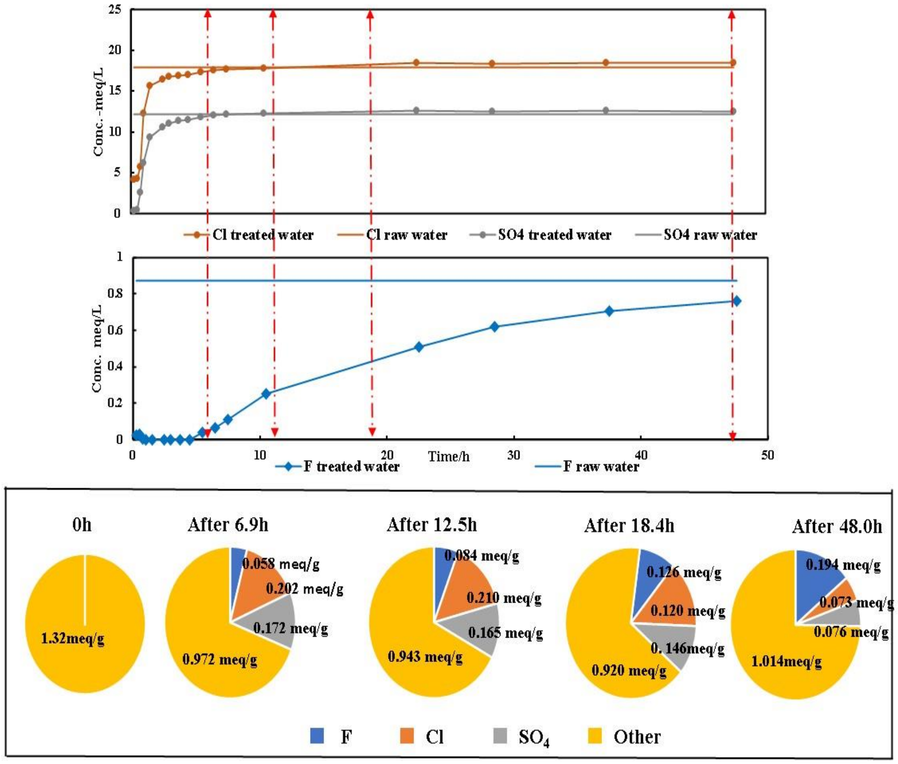

Figure 18: Breakthrough curves of Cl^-, SO_4^{2-}, and F^- ions with granular SAM118 by column test at a space velocity (SV) of 1.09/h using Matsue Shinjiko Onsen hot spring water, illustrating the transition of adsorbates and the adsorption capacity of SAM118.

3.11 Adsorption Mechanism of SAM118:

Granular SAM118 is composed of silicon (Si), aluminum (Al), and magnesium (Mg), and it shares similarities with hydrotalcite-like compounds but lacks a fully layered structure. The analyzed sample has a molar ratio of Al:Mg of 1:8, indicating a significant excess of magnesium. This excess Mg plays a crucial role in the adsorption of fluoride ions (F^-) from aqueous solutions.

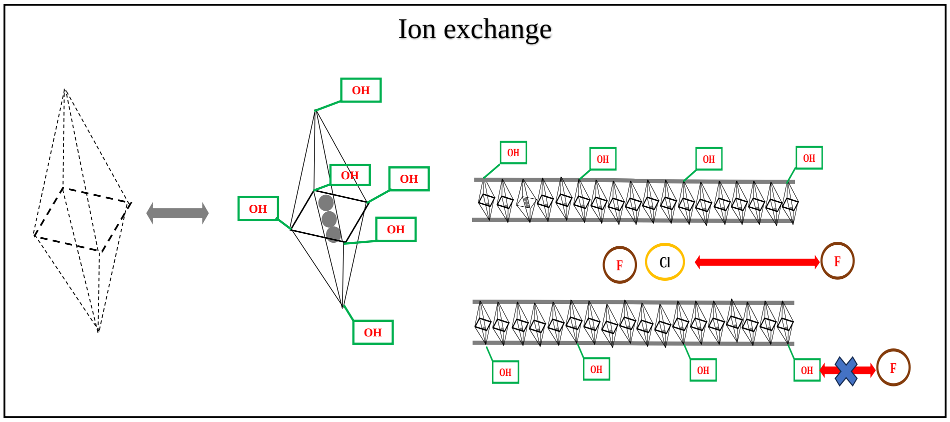

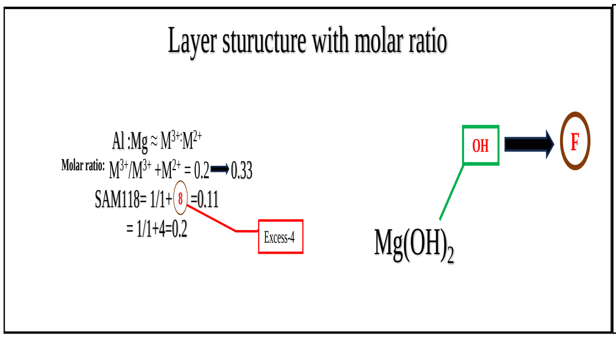

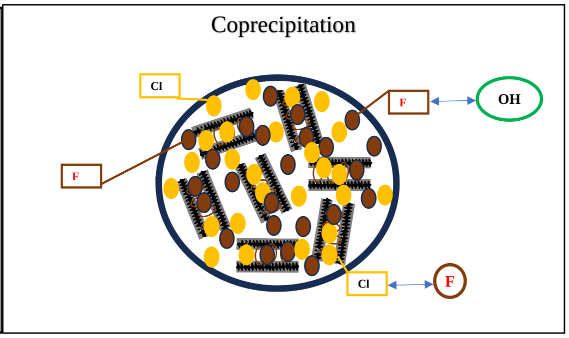

Chemical Reactions and Mechanism:

i) Ion Exchange Mechanism:

The primary fluoride adsorption process occurs through ion exchange between Mg $(OH)_2$ in SAM118 and fluoride ions in the solution. In this reaction, hydroxyl (OH^-) groups in Mg $(OH)_2$ are replaced by fluoride ions, forming magnesium fluoride (MgF_2) and releasing hydroxide ions into the solution:

$$Mg(OH)_2 + 2F^- \rightarrow MgF_2 + 2OH^-$$

This mechanism ensures effective fluoride removal, leveraging the high reactivity of $Mg(OH)_2$.

ii) Co-precipitation Mechanism:

The excess Mg $(OH)_2$ in SAM118 promotes the co-precipitation of fluoride ions within its amorphous matrix. This mechanism is enhanced by the hydrotalcite-like structure, which, although not fully layered, provides ample active sites for fluoride entrapment during synthesis.

Thermal Crystallization Effects:

The high-temperature synthesis process (80–110°C) encourages partial crystallization of Mg $(OH)_2$ into a more stable hydrotalcite-like structure. This crystallized form enhances the material's ion exchange capacity and strengthens chemical adsorption due to its increased structural stability.

Overall, the fluoride adsorption mechanism of SAM118 is a combination of ion exchange, co-precipitation, and chemical adsorption processes. Magnesium hydroxide (Mg $(OH)_2$) serves as the active phase for fluoride removal, with its effectiveness further enhanced by the partially crystallized hydrotalcite-like structure resulting from thermal treatment. These combined mechanisms make SAM118 a robust material for fluoride adsorption in water treatment applications.

3.12 Conclusion

This study thoroughly investigated the fluoride adsorption properties of SAM118, both in its powdered and granular forms, under varying conditions, including complex environments like the Matsue Shinjiko Onsen hot spring water. The physicochemical characterization of SAM118—through metal element composition analysis, XRD, TG-DTA, and FTIR—supports its suitability as an effective adsorbent for fluoride ions. The fluoride adsorption capacity of SAM118 was found to be influenced by several factors, such as particle form, flow velocity, and pH, all of which must be carefully controlled to optimize its performance in practical applications.

Key Findings:

1. **Fluoride Adsorption Capacity:** The granular form of SAM118 exhibited an impressive fluoride adsorption capacity of 7.793 mg g^{-1}, maintaining its performance even when bound with polyacrylamide. Although the granulation process did not significantly reduce the overall adsorption capacity, it affected the adsorption rate, emphasizing the need for optimization in practical applications.

2. **Effect of pH:** The study revealed that pH had a minimal impact on fluoride adsorption. This finding is crucial as it demonstrates that SAM118 can function effectively across a wide range of pH conditions, making it highly adaptable for diverse water environments.
3. **Impact of Granulation:** Although granulation preserved the core adsorption properties of SAM118, the adsorption rate decreased compared to its powdered form. This highlights the trade-offs between particle form and performance, suggesting that optimizing the granulation process is necessary to enhance adsorption efficiency in practical systems.
4. **Column Adsorption Performance:** Column tests with granular SAM118 confirmed its effectiveness in removing fluoride ions from both artificial and natural hot spring waters, even in the presence of coexisting anions. This demonstrates the material's versatility and efficacy in real-world water treatment applications, paving the way for scalable use in water treatment systems.
5. **Space Velocity and Adsorption Efficiency:** The study found that space velocity is a critical factor in determining the fluoride removal efficiency of SAM118 in column adsorption systems. Optimizing the flow rate is essential to maximize the adsorbent's capacity, especially under dynamic conditions typical of practical applications.

In conclusion, this research highlights the potential of SAM118, particularly in its granular form, as a highly promising solution for fluoride removal in diverse aqueous environments. The material demonstrated significant adsorption capacity and resilience, even under challenging conditions such as the presence of competing anions and varying pH levels. Given its effective performance in both conventional water systems and unique environments like hot spring waters, SAM118 is a versatile candidate for fluoride remediation in water treatment applications.

The findings from this study provide a solid foundation for future research aimed at optimizing SAM118-based adsorbents for large-scale, real-world water treatment systems. Further studies should focus on enhancing the adsorption process and evaluating SAM118's performance across a broader spectrum of environmental conditions, including industrial and naturally contaminated waters.

3.13 References

1) Kuwabara, T., Sato, T., and Onodera, Y. (2010) Synthesis of Si–Al–Mg mixed hydrous oxides and their ion adsorption behavior. *Journal of the Society of Inorganic Materials, Japan*, **17**, 81–88 [in Japanese with English abstract].

2) Kurozumi, M., Yano, Y., Kiyo Yama, S., Kumar, A., & Shiomori, K. (2015). Adsorption Properties of Arsenic(V) by Polyacrylamide Cryogel Containing Iron Hydroxide Oxide Particles Prepared by in situ Method. *Resources Processing*, 62, 17-23. https://doi.org/10.4144/rpsj.62.17.

3) Kurozumi, M., Yano, Y., & Kiyo Yama, S. (2016). Preparation of polyacrylamide Cryogels containing iron hydroxide oxide nanoparticles by particle addition method and their arsenic adsorption properties. *Science and Technology studies*, 5(1), 23-28. https://doi.org/10.11425/sst.5.23.

4) Ni, T., Huang, GS., Zheng, J. (2010). Research on the crosslinking mechanism of polyacrylamide/resol using molecular simulation and X-ray photoelectron spectroscopy. *Polym Journal* 42, 357–362. https://doi.org/10.1038/pj.2010.10.

5) Sarma, G., & Rashid, M. (2018). Synthesis of Mg/Al Layered Double Hydroxides for Adsorptive Removal of Fluoride from Water: A Mechanistic and Kinetic Study**.** *Journal of Chemical & Engineering Data*, *63*(8). https://doi.org/10.1021/acs.jced.8b00242.

6) Mohammad U., (2017). A review on the adsorption of heavy metals by clay minerals, with special focus on the past decade. *Chemical Engineering Journal*, 308,438-462. https://doi.org/10.1016/j.cej.2016.09.029.

Chapter 4: Evaluation of the arsenic adsorption capacity of Si-Fe-Mg (SFM) mixed hydrous oxides

4.1 Introduction:

The present study investigates the effectiveness of a mixed hydrous oxide composed of silicon (Si), iron (Fe), and magnesium (Mg) — referred to as SFM powder — with a high iron ratio for the removal of arsenic from groundwater. Arsenic contamination in drinking water is a pressing global health concern, necessitating the development of efficient removal technologies (Centeno et al., 2002, World Health Organization. (2011). The synthesized SFM powder's physical properties and arsenic adsorption capacity were thoroughly evaluated, providing a foundation for understanding its potential application in water treatment.

In addition to assessing the adsorption capacity of SFM powder, this study included adsorption tests conducted with actual groundwater samples to better mimic real-world conditions. Given that groundwater often contains various coexisting materials that may affect arsenic adsorption, we also examined the influence of these substances on the adsorption process. The results highlight the SFM powder's ability to maintain its arsenic removal efficiency in the presence of competing ions and other coexisting materials.

This paper presents the findings from these experiments, offering valuable insights into the potential of SFM powder as an effective adsorbent for arsenic removal from contaminated groundwater. By elucidating the factors that influence arsenic adsorption, this study aims to contribute to the development of practical solutions for addressing arsenic contamination in water resources.

4.2 Experimental Methodology:

4.2.1 Preparation of SFM05905

4.2.2 Materials and reagent.

In this study, the following materials were employed for the synthesis of the mixed hydrous oxide (SFM) powder:

- Sodium Silicate Solution No. 3 ($Na_2O\cdot nSiO_2\cdot xH_2O$, Kishida Chemical, Osaka, Japan)
- Ferric Chloride Hexahydrate ($FeCl_3\cdot 6H_2O$)
- Magnesium Chloride Hexahydrate ($MgCl_2\cdot 6H_2O$)
- Hydrochloric Acid (Fujifilm Wako Pure Chemical Corp., Osaka, Japan)

Additionally, ultrapure water (Milli-Q, Merck Millipore, Darmstadt, Germany) was utilized throughout the synthesis process as well as for all water quality analyses, ensuring high accuracy and reliability of the experimental results. These materials were selected based on their availability and suitability for synthesizing an effective adsorbent for arsenic removal from groundwater.

4.2.3 Synthesis of SFM05905:

The Si-Fe-Mg mixed hydrous oxide sample, designated as SFM05905, was synthesized using the neutralization-precipitation method. The synthesis process involved the following steps:

①. **Reagent Preparation**: A specific amount of sodium silicate solution ($Na_2O\cdot nSiO_2\cdot xH_2O$), ferric chloride hexahydrate ($FeCl_3\cdot 6H_2O$), and magnesium chloride hexahydrate ($MgCl_2\cdot 6H_2O$) was dissolved in an aqueous hydrochloric acid (HCl) solution.

②. **pH Control**: The mixed acidic solution was simultaneously added to a sodium hydroxide (NaOH) solution (6 mol/kg) while stirring. The pH was initially maintained between 10.0 and 10.5, and then gradually adjusted to 12.2 through dropwise addition.

③. **Synthesis Conditions**: The synthesis was conducted under controlled conditions of temperature, agitation rate, and dripping rate of the mixed acidic solution, as the ion adsorption properties of hydrous oxides are highly sensitive to these parameters (Qureshi et al., 1991).

④. **Homogenization**: Following synthesis, the composite hydrous oxide slurry was stirred for 40 minutes to achieve homogeneity and then allowed to rest at 40°C for 24 hours.

⑤. **Centrifugation**: The slurry was centrifuged at 8,000 rpm for 15 minutes at 20°C, and the precipitate was collected.

⑥. **Drying and Pulverization**: The collected precipitate was dried at 80°C for 24 hours, followed by pulverization. The powder was then washed with ultrapure water, dried again, pulverized, and passed through a 100-mesh sieve.

⑦. **Characterization:** The resulting powder was stored in a plastic bottle for further use.

The metal element composition ratio of SFM05905 was determined using the dissolution method. The sample was dissolved in nitric and perchloric acids, and the gel was collected using quantitative filter paper. The weight of the gel was measured to determine the SiO_2 content. The filtrate was analyzed using ICP-MS (Agilent 8800, Agilent Technologies, Inc., California, USA) to measure the magnesium and iron content. Figure 1 shows the synthesized SFM05905 powder, which will be utilized in subsequent experiments for arsenic removal from groundwater.

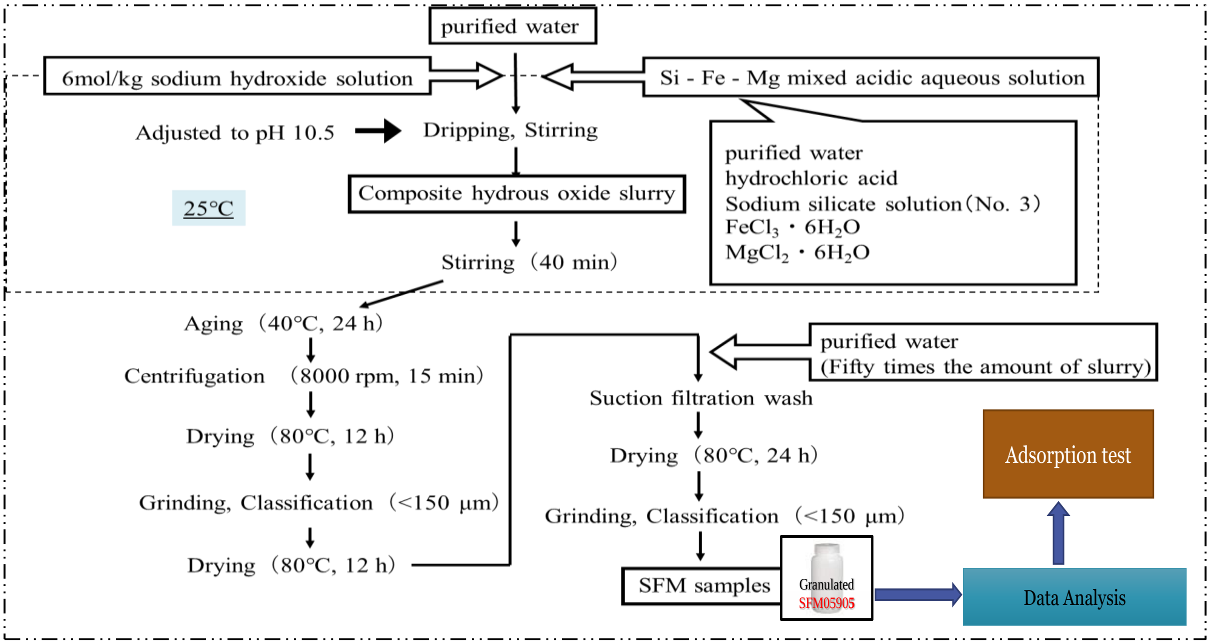

Figure 1: Illustrates the step-by-step process used to synthesize the Si-Fe-Mg mixed hydrous oxide (SFM05905) sample.

4.2.4 Characterization of physical properties of metal element composition ratio of SFM05905:

The physical properties and metal element composition of the Si-Fe-Mg mixed hydrous oxide sample (SFM05905) were characterized using a combination of analytical techniques. The metal element composition (Si: Fe: Mg) ratio was determined through inductively coupled plasma mass spectrometry (ICP-MS). The sample preparation involved dissolving the synthesized SFM05905 in an acidic solution to ensure complete dissolution of the metal ions for accurate measurement. The metal composition ratio was found to be 0.048 Si: 0.907 Fe: 0.046 Mg, which corresponds closely to the expected formulation.

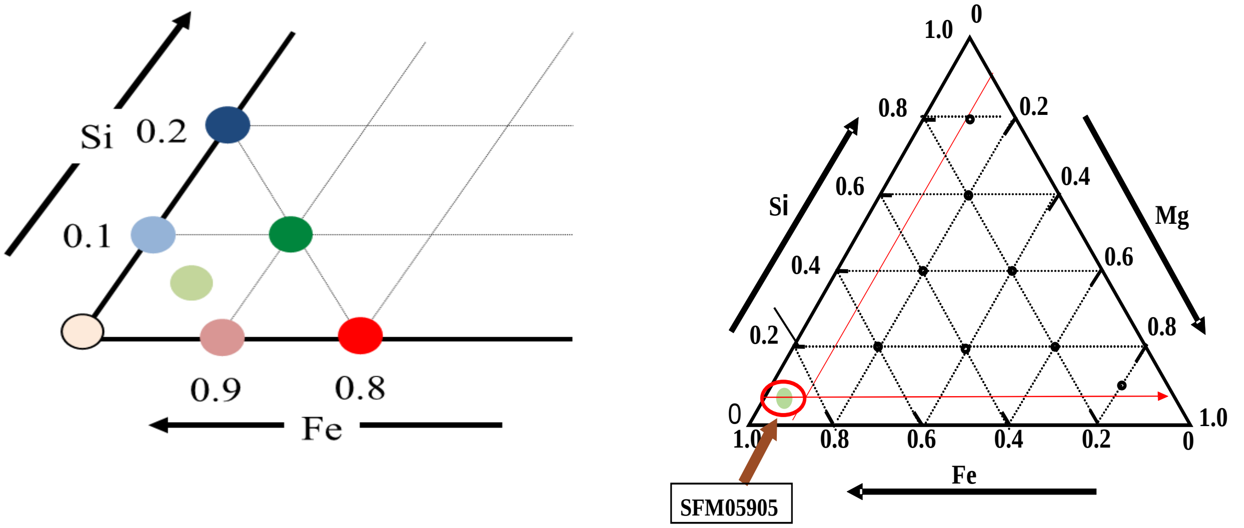

Figure 2: The metal element composition and structural features of the SFM05905 sample, highlighting the specific ratios of silicon, iron, and magnesium.

In addition to composition analysis, the structural features of SFM05905 were investigated using X-ray Diffraction (XRD) to confirm the crystalline phases and the homogeneity of the mixed hydrous oxide structure. The relationship between the metal element ratios and arsenic adsorption capacity was also evaluated based on previous findings (Kuwabara et al., 2007), which suggest a correlation between the Mg and Fe ratios and arsenite ion adsorption efficiency.

4.3 Characterization of the SFM05905:

The characterization of SFM05905 was conducted using X-ray diffraction (XRD) and thermogravimetric-differential thermal analysis (TG-DTA) to assess its structural and thermal properties.

4.3.1 Characterization of XRD Analysis

The X-ray diffractometer (MiniFlex II, Rigaku, Tokyo, Japan) was employed with an excitation voltage of 40 kV and a current of 40 mA, utilizing Ni (β) and Cu-Kα rays. Scanning was performed over the range of 2θ = 5 to 80 ° with a scanning width of 0.02 ° and a speed of 2 °/min. Figure 3 presents the XRD diffractograms of the SFM05905 powder, which revealed no distinct patterns or diffraction peaks. This observation suggests that the predominant component of SFM05905 is likely an amorphous Fe hydrous oxide, contrasting with previous studies on SFM010 that identified α-FeOOH (Goethite) as the main component when synthesized solely with iron. In samples with decreased Fe/Mg ratios, peaks indicative of layered double hydroxides became more pronounced (Kuwabara et al., 2007).

Prior to the analysis, the SFM05905 powder was carefully ground to a fine consistency to improve the homogeneity of the sample, thereby minimizing the risk of preferential orientation effects during measurement. The prepared sample was then subjected to XRD scanning over a wide angular range (2θ = 5° to 80°) to capture all possible diffraction peaks corresponding to various crystalline phases. The scanning was performed with a step size of 0.02°, which provided high-resolution data, and a scanning speed of 2° per minute to ensure the reliability of the collected diffractograms. This method allowed for the identification of any crystalline structures present in the sample, with specific attention to detecting layered double hydroxides (LDHs) or other iron and magnesium oxide phases, as anticipated based on the sample's Fe/Mg composition ratio. The results obtained from the XRD analysis were compared with existing literature data to assess structural similarities or deviations in the synthesized material.

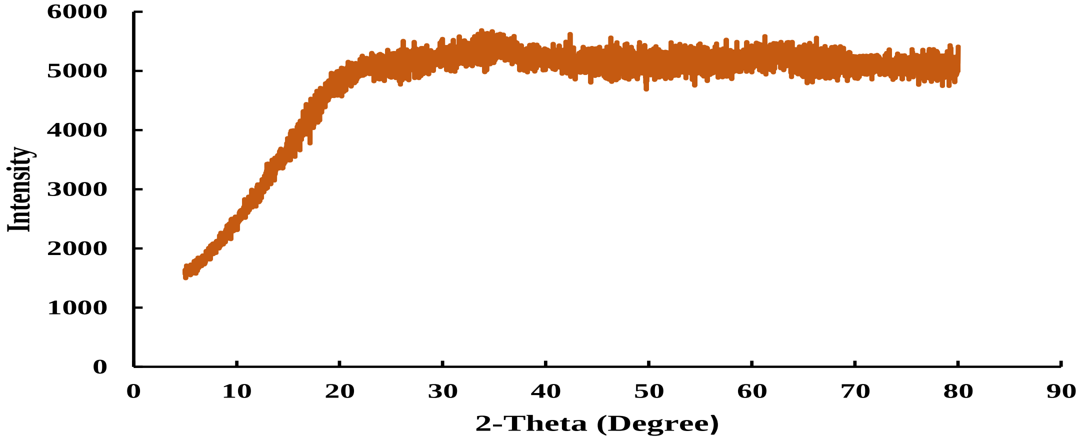

Figure 3: XRD pattern of the synthesized SFM05905.

4.3.2 Characterization of TG-DTA Analysis

The thermal properties of the SFM05905 sample were evaluated using a Thermo gravimetric differential thermal analyzer (ThermoPlus TG8120, Rigaku, Tokyo, Japan). The analysis was performed under a nitrogen atmosphere with a flow rate of 200 mL/min, over a temperature range of 25°C to 1000°C, and a heating rate of 10°C/min. Al_2O_3 powder was used as a reference material to calibrate the system and provide a baseline for differential thermal analysis.

During the experiment, the thermal behavior of the sample was observed through the TG-DTA curves, which are presented in Figure 4. The DTA curve showed an endothermic peak around 100°C, attributed to the dehydration of water molecules, while the TG curve indicated a gradual weight loss due to dehydration up to 400°C. These findings are consistent with previously reported data (Kuwabara et al., 2007) suggesting that the dehydration process is responsible for the endothermic peaks observed in the DTA curve. The TG-DTA analysis was instrumental in identifying key thermal transitions in the SFM05905 sample. The simultaneous recording of weight changes (TG curve) and heat flow (DTA curve) revealed that the dehydration process likely impacts the structural characteristics of the material. The absence of a layered structure in SFM05905 may be linked to this dehydration process, as indicated by the thermal analysis results. These findings provide valuable insights into the thermal stability and composition of the sample.

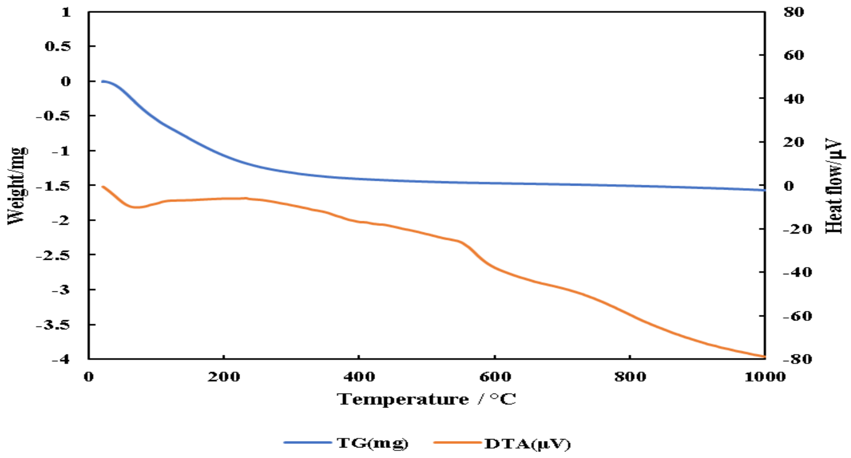

Figure 4: TG-DTA pattern of the synthesized SFM05905.

4.3.3 Characterization of FTIR analysis:

The FTIR spectrum presented in Figure 5 for the SFM05905 composite material reveals several key features that confirm its structural components.

Key Observations:

- **Hydroxyl Groups:** A strong, broad band at 3392 cm^{-1} suggests the presence of hydroxyl (-OH) groups, which are crucial for the chemical reactivity of the material.
- **Aromatic Cycles:** A significant peak at 1629 cm^{-1} indicates stretching vibrations associated with the C–H bonds in aromatic rings, confirming the existence of aromatic cycles within the extracts.
- **C–O Bond:** Vibrations in the C–H region around 1100 cm^{-1} correspond to the C–O bond, further supporting the presence of alcohols or ethers in the composition.
- **Fe–O Bond:** The peak observed at 577 cm^{-1} is attributed to the Fe–O bond, providing additional evidence of the SFM05905 structure.

These peaks collectively affirm the presence of hydroxyl and Fe–O bonds, which are essential for the reduction of salt precursors to SFM05905, attributed to their lower redox potential. The Fe–O bond at 577 cm^{-1} specifically indicates the presence of iron-containing species in the composite. These bonds likely result from Fe-OH stretching and bending vibrations of hydroxyl groups, derived from the conversion of iron oxide into forms such as Fe-OH, $Fe(OH)_2$, or the α-FeOOH (Goethite) phase. Importantly, these materials are recognized for their environmental friendliness, making them suitable for various applications.

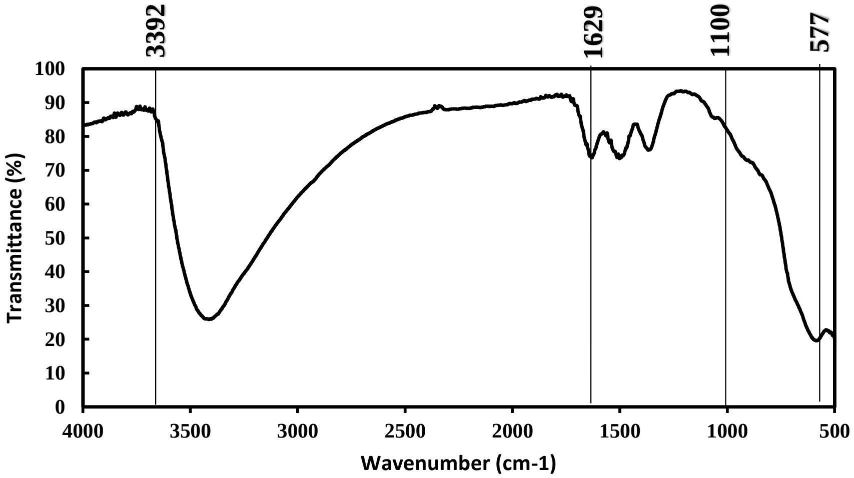

Figure 5 : FTIR pattern of SFM05905.

4.4 Adsorption rate and equilibrium adsorption amount:

4.4.1 Batch adsorption method.

The adsorption process was conducted in batch experiments to evaluate the effectiveness of SFM05905 in removing arsenic from aqueous solutions. A stock solution of arsenic (As) at approximately 1000 mg/L was prepared by dissolving dibasic sodium arsenate ($Na_2HAsO_4·7H_2O$) and diarsenic trioxide (As_2O_3), obtained from Fujifilm Wako Pure Chemical Corporation and Kanto Chemical Co., Inc., respectively, in deionized water. Table 1 represent that the working solutions with varying arsenic concentrations (10, 20, 50, 100, and 150 mg L^{-1})

were freshly prepared, and the sample pH was adjusted to 6.8 using 1 mol kg^{-1} HCl and 1 mol kg^{-1} NaOH solutions. The batch adsorption experiments were carried out at different temperatures (25°C, 35°C, and 45°C) using a Mixed Rotor apparatus (VMRC-5, AS ONE, Japan), with SFM05905 added at a concentration of 0.5% (w/v). The mixture was agitated for 72 hours, with three replicates for each concentration. After agitation, the sample solution was filtered through a 0.2 µm membrane filter (HP020AN, Advantec, Tokyo, Japan), and the arsenic concentration in the filtrate was analyzed using inductively coupled plasma mass spectrometry (ICP-MS) (Agilent 8800, Agilent Technologies, Inc., California, USA). The pH of the filtered solution was measured with a pH meter (LAQUAtwin AS-712, HORIBA, Kyoto, Japan). The adsorption amount of arsenic ions per gram of SFM05905 was calculated using the equation (1).

$$W_g = V\,(C_0 - C_t)/w \qquad (1)$$

Where,

W_g: Adsorption amount per 1 g of SFM05905 (mg/g);
C_0: Initial concentration (mg/L);
C_t: Concentration in sample water after t hours of shaking (mg/L);
V: water volume of the sample (L);
w: Added quantity of SFM05905 (g).

Adsorption isotherms for both As (III) and As(V) were constructed at each temperature, and the effects of temperature, equilibrium time, and adsorption amounts of As(V) and As (III) were thoroughly investigated.

Table 1: Experimental conditions for Batch test of arsenic adsorption.

As species	**Initial concentration (mg /L)**	**Sample volume (mL)**	**Material addition (w/v) %**	**Initial pH**	**Rotational Speed (rpm)**	**Time Intervals (hr.)**	**Temperature intervals (^{0}C)**
As(III) As(V)	10,20,50,100,150.	30	0.5%	6.8	100 max.	0,6,12,18,24	25,35, 45

4.4.2 Evaluation by adsorption isotherm.:

Adsorption isotherms for both As (III) and As(V) were measured at three temperatures (25°C, 35°C, and 45°C), as shown in Figure 6. The adsorption amounts of As (III) and As(V) on SFM05905 reached approximately 25 mg g^{-1} at equilibrium concentrations of less than 2.5 mg L^{-1} and 25 mg L^{-1}, respectively. Comparatively, in a previous study (Kuwabara et al., 2007), the adsorption capacity of As (III) on SFM118 was 10 mg g^{-1} at an equilibrium concentration of 1.3 mg L^{-1}, and As(V) adsorption reached 15 mg/g at an equilibrium concentration of 24 mg L^{-1}. These findings highlight a significant improvement in the adsorption capacities of SFM05905, which has a higher Fe content, compared to SFM118.

To further analyze these results, both the Langmuir and Freundlich models (Langmuir et al., 1916), (Freundlich et al., 1906) were applied to describe the adsorption isotherms. The Freundlich equation (2) is expressed as:

$$q_e = k_F Ce^{1/n} \qquad (2)$$

where q_e is the amount of arsenic adsorbed on the solid phase (mg g^{-1}), Ce is the equilibrium concentration of arsenic in the solution (mg L^{-1}), k_F represents the adsorption capacity (mg g^{-1}), and n is the heterogeneity factor, which decreases as surface heterogeneity increases.

The Langmuir model, initially developed for gas adsorption on solid surfaces (Langmuir et al., 1916), is based on the following assumptions: (1) a fixed number of accessible sites with identical energy levels exist on the adsorbent surface; (2) adsorption is reversible; (3) once an adsorbate occupies a site, no further adsorption occurs at that site; and (4) no interaction occurs between adsorbate molecules. The Langmuir equation (3) is given by:

$$q_e = \frac{q_m k_L C_e}{(1+k_L C_e)} \qquad (3)$$

Where q_e and C_e are as previously denoted, K_L is the equilibrium adsorption constant related to the affinity of binding sites (mg L^{-1}) and q_m is the maximum amount of the arsenic per unit weight of adsorbent for complete monolayer coverage. The Langmuir model is often linearized into different forms for parameter estimation, including:

Hanes-Woolf linearization:

$$\frac{\mathrm{Ce}}{\mathrm{qe}} = (\frac{1}{\mathrm{qmax}})\ \mathrm{Ce} + \frac{1}{\mathrm{qmaxKL}} \tag{4}$$

Lineweaver-Burk linearization:

$$\frac{1}{\mathrm{qe}} = (\frac{1}{\mathrm{qmaxKL}})\frac{1}{\mathrm{Ce}} + \frac{1}{\mathrm{qmax}} \tag{5}$$

Eadie-Hofstee linearization:

$$q_e = (-\frac{1}{\mathrm{KL}})\frac{\mathrm{qe}}{\mathrm{Ce}} + \mathrm{qmax} \tag{6}$$

Scatchard linearization:

$$\frac{qe}{Ce} = -K_L\ q_e + q_{max}\ K_L \tag{7}$$

In these equations qmax (mg g^{-1}) is the maximum saturated monolayer adsorption capacity of an adsorbent, Ce (mg L^{-1}) is the adsorbate concentration at equilibrium, qe (mg g^{-1}) is the amount of adsorbate uptake at equilibrium, and K_L (mg L^{-1}) is a constant related to the affinity between an adsorbent and adsorbate. For a good adsorbent, a high theoretical adsorption capacity qmax and a steep initial sorption isotherm slope (i.e., high K_L) are generally desirable (Paritam et al.,2017, Mólgora et al.,2013). However, the limitations of using these linear forms of the Langmuir model have been identified in previous studies (Bien et al.,2019), which emphasize potential errors in parameter estimation due to assumptions and data transformations. The adsorption isotherms and their linearized expression of SFM05905 shows in Table 2.

Table 2: Adsorption Isotherms and their linearized expressions of SFM05905.

Isotherm	Equations	Linear expressions	Parameter
Freundlich	$q_e = ln\, k_F(c_e)\left(\frac{1}{n}\right)$	$lnqe = lnKF + 1/n\ lnCe$	K_F =exp(intercept), n=1/(slope)
Langmuir	$q_e = \frac{q_m k_L C_e}{(1 + k_L C_e)}$	$C_e/q_e=(1/K_Lq_m) + (C_e/q_m)$	q_m=1/(slope), K_L=slope/(intercept)

4.5 Result and discussion

This chapter presents the experimental results and an in-depth discussion of the adsorption properties of SFM05905, specifically focusing on its metal composition, structural analysis, and adsorption behavior. The goal was to assess the material's efficacy for arsenic removal, thermodynamic parameters, and temperature effects. The data obtained from XRD, TG-DTA, and adsorption experiments are analyzed to highlight the relationship between SFM05905's composition and its performance in arsenic removal.

4.5.1 Metal elements composition ratio of powder SFM05905.:

The metal composition ratio of powder SFM05905 was 0.048 Si:0.907Fe:0.046Mg which is shown in Table 3**.** The metal element composition ratio of powder SFM05905 was the same as the prepared solution of dissolving reagents during the synthesis of SFM05905. The Si, Fe and Mg content of the powder SFM05905 was 0.533 mmol g^{-1}, 10.514 mmol g^{-1} and 0.530 mmol g^{-1}. Thus, the specific gravity of the powder SFM05905 was 3.81g cm^{-3}.

Table 3: The metal element composition ratio of the powder

SFM05905 Powder					
Target Composition ratio	Si (mol/g)	Fe (mol/g)	Mg (mol/g)	Obtained Composition ratio	Specific gravity (g/cm^3)
SFM05905 = (Si: Fe: Mg) = (0.05:0.9:005)	0.533	10.514	0.530	0.048 Si:0.907Fe:0.046Mg	3.81

4.5.2 XRD and TG-DTA analysis of powder SFM05905.

SFM05905 was analysed by XRD to assess the physicochemical characteristics of the materials. XRD patterns of the powder SFM05905 are shown in Figure 3**.** The XRD patterns of SFM05905 was not specific and no diffraction peaks. In a previous report, based on the X-ray diffraction results, layered double hydroxide peaks were clearly detected in the SFM samples with a small

Fe/Mg ratio such as SFM118, but when the Fe/Mg ratio increased, the specific peaks were could not be observed (Kuwabara et al., 2007). It was also shown that the main component of SFM010 synthesized using only Fe was α-FeOOH (Goethite). Therefore, main component of SFM05905 was assumed amorphous Fe hydrous oxide. Using a Thermo gravimetric differential thermal component analyzer (ThermoPlus TG8120, Rigaku, Tokyo, Japan) under a nitrogen atmosphere (200 mL/min) and a heating rate of 10 °C/min, the thermal properties of SFM05905 were examined over a temperature range of 25-1000 °C. Figure 4 presents the TG-DTA curves of SFM05905 with Al_2O_3 powder as a reference material. The DTA curve indicated an endothermic peak at around 100°C, which was attributed to dehydration, while the TG curve showed a gradual decrease in weight loss up to 400°C, also due to dehydration. These results are in line with previous studies (Kuwabara et al., 2007) and suggest that the endothermic peaks in the DTA curve are related to the dehydration process, which may be responsible for the lack of a layer structure in SFM05905.

4.5.3 Adsorption Isotherm of powder SFM05905:

Adsorption isotherms were generated to examine the adsorption of As(III) and As(V) on SFM05905 at various initial concentrations (10~150 mg L^{-1}) and temperatures (25°C, 35°C, and 45°C). The equilibrium concentration of SFM05905 was found to be in the range of 2-5 mg L^{-1}, and the adsorption capacity was observed to be approximately 20-25 mg $g^{-1}$for both As(III) and As(V) at temperatures between 25°C to 45°C, as shown in Figure 6. The adsorption behavior of SFM05905 was analyzed using adsorption isotherm curves with respect to concentrations ranging from 10 to 150 ppm. The distribution of molecules between the liquid and solid phases at equilibrium state was considered as a fundamental factor in determining the sorption capacity (Padmavathy et al., 2008). The experimental data obtained for As(V) were reasonably well described by the Freundlich model.

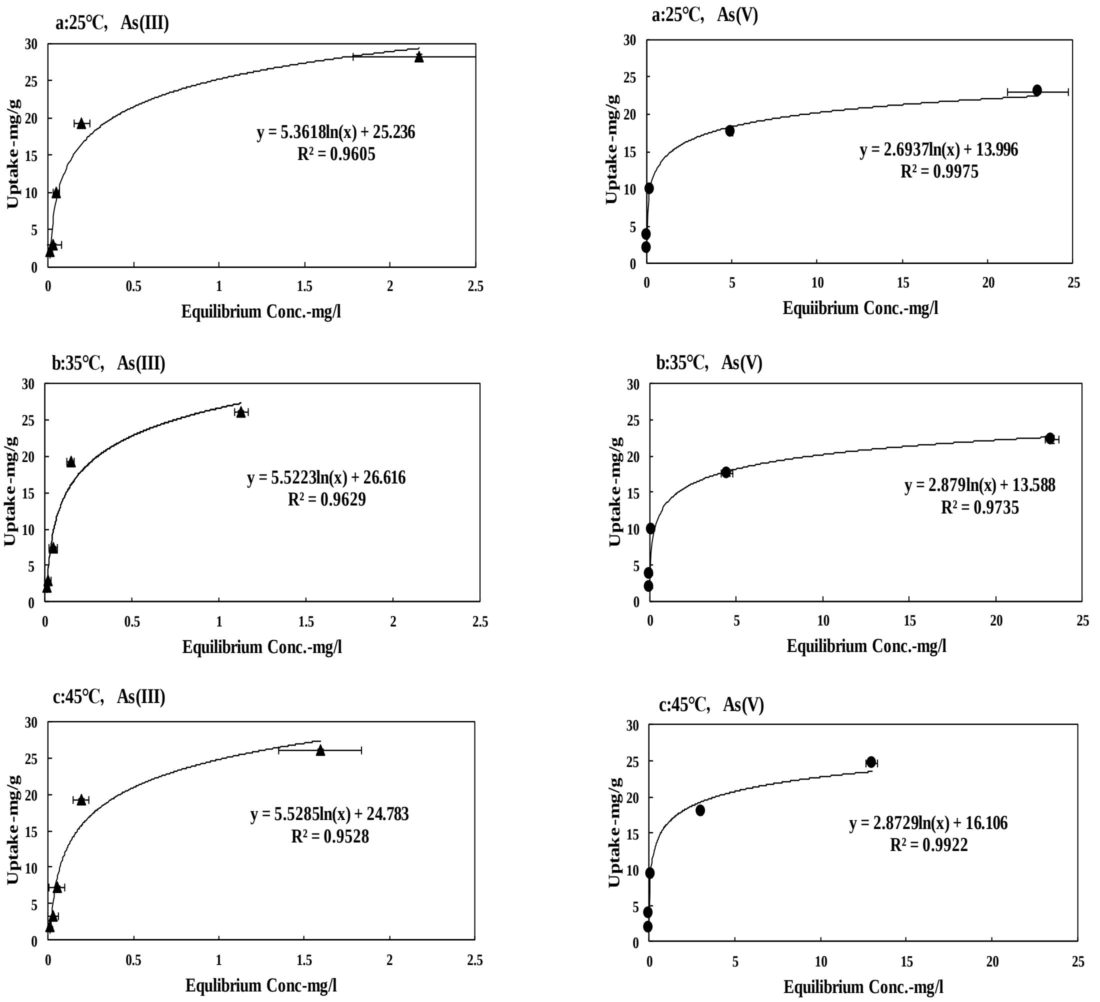

Figure 6: Changes in the adsorption amount of As (III) and As(V) at various temperatures (25℃, 35℃, and 45℃) for concentrations ranging from 10-150 mg L−1. ※ Error bars in the figure indicate the standard deviation of the data.

The value of 1/n in the Freundlich equation for arsenic was found to be 0.5 or less, indicating a high affinity of arsenic for SFM05905. Figure 7 shows that As(V) exhibited a high affinity (1/n < 0.5) for SFM05905, with adsorption ability demonstrated over a wide range of concentrations and little effect of concentration. However, As(III) exhibited low affinity (1/n > 0.5), with adsorption ability depending on concentration and increasing at higher concentrations. However, low uptake was observed at low concentrations. Therefore, the Langmuir model was employed to describe the adsorption behavior of arsenic by SFM05905, as it provided the best correlation coefficient (R^2). However, the Langmuir isotherm failed to describe the adsorption behavior due to the amorphous nature of the material and the assumption that adsorption occurs on a homogeneous surface (Langmuir et al. 1916). The Langmuir adsorption capacities for As(III) and As(V) were calculated to be 31.948 mg/g and 24.451 mg/g, respectively, with the highest correlation coefficient [As(V)-(R^2 = 0.998), As(III)-(R^2=0.981)] , as shown in Table 4. As shown in Figure 8, an increase in temperature resulted in a decrease in saturation values (q_m) for As(III), whereas saturation values (q_m) for As(V) was not affected by temperature, with only a slight change observed at 45°C. Therefore, it can be concluded that the temperature did not affect the adsorption of arsenic by SFM05905 for both As(V) and As(III) removal.

Table 4: Arsenic adsorption parameter through Freundlich and Langmuir isotherm and their respective parameters.

Arsenic species		**Freundlich model**			**Langmuir model**		
As (III)	Temperature	K_F(mg/g)	1/n	R^2	K_L(L/mg)	q_m (mg/g)	R^2
	25°C	9.157	0.644	0.709	5.782	31.948	0.989
	35°C	14.277	0.751	0.818	4.575	29.815	0.926
	45°C	10.585	0.684	0.857	5.160	30.377	0.981
As (V)	25°C	9.477	0.296	0.928	1.834	21.673	0.996
	35°C	9.609	0.306	0.841	2.218	21.711	0.997
	45°C	12.284	0.301	0.936	2.539	24.451	0.998

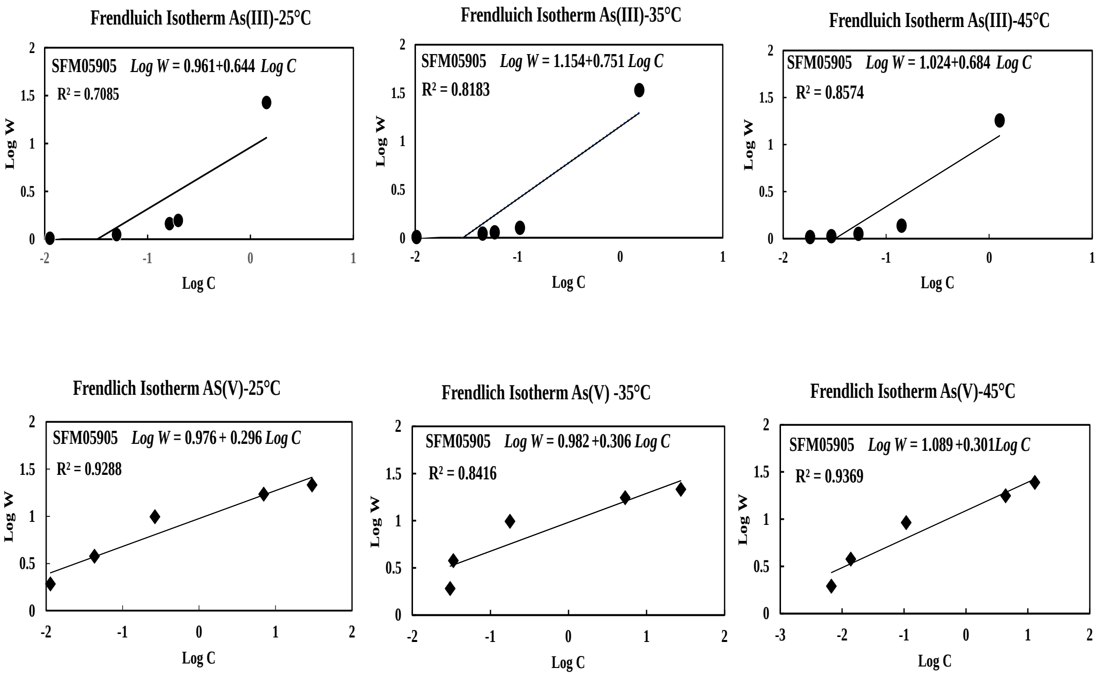

Figure 7: Freundlich isotherm of SFM05905 on As (III) and As(V).

The Langmuir model was employed to describe arsenic adsorption by SFM05905, and while its fit, as indicated by the correlation coefficient (R^2), is recognized, its limitations for amorphous materials and its assumption of adsorption on a homogeneous surface should be noted (Frsc et al., 2005). The capacity of the Langmuir isotherm for pattern recognition is also discussed, with Equation (11) evaluated for its fit to modified Langmuir isotherms:

$$\frac{\mathrm{Ce}}{\mathrm{Wg}} = \left(\frac{1}{\alpha \mathrm{qm}}\right) + \left(\frac{1}{\mathrm{qm}}\right)\mathrm{c} \qquad (11)$$

where C_e is the equilibrium adsorption concentration (mg L^{-1}), W_g is the adsorption amount per 1 g of SFM05905 (mg g^{-1}), q_m is is the maximum amount of the arsenic per unit weight of adsorbent for complete monolayer coverage (mg g^{-1}).

Table 4 presents the Langmuir adsorption capacities for As(III) ranging from 30 to 32 mg g^{-1}, and for As(V) between 21 to 24 mg g^{-1}, with respective correlation coefficients. However, when examining maximum adsorption capacities for As(III), the trend follows: at 25°C (31.948 mg g^{-1}) > 45°C (30.377 mg g^{-1}) > 35°C (29.815 mg g^{-1}) at 100 rpm. For As(V), the order is: at 25°C (21.673 mg g^{-1}) > 35°C (21.711 mg g^{-1}) > 45°C (24.451 mg g^{-1}) at 100 rpm. This variation is likely due to the adsorption process nearing equilibrium at different temperatures, particularly at lower concentrations. Recent findings have raised questions about the effects of agitation rates on adsorption capacity. For example, (Chu et al., 2005) demonstrated that the adsorption capacity of vitamin E onto silica varied with agitation rate, while (Ming-Cheng et al., 2005) observed that agitation rate primarily influenced the speed at which equilibrium was achieved rather than the equilibrium state itself.

In Figure 8, increasing the temperature for As(III) resulted in a decrease in the saturation value (q_m), while for As(V), it remained relatively stable, with minor fluctuations at 45°C. Thermodynamic parameters (ΔG°, ΔH°, ΔS°) of SFM05905 were investigated between 25–45°C for both As(III) and As(V), but due to time-dependence and comparison constraints, a full kinetic analysis of thermodynamic parameters was not feasible. Consequently, only experimental data were compared with adsorption isotherms, Freundlich constant (K_F), and Langmuir constant (K_L). In conclusion, temperature did not significantly influence the adsorption behavior of SFM05905 for the removal of both As(III) and As(V).

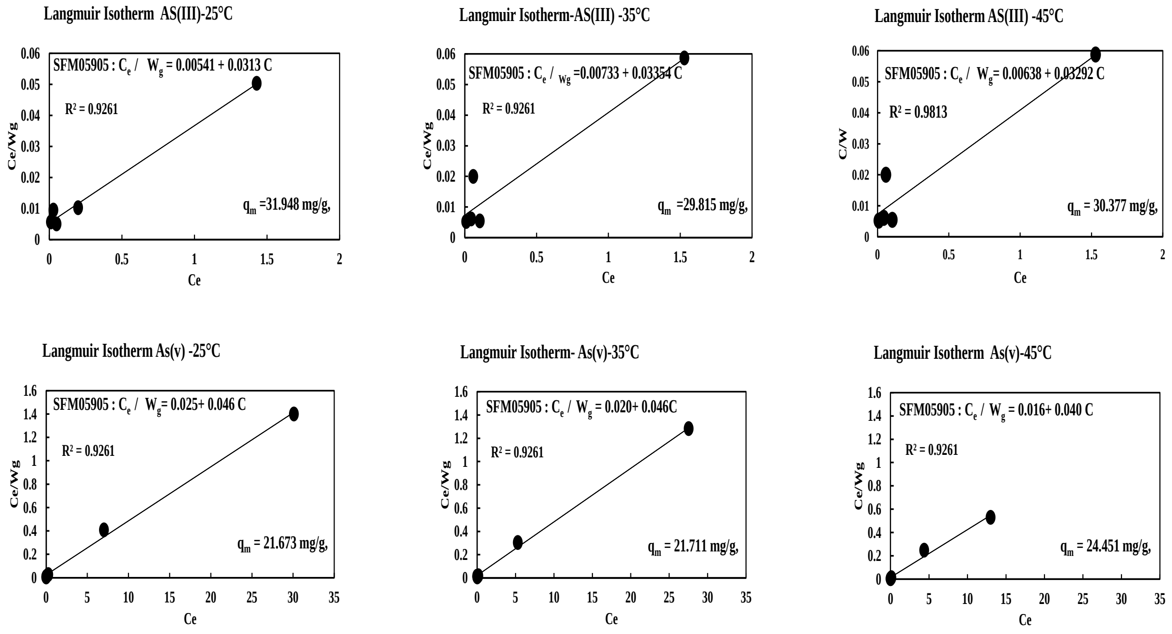

Figure 8: Langmuir isotherm of SFM05905 on As (III) and As(V).

4.6 Adsorption of anion selectivity for SFM05905.

The adsorption capacity of SFM05905 for arsenic was evaluated using single element samples, as presented in Table 5. The results indicated that SFM05905 exhibited higher anion selectivity for As (III) and PO_4 ions compared to As(V) ion. The selectivity for SO_4, F, NO_3, and CO_3 ions was found to be lower and different from that of arsenic. These ions were observed to have a minimal effect on the arsenic adsorption. PO_4 ion, which behaves chemically similar to arsenite ion, was considered to inhibit the adsorption. Therefore, the selectivity ratio of each anion was calculated based on the highest selectivity of arsenite and phosphate ion.

Table 5: Distribution coefficient (Kd) and adsorption amount (mmol. g^{-1}) of SFM05905 using Single anions.

Kd	**SFM05905**
As (III)	539,000
As(V)	158,000
PO_4	531,000
SO_4	300
F	400
NO_3	200
CO_3	<1

Table 6 shows the variation of the distribution coefficient (kd) for As (III) and As(V) in binary conditions with PO_4. The distribution coefficient value increased for both As (III) and As(V) in the presence of PO_4. However, As(V) exhibited a lower kd value compared to As(III).

Table 6: Distribution coefficient (Kd) and adsorption amount (mmol. g^{-1}) of SFM05905 using binary and tertiary anions.

Kd	**SFM05905**			
	As (III)+PO_4	**As(V)+PO_4**	**AS(III)+ AS(V)**	**AS(III) + AS(V) +PO_4**
As(III)	122,000	-	42,700	122,000
As(V)	-	36,600	31,200	16,800
PO_4	7,040	8,870	-	5,030

The anion selectivity of SFM05905 was found to have a significant effect on the adsorption of arsenic in both single and mixed conditions. In the tertiary system, the distribution coefficient (kd) value of PO_4 was lower than that of As (III) and As(V), indicating that [As (III)+PO_4] had a higher affinity than [As(V) +PO_4]. Therefore, it was observed that the anion selectivity of PO_4 differed greatly between single and mixed conditions of the SFM05905 adsorbent.

4.7 Time dependent variation of arsenic removal from chloride concentration with SFM05905.:

In this study, the initial concentration was adjusted using 0.1M HCl, making it difficult to estimate the chloride concentration from the solid materials, as discussed in Figure 9. Due to the small amount of chloride concentration obtained from the extraction, it was necessary to measure the equilibrium constant (Kd). The data obtained from this experiment was time-dependent and compared the adsorption of As (III) and As(V). However, it was not possible to determine the kinetic analysis with thermodynamic parameters due to the equilibrium constant, which reacts directly with Gibbs free energy ($\Delta G° = - RTInK$). Therefore, only experimental data can be compared with adsorption isotherm, Freundlich constant (K_F), and Langmuir constant (K_L).

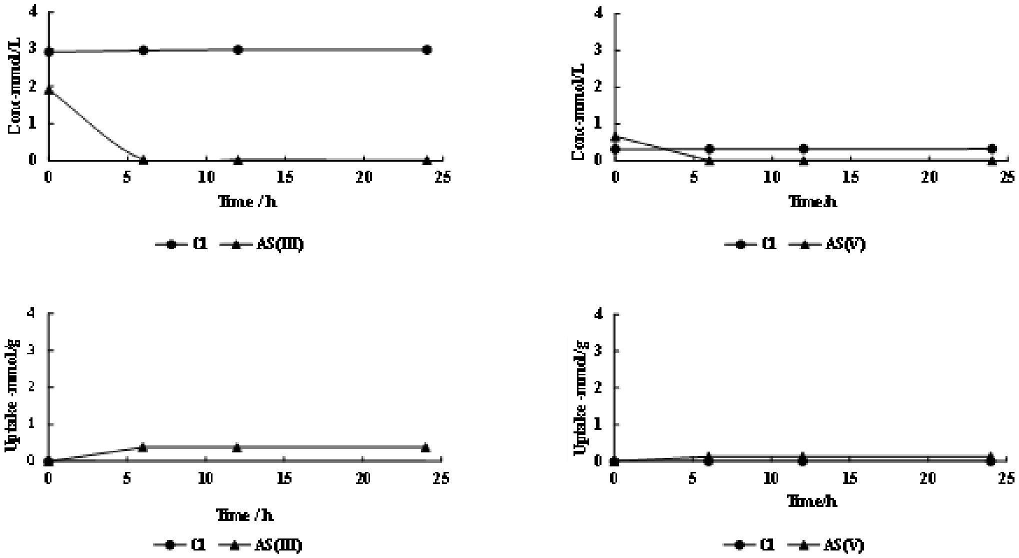

Figure 9: Illustrates the time-dependencies variation of chloride ion from aqueous solutions using SFM05905.

4.8 Effect of temperature on the adsorption.

The effect of temperature on the adsorption of arsenic ion on SFM05905 was investigated at various temperatures ranging from 25-45°C, as presented in Figure 10. The results revealed that as the temperature increased, the arsenic ion removal and adsorption capacity also increased up to a certain point, beyond which there was no significant impact on the adsorption process. A rapid adsorption stage was observed within 12-24 h of contact time at different temperatures, after which adsorption reached equilibrium. Notably, the time required to reach the adsorption equilibrium was unaffected by the increase in temperature from 25-45°C. The increase in temperature provides enough energy to overcome the resisting hydration energy acting on diffusion metal ions and thereby increases the mobility of the metal ion towards the adsorbent surface. However, the slight change in saturation values (q_e) (23.0-23.6 mg g^{-1}) observed for SFM05905 in the tested temperature range indicated a non-significant influence of temperature rise on the adsorption removal of arsenic ions (Itsuki et al., 2024).

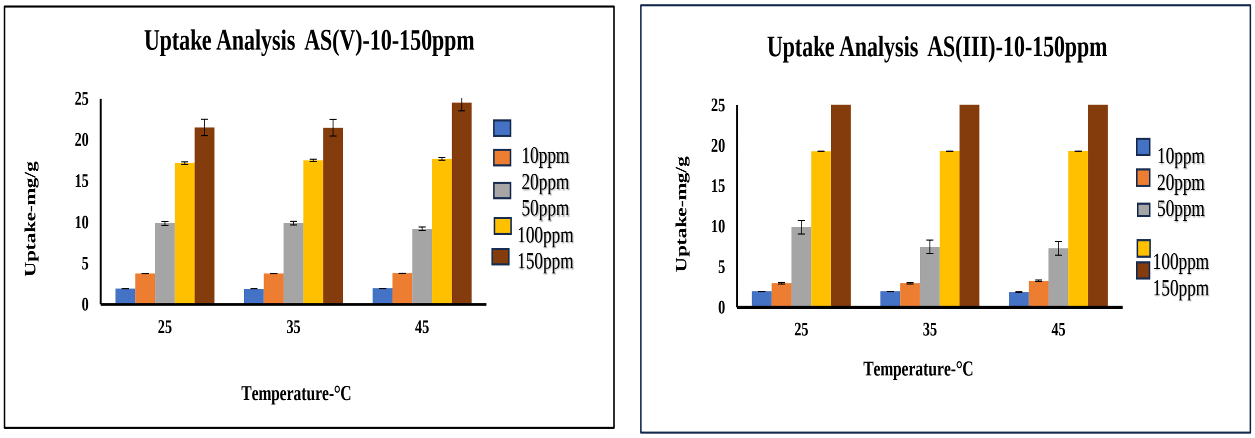

Figure 10: Effect of temperatures and adsorption capacity by using SFM05905.

4.9 Adsorption Thermodynamics.

Thermodynamic parameters for SFM05905 adsorption were determined by evaluating the Gibbs free energy change (ΔG°), enthalpy change (ΔH°), and entropy change (ΔS°) using equations (8) and (9). The values of ΔH° and ΔS° were calculated from the slope and intercept of the lnK versus 1/T plot. These values can be expressed in the following equation:

$$\Delta G^\circ = - RTInk, \tag{8}$$

$$\Delta G^\circ = \Delta H^\circ - T\Delta S^\circ \tag{9}$$

Here, ΔG° is measured in kJ/mol, ΔH° and ΔS° are the changes in enthalpy and entropy, respectively, also in kJ/mol. The temperature (T) is expressed in Kelvin, and R represents the gas constant (8.314×10−3 kJ/mol·K). The equilibrium constant (K) is obtained from experimental data, specifically from the slope and intercept of the plot of ln K versus 1/T. The thermodynamic parameters for the adsorption of SFM05905 are summarized in Table 7.

Table 7: Thermodynamics parameter of AS(v) AND As(iii) ion adsorption on SFM05905.

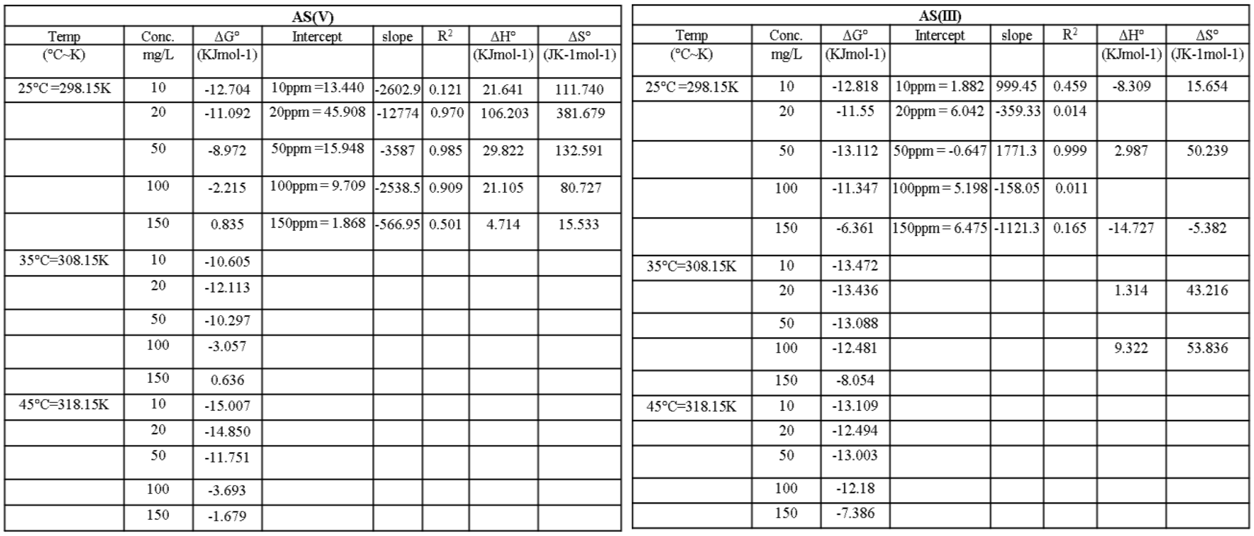

AS(V)

Temp (°C~K)	Conc. mg/L	ΔG° (KJmol-1)	Intercept	slope	R^2	ΔH° (KJmol-1)	ΔS° (JK-1mol-1)
25°C =298.15K	10	-12.704	10ppm =13.440	-2602.9	0.121	21.641	111.740
	20	-11.092	20ppm = 45.908	-12774	0.970	106.203	381.679
	50	-8.972	50ppm =15.948	-3587	0.985	29.822	132.591
	100	-2.215	100ppm = 9.709	-2538.5	0.909	21.105	80.727
	150	0.835	150ppm = 1.868	-566.95	0.501	4.714	15.533
35°C=308.15K	10	-10.605					
	20	-12.113					
	50	-10.297					
	100	-3.057					
	150	0.636					
45°C=318.15K	10	-15.007					
	20	-14.850					
	50	-11.751					
	100	-3.693					
	150	-1.679					

AS(III)

Temp (°C~K)	Conc. mg/L	ΔG° (KJmol-1)	Intercept	slope	R^2	ΔH° (KJmol-1)	ΔS° (JK-1mol-1)
25°C =298.15K	10	-12.818	10ppm = 1.882	999.45	0.459	-8.309	15.654
	20	-11.55	20ppm = 6.042	-359.33	0.014		
	50	-13.112	50ppm = -0.647	1771.3	0.999	2.987	50.239
	100	-11.347	100ppm = 5.198	-158.05	0.011		
	150	-6.361	150ppm = 6.475	-1121.3	0.165	-14.727	-5.382
35°C=308.15K	10	-13.472					
	20	-13.436				1.314	43.216
	50	-13.088					
	100	-12.481				9.322	53.836
	150	-8.054					
45°C=318.15K	10	-13.109					
	20	-12.494					
	50	-13.003					
	100	-12.18					
	150	-7.386					

To determine the thermochemical parameters ΔH and ΔS, van't Hoff's plot was utilized by applying the concept that the Gibbs free energy is the product of the difference between the adsorption enthalpy and adsorption entropy with the temperature.

$$\ln K = -\Delta H^\circ/RT + \Delta S/R \tag{10}$$

Equation (10) was used to construct the plot, where lnK is plotted against 1/T, and the slope and intercept were used to calculate ΔH° and ΔS°, respectively. The universal gas constant R (8.314 J mol−1 K−1) and T (K) were also used in the equation.

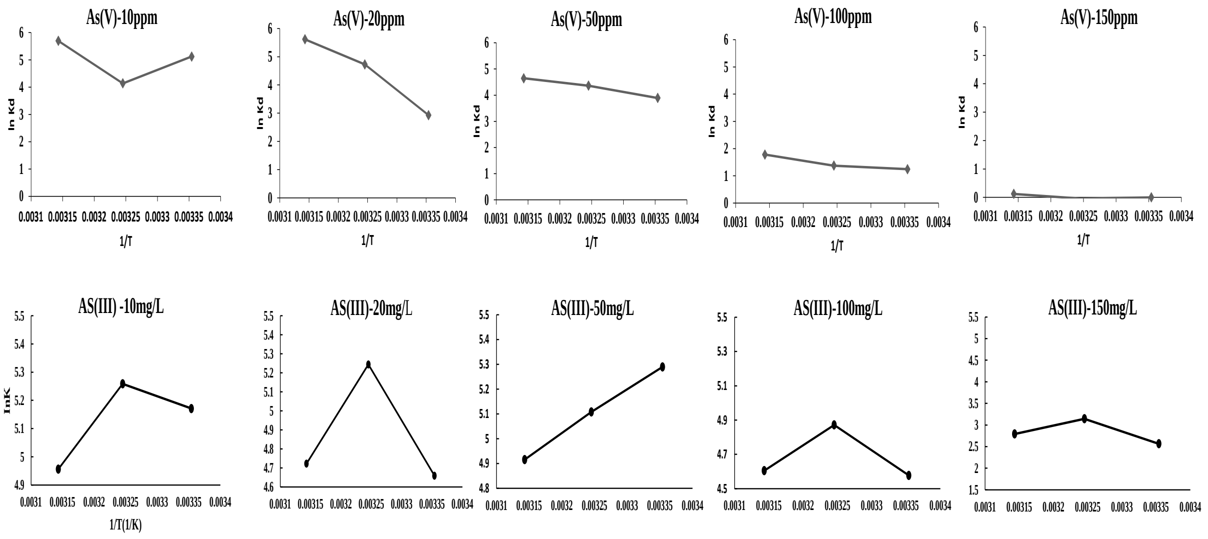

Figure 11: Van’t Hoff plot for the AS(V) and As(III) adsorption by using of SFM05905.

In Figure 11, the Van't Hoff plot is shown with a correlation coefficient (R^2) of 0.99, demonstrating a strong fit with the experimental data. The calculated Gibbs free energy (ΔG) values ranged from -15.6 to 1.0 kJ mol^{-1}, indicating that the adsorption process is spontaneous but becomes less favorable at higher temperatures. This trend suggests that, as temperature increases, the adsorption rate decreases, a finding consistent with previous studies (Paritam et al., 2004).

The enthalpy change (ΔH) of -112.7 kJ mol^{-1} confirms the exothermic nature of the adsorption process observed that such enthalpy values, ranging between -40 and -800 kJ mol^{-1}, are typical of chemical adsorption. The negative entropy change (ΔS = -0.338 kJ mol^{-1} K^{-1}) indicates decreased randomness at the solid-liquid interface during adsorption.

Therefore, the negative ΔH and ΔS values suggest that enthalpy plays a dominant role in the process, contributing to the observed negative ΔG values, which are in line with previous thermodynamic studies on adsorption processes, including for arsenic adsorption with SFM05905.

Table 8: Isotherm parameters for removal of SFM05905.

SFM05905 Powder							
As(V)				**As (III)**			
Langmuir isotherm				**Langmuir isotherm**			
	298.15K	**308.15K**	**318.15K**		**298.15K**	**308.15K**	**318.15K**
K_L x10^{-4} (L mol-1)	**0.024**	**0.029**	**0.033**	**K_L x10^{-4} (L mol-1)**	**0.077**	**0.061**	**0.068**
q_m x10^{6} (mol g-1)	**0.2893**	**0.2898**	**0.326**	**q_m x10^{6} (mol g-1)**	**0.426**	**0.397**	**0.405**
R^2	**0.996**	**0.997**	**0.998**	**R^2**	**0.989**	**0.926**	**0.981**
Freundlich isotherm				**Freundlich isotherm**			
K_F x10^{2} ((mol g-1) (mol L-1)$^{-1/n}$	**0.126**	**0.128**	**0.163**	**K_F x10^{2} ((mol g-1) (mol L-1)$^{-1/n}$**	**0.122**	**0.190**	**0.141**
1/n	**0.296**	**0.306**	**0.301**	**1/n**	**0.644**	**0.751**	**0.684**
R^2	**0.928**	**0.841**	**0.936**	**R^2**	**0.709**	**0.818**	**0.857**

As shown in Table 8, the Langmuir isotherm for AS(V) exhibited the best correlation coefficients in the order of 318.15K > 308.15K > 298.15K, whereas for AS(III), the best correlation coefficients were observed at 298.15K > 318.15K > 308.15K. Furthermore, the Langmuir saturation values (q_m) for AS(V) were found to be in the order of 318.15K > 308.15K > 298.15K, while for AS(III), they were in the order of 298.15K > 318.15K > 308.15K. The results suggest that the interaction between SFM05905 and arsenic is more prominent in this temperature range due to the presence of a higher number of exposed adsorption sites. However, at higher temperatures, the physical interaction between SFM05905 and arsenic weakens due to the weakening of hydrogen bonds and van der Waal interactions, as observed in the adsorption of Congo Red by chitosan hydro beads (Dinesh et al., 2007). Additionally, the K_L parameter of the Langmuir model indicates that monolayer saturation values (q_m) were achieved at higher equilibrium concentrations (C_e), suggesting higher adsorption intensity (1/n) values of the Freundlich isotherm model for AS(III) at lower temperatures, consistent with previous studies by (Itsuki et al. (2024), and Freundlich et al. (1906).

4.10 Conclusion

This study aimed to evaluate the efficacy of SFM05905 as an adsorbent for the removal of arsenic species (As(III) and As(V)) from aqueous solutions. Arsenic contamination in water is a significant environmental and public health issue, particularly in areas where industrial processes and natural sources contribute to elevated arsenic levels. This research explored the adsorption capacity of SFM05905 under various experimental conditions, including different concentrations and temperatures. By assessing both the physical and chemical properties of SFM05905, this study aimed to provide valuable insights into its potential application in water treatment systems.

Summary of Key Findings

1. **Adsorption Capacity:** The adsorption capacity of SFM05905 for As(III) and As(V) was determined to be 30 mg/g and 25 mg/g, respectively, at temperatures between 25°C and 45°C. The results showed that the adsorption increased with increasing equilibrium concentration, regardless of temperature. Notably, the initial concentration of arsenic in the solution played a critical role in modifying the adsorption capacity.
2. **Effect of Temperature on Adsorption**: The adsorption capacity of SFM05905 showed a consistent trend across a wide range of temperatures. Although temperature changes did not significantly affect the saturation values, the adsorption process was found to be spontaneous, as evidenced by the negative Gibbs free energy ($\Delta G°$) values.
3. **Structural and Physical Characterization**: X-ray diffraction (XRD) analysis revealed that SFM05905 composites primarily consisted of iron (Fe) and exhibited an amorphous structure. The silica and magnesium content in the composites was low, suggesting that the material's adsorption capacity is primarily influenced by iron-based functional groups.
4. **Thermogravimetric Analysis (TGA):** Thermogravimetric analysis (TGA) confirmed that SFM05905 exhibited a single-layer structure and an amorphous nature. This characteristic is beneficial for adsorption because it allows for greater surface area and more available binding sites for arsenic ions.
5. **Modeling the Adsorption Process**: The Langmuir adsorption isotherm model best fitted the experimental data, showing maximum adsorption capacities of 31.948 mg/g for As(III) and 24.451 mg/g for As(V). The high correlation coefficients demonstrated that

SFM05905 follows monolayer adsorption. Additionally, the Freundlich model indicated that the material has a high affinity for arsenic ions, and adsorption is favored at lower concentrations with a preference for high-affinity sites.

6. **Thermodynamic Considerations**: Thermodynamic parameters indicated that the adsorption process is spontaneous, with the negative values of $\Delta G°$ confirming that arsenic removal by SFM05905 is a thermodynamically favorable reaction. This enhances the material's potential for real-world applications in arsenic-contaminated water treatment.

Implications for Water Treatment

The findings of this study suggest that SFM05905 has significant potential as an adsorbent material for the removal of arsenic from wastewater. Its high adsorption capacity, along with its thermodynamically favorable properties, indicates that it could be an effective solution for addressing arsenic contamination in both drinking water and industrial wastewater. Furthermore, the simplicity of the adsorption process and the material's stability under varying conditions make it a promising candidate for large-scale applications in environmental remediation.

Given its amorphous structure and iron-rich composition, SFM05905 has the potential to outperform traditional adsorbents in terms of both efficiency and cost-effectiveness. This makes it a viable option for use in regions where access to clean water is limited due to high arsenic concentrations.

Limitations and Areas for Future Research

While SFM05905 shows considerable promise, several factors require further investigation. Future studies should explore the following:

- **Long-Term Stability and Regeneration**: The long-term stability of SFM05905 under repeated adsorption cycles should be assessed. Additionally, research into the regeneration and reuse of the adsorbent could enhance its sustainability and reduce operational costs.

- **Effect of Coexisting Contaminants:** The presence of other ions or contaminants in wastewater may impact the adsorption efficiency of SFM05905. Investigating the material's performance in complex water matrices, such as those with competing ions (e.g., sulfate, chloride), is essential for understanding its behavior in real-world conditions.
- **Field-Scale Applications:** Scale-up studies are necessary to evaluate the practical feasibility of using SFM05905 in large-scale water treatment systems. This includes assessing its performance in different water sources and optimizing the adsorption process for industrial and municipal applications.
- **Environmental Impact Assessment**: An assessment of the environmental impact of using SFM05905 in water treatment should be conducted, including any potential leaching of harmful components and the ecological impact of waste disposal from spent adsorbents.

In conclusion, SFM05905 proves to be a highly effective adsorbent for the removal of arsenic from wastewater, with favorable adsorption characteristics and thermodynamic properties. The material demonstrated a high adsorption capacity, particularly for As(III), and performed well across a range of temperatures and concentrations. Its structure and composition were found to be conducive to arsenic ion removal, and the findings suggest its potential for large-scale application in arsenic remediation.

While the results of this study highlight the potential of SFM05905, further research is needed to explore its long-term effectiveness, regeneration potential, and real-world applications. Nonetheless, this study contributes significantly to the field of water treatment, offering a promising solution to address the pressing issue of arsenic contamination in wastewater.

4.11 References

1. Ali Basem, Dheyaa J. Jasim, Hasan Sh Majdi, Rawaa M. Mohammed, Mohsen Ahmed, Ameer H. Al-Rubaye, Ehsan kianfar, (2024). Adsorption of heavy metals from wastewater by chitosan: A review, *Results in Engineering*, ,23,102404. https://doi.org/10.1016/j.rineng.2024.102404.

2. Centeno JA, M. F. (2002). Pathology related to chronic arsenic exposure. *Environ Health Perspect.*, 883-6. https://doi.org/10.1289/ehp.02110s5883.

3. Paritam K. Dutta, Ajay K. Ray, Virender K. Sharma, Frank J. Millero, (2004). Adsorption of arsenate and arsenite on titanium dioxide suspensions. *Journal of Colloid and Interface Science*, 278(2), 270-275. https://doi.org/10.1016/j.jcis.2004.06.015.

4. Bien, N. Q., & Ha, N. T. H. (2019). Adsorption of arsenic and heavy metals from solutions by modified iron ore sludge. *Vietnam Journal of Earth Sciences*, 41(3), 259–271. https://doi.org/10.15625/0866-7187/41/3/13947.

5. Grégorio Crini, (2006). Non-conventional low-cost adsorbents for dye removal: A review, *Bioresource Technology*, 97(9), 1061-1085. https://doi.org/10.1016/j.biortech.2005.05.001.

6. Freundlich, H. (1906). Over the Adsorption in Solution. *The Journal of Physical Chemistry*., 57, 385-471.

7. World Health Organization. (2011). Guidelines for Drinking-water Quality. *World Health Organization (WHO)*, WHO 178. Retrieved from https://bit.ly/3fLo0li.

8. Mólgora, C. C., Domínguez, A. M., Avila, E. M., Drogui, P., & Buelna, G. (2013). Removal of arsenic from drinking water: A comparative study between electrocoagulation-microfiltration and chemical coagulation-microfiltration processes,

Sep. Purif. Technol, 118, 645-651. https://doi.org/10.1016/j.seppur.2013.08.011.

9. Cui, J., Jing, C., Che, D., Zhang, J., & Duan, S. (2015). Groundwater arsenic removal by coagulation using ferric (III) sulfate and polyferric sulfate: A comparative and mechanistic study, *J. Environ. Sci.*, 32, 42-53. https://doi.org/10.1016/j.jes.2014.10.020.

10. Kuwabara, T., Kimura, H, Sunayama, S., (2007). Removal Characteristics of Phosphate and Nitrate Ions with an Mg-Fe-Al-Cl Form Hydrotalcite. *Journal of the Society of Inorganic Materials, Japan,* 14(326),17-25.

11. Kuwabara, T., Arakawa, K., Sato, T., Onodera, Y. (2007). Adsorption Properties of Synthetic Si-Fe-Mg Mixed Hydrous Oxides. *Journal of Japan Society on Water Environment* 30(3):133-138. https://doi.org/ 10.2965/jswe.30.133.

12. Langmuir, I. (1916). The Constitution and Fundamental Properties of Solids and Liquids. Part I. Solids. *Journal of the American Chemical Society*., 38, 2221-2295. https://doi.org/ 10.1021/ja02268a002.

13. Itsuki T., Tomohito K., Shogo K., Yuko S., Yasuyuki N., Daiki K., Toshiaki Y., (2024). Synthesis of an Mg–Fe–Al layered double oxide with a high arsenic anion adsorption capacity and the establishment of an arsenic anion desorption process, *Journal of Physics and Chemistry of Solids,* 190, 112017, https://doi.org/10.1016/j.jpcs.2024.112017.

14. Dinesh M., Charles U., Pittman, (2007). Arsenic removal from water/wastewater using adsorbents—A critical review, *Journal of Hazardous Materials*, 142(1-2), 1-53,. https://doi.org/10.1016/j.jhazmat.2007.01.006.

15. FRSC, S. M. C. C. (2005). New development of inorganic ion exchanger: Synthesis and Ion Uptake Properties of Ternary Mixed Hydrous Oxides as Environmentally Harmonious Material. *Journal of Ion Exchange.*

16. Qureshi, M. (1991). Inorganic Ion Exchangers in Chemical Analysis (1st ed.). CRC Press. https://doi.org/10.1201/9780203750780.

17. V. Padmavathy (2008). Biosorption of nickel (II) ions by baker's yeast: Kinetic, thermodynamic and desorption studies, *Bioresource Technology*, 99(8), 3100-3109, https://doi.org/10.1016/j.biortech.2007.05.070.

18. Ming-Cheng Shih, (2005). An overview of arsenic removal by pressure-driven membrane process Desalination. Desalination, 172, 85–97. https://doi.org/10.1016/j.desal.2004.07.031.

Chapter 5: Granulation of SFM05905 and evaluation of arsenic adsorption capacity of granular SFM05905

5.1 Introduction:

This chapter focuses on the preparation, characterization, and evaluation of Si-Fe-Mg (SFM) granular mixed hydrous oxides, specifically SFM05905, as adsorbents for arsenic removal from aqueous solutions. The study highlights the synthesis of granular SFM05905 via the Iron Hydroxide Oxide on Polyacrylamide Cryogel technique, as reported by (Kurozumi et al., 2015 and Kurozumi et al., 2016), and investigates its potential for removing both arsenite (As(III)) and arsenate (As(V)) ions from water. The study also delves into the process conditions, material characterization, and performance of SFM05905 in a column adsorption system for various arsenic concentrations and mixed anion solutions. The goal of this chapter is to provide a comprehensive analysis of the methods used to prepare granular SFM05905, followed by its detailed application in a column adsorption setup for the removal of arsenic species. This chapter discusses the synthesis process, experimental conditions, and the adsorption performance of SFM05905 in terms of its efficiency in removing arsenic from contaminated water (Yao et al., 2020).

5.2 Experimental Methodology:

5.2.1 Preparation of granular SAM05905.

5.2.2 Materials and reagents:

For the column adsorption experiment, the reagents and materials used included monomeric acrylamide (AAm) and ammonium peroxydisulfate (APS) from Fujifilm Wako Pure Chemical Corp. (Osaka, Japan), N, N- methylene bis acrylamide (MBAAm) from Alfa Aesar Ward Hill, USA, and N, N, N; N- Tetramethyl ethylene diamine (TEMED) from Combi-Blocks, San Diego, USA. The polyacrylamide granular SFM05905 was prepared using SFM05905 powder and degassed water.

5.2.3 Preparation of granular SFM05905 by using polyacrylamide.

In the preparation of granular SFM05905, 200 mL of pre-degassed water was placed in a 500 mL beaker and cooled to 0°C using an ice bath. SFM05905 (20 g) was dispersed in the degassed water while stirring with a magnetic bar. AAm (8 g) and MBAAm (2 g) were then dissolved in this mixture with vigorous stirring for 1.5 hours, after which nitrogen gas (N_2) was passed through the solution for 3 minutes. Following this, a solution of ammonium persulfate (APS), consisting of 1.0 g of APS dissolved in 1.0 mL of degassed water, was added to the monomer solution and stirred for an additional 0.5 hours. TEMED (0.24 g) was added quickly, and approximately 10 mL of the mixture was poured into syringes. These syringes were sealed and placed in a program-controlled refrigerator, where the solution was frozen at -15°C for 24 hours.

After freezing, the syringes were thawed in a warm bath and washed with distilled water until the solution reached a neutral pH. The polyacrylamide (PAAm) containing SFM05905 was then cut into pieces smaller than 1.0 cm^3 (as shown in Figure 12) and dried using a freeze dryer (VD-800R, TAITEC, Koshigaya, Japan).

Lastly, the SFM05905 content in the granular form was determined using a heating and melting method. The sample was heated on a hot plate at 100-150°C. If decomposition was insufficient, a mixture of nitric acid and sulfuric acid was added. The mixture was then cooled, releasing white smoke, and boiled slowly to settle the insoluble matter. The resulting solution was filtered, and the iron (Fe) concentration in the filtrate was measured to calculate the content of powder SFM05905 in the granular form.

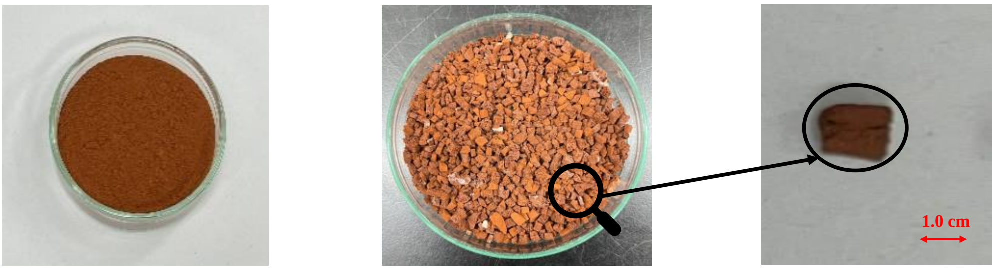

Powder SFM05905   Granular SFM05905   Particle size of the granular SFM05905

Figure 12. Photograph depicting powder SFM05905, granular SFM05905, and its expansion particles.

5.2.4 Measurement process for SFM05905 content in Cryogels.:

The continuous flow arsenic adsorption experiment was conducted using the adsorption column method, as depicted in Figure 13. The experimental conditions for column adsorption are detailed in Table 9. A polyethylene column, 20.0 cm in length and with an internal diameter of ø 1.6 cm, was employed. Dry granular SFM05905 was packed into the column, and water was used to remove air from the granular samples by applying negative pressure.

The experiment involved various adsorbate systems, including single-component [As(III)], [As(V)], and [PO4], binary mixtures [As(III) + PO4], [As(V) + PO4], and [As(III) + As(V)], and a ternary mixture [As(III) + As(V) + PO4]. The concentration of each anion in the aqueous solution was adjusted to 0.015 mmol L^{-1}. The solutions were passed through the column in an upward flow using a silicon tube connected to the column's base. Treated water was collected from the outlet at the top of the column at regular time intervals, and the residual arsenic concentrations and pH were measured. For this study, the space velocity (SV) was maintained at approximately 3.3 /h.

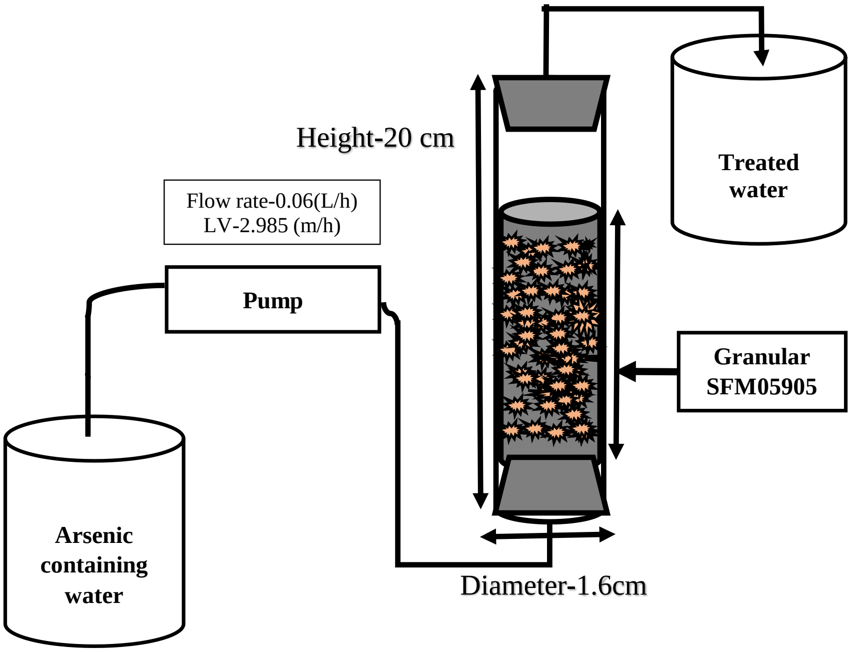

Figure 13: Column adsorption with granular SFM05905.

Table 9 Experimental condition for column test.

Sample in aqueous water (0.015mmol/L)	Space velocity (/h)	Packed granule SFM05905 (g)	Volume of packed granular SFM05905(cm^3)	Length of packed granular SFM05905 (cm)	
				Dry condition	**Wet condition**
As(V)	3.5	2.505	1.03	7.5	8.5
As (III)	3.2	2.516	1.04	8.2	9.4
PO_4	3.6	2.514	1.04	7.2	8.3
[As(V) +PO_4]	3.7	2.503	1.03	7.5	8
[As (III) +PO_4]	3.3	2.515	1.04	8.1	9
[As (III)+As(V)]	3.7	2.513	1.04	7.5	8
[As (III)+As(V)+PO_4]	3.7	2.504	1.03	7.5	8

5.3 SFM05905 in Cryogels Content measurement:

The content of SFM05905 in its granular form was determined using a heating and melting method involving nitric acid and sulfuric acid, as shown in Figure 14. After dissolution in the acids, the resulting gel was collected on quantitative filter paper (5B, Toyo Roshi Kaisha, LTD., Tokyo, Japan). The concentration of iron (Fe) in the filtrate was measured to calculate the SFM05905 powder content in the granular form. Additionally, the filtrate was analyzed using inductively coupled plasma mass spectrometry (ICP-MS) (Agilent 8800, Agilent Technologies, Inc., California, USA) to determine the concentrations of magnesium (Mg) and iron (Fe).

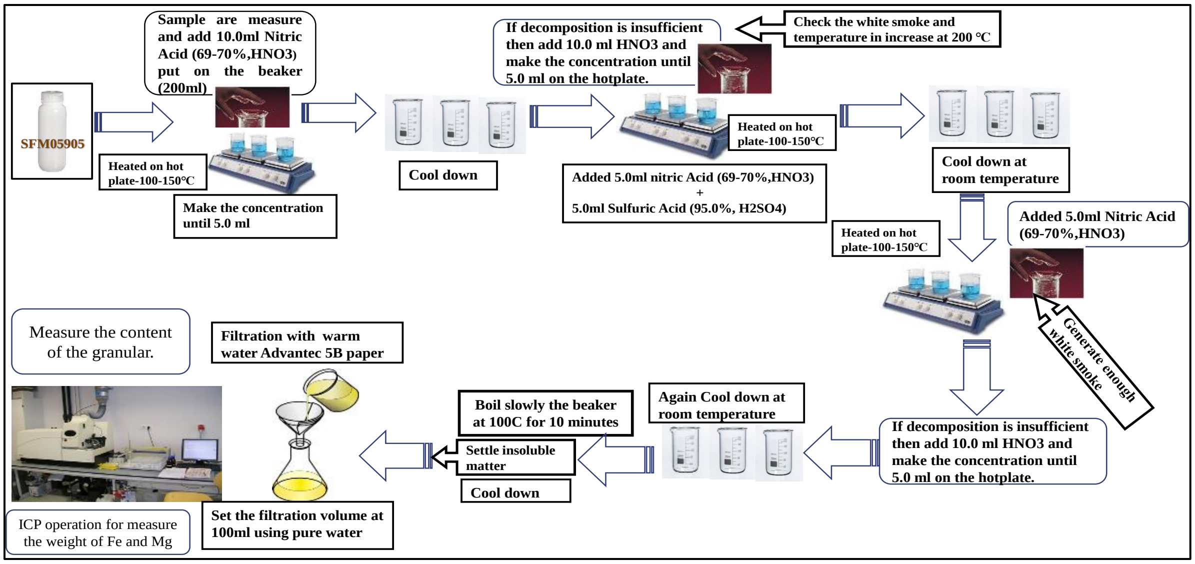

Figure 14: SFM05905 in Cryogels Content measurement procedure.

①. **Dissolution and Filtration**: The granular SFM05905 sample was dissolved in a mixture of nitric and sulfuric acid, and the solution was filtered to separate any insoluble matter. The filtrate was then analyzed for iron and magnesium content.

②. **ICP-MS Analysis**: The concentration of Fe and Mg was measured using ICP-MS, which provided precise quantification of the elements present in the SFM05905. This analysis was crucial for confirming the composition of the granular material and ensuring that it met the desired specifications for effective arsenic adsorption.

5.4 Result and discussion

This chapter presents the experimental results and a discussion of the findings regarding the fluoride adsorption capacity of the SFM05905 sample, along with the analysis of its metal composition and structural properties. The adsorption behavior under varying conditions such as equilibrium concentrations, temperatures, and competing anions is also discussed. The chapter integrates metal element composition analysis, X-ray diffraction (XRD), thermogravimetric-differential thermal analysis (TG-DTA), and adsorption isotherm models to explain the material's adsorption performance.

5.4.1 Metal elements composition ration XRD and TG-DTA analysis of SFM05905.

The analysis revealed a composition ratio of Si-Fe-Mg-mixed hydrous oxide as 0.048 Si:0.907 Fe:0.046 Mg, which aligns with the intended metal element ratio in the solution used for synthesizing SFM05905. Comparing the Fe content, the carrying ratio of SFM05905 in its granular form was found to be 56.0 wt.%. This result confirms that the SFM05905 powder effectively carried the metal oxide, as detailed in Table 10.

Table 10: Metal element composition ratio of SFM05905.

Contents		Si	Fe	Mg	Density (g/cm^3)	Carrying ratio of SFM05905 (%)	Particle size
Powder SFM05905	**Content (mmol/g)**	**0.53**	**10.51**	**0.53**	**3.81**	**-**	**＜250μm**
	Obtained composition ratio	**0.048**	**0.907**	**0.046**			
	(Target composition ratio	**0.05**	**0.9**	**0.05)**			
Granular SFM05905	**Content (mmol/g)**	**Not calculated**	**5.884**	**Not calculated**	**2.41**	**56.0**	**Less than <1 cm^3**

In the previous study, the correlation between the metal element composition ratio and the adsorption of various ions was investigated (Kuwabara et al., 2007). The results showed a positive correlation between the Mg and Fe ratios and the adsorption amount of arsenite ions. This suggests that the adsorption of arsenite ions is influenced by both Mg and Fe ratios. To further investigate the physicochemical properties of SFM05905, XRD analysis was performed and the results showed that the sample consisted mainly of amorphous Fe hydrous oxide. Additionally, TG-DTA measurements indicated that dehydration occurred at around 100°C and weight loss gradually decreased up to 400°C. This weight loss was attributed to the dehydration process and suggests that SFM05905 does not have a layered structure. These findings provide insight into the properties and behavior of SFM05905 in various applications.

5.5 Arsenic adsorption capacity of SFM05905 by the column adsorption method.

The experimental conditions for column adsorption were investigated in order to determine the arsenic adsorption capacity. The desorption efficiency of PO_4 uptake amount was observed to occur at the breakthrough point at 80 h of the tertiary mixing column. The adsorption amount was calculated using the breakthrough area at 80 h for all components shown in Figure 15. In the single adsorbate system of the column adsorption, the uptake amounts of As(III), As(V), and PO_4 were 0.032 mmol/g, 0.016 mmol/g, and 0.014 mmol/g, respectively.

In the binary adsorbate system, the adsorption uptake amounts [As(III)+PO_4] (0.032+0.017) mmol g^{-1} and [As(V)+PO_4] (0.023+0.015) mmol g^{-1} were observed. In the [As(III)+PO_4] system, PO_4 increased compared to the single adsorbate system, while in the [As(V)+PO_4] system, both As(V) and PO_4 increased compared to the single adsorbate system. [As(III) + As(V)] - (0.026+0.023) mmol g^{-1} showed that As(III) initially increased and then decreased, while As(V) initially decreased and then increased.

The tertiary [As(III) + As(V) + PO_4] - (0.026+0.016+0.010) mmol g^{-1} adsorbate system showed that the adsorption of As(III), As(V), and PO_4 was lower than in the single adsorbate system of the column adsorption in Table 11. PO_4 exhibited almost the same adsorption phenomenon as the single adsorbate system and gradually increased below 0.005 mmol L^{-1}. However, the PO_4 concentration gradually increased even after 80 h, which is the breakthrough point, indicating a shift from adsorption to desorption. The Kd value of the single component PO_4 was higher than As(V), but almost the same as As(III). In the tertiary condition, the Kd value indicated that PO_4 selectivity was lower than As(III) and As(V).

The distribution coefficient (Kd) value of granular SFM05905 is an important factor in actual groundwater or hot spa water, where many components or anions are included. However, the Kd value cannot be used to refer to the actual selectivity with the mixing condition, and it is useful to use in the column adsorption process. In conclusion, it was found that As(III) and PO_4 affected each other, while As(V) selectivity was higher than PO_4 in the Kd value and As(V) was not affected by PO_4 in the mixing condition.

Table 11: A summary of the adsorption amounts obtained from the column method experiments.

mmol g^{-1}	**SFM05905 column adsorption amount**						
	As (III)+PO_4	**As(V)+PO_4**	**AS(III)+ AS(V)**	**AS(III)**	**AS(V)**	**PO4**	**AS(III) + AS(V) +PO_4**
As(III)	**0.032**	**-**	**0.026**	**0.032**	**-**	**-**	**0.026**
As(V)	**-**	**0.023**	**0.023**	**-**	**0.016**	**-**	**0.016**
PO_4	**0.017**	**0.015**	**-**	**-**	**-**	**0.014**	**0.010**

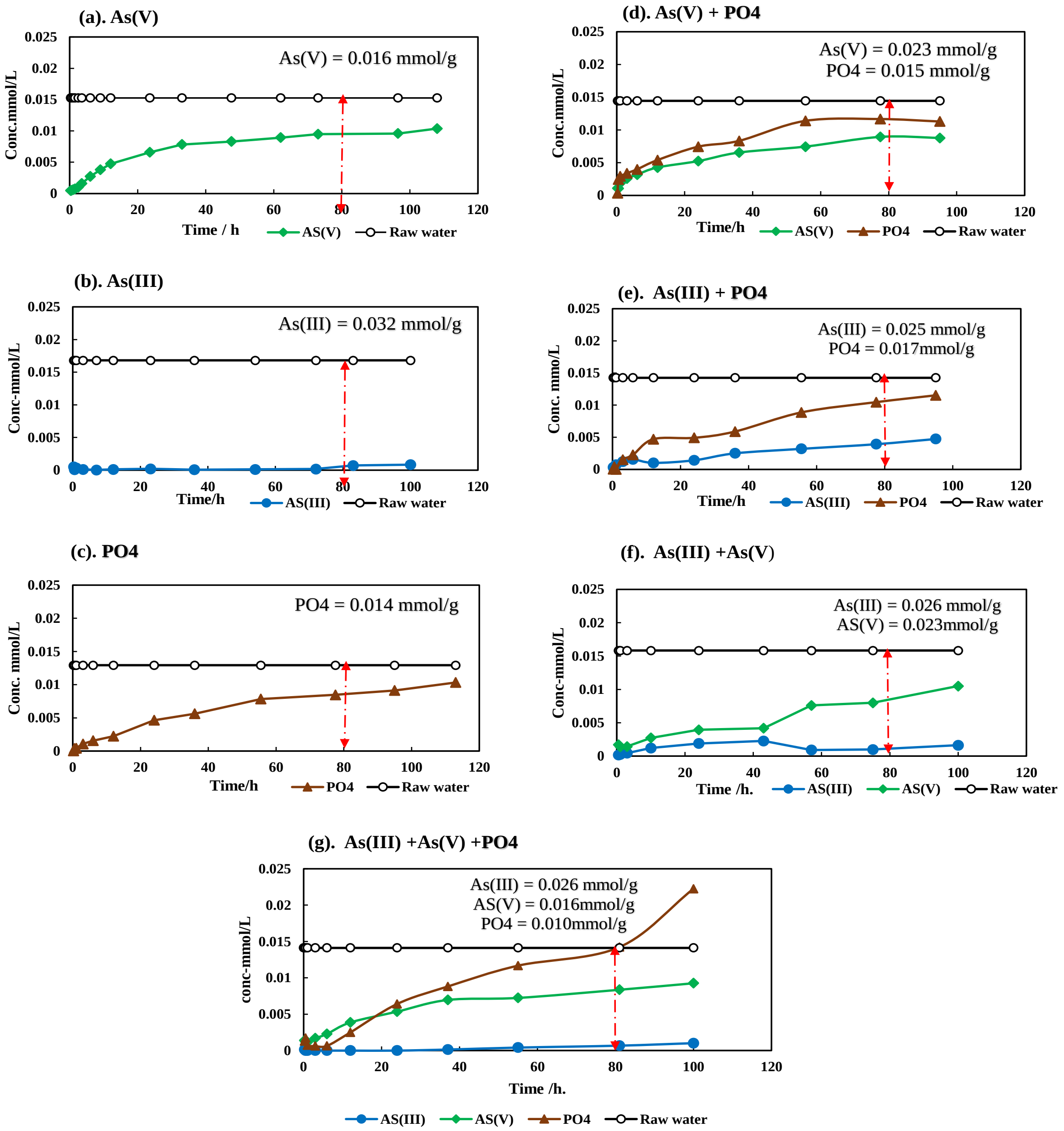

Figure 15: Schematic conditions for column test with granular SFM05905.

5.6 Adsorption Mechanism of SFM05905:

Granular SFM05905 is an amorphous Si-Fe-Mg mixed hydrous oxide that utilizes both chemical bonding and electrostatic interactions for adsorption. This material demonstrates strong selectivity for arsenic species (As (III) and As(V)) and moderate efficiency for phosphate in the adsorption process.

Chemical Reactions and Mechanism:

i) **Arsenic Adsorption via Chemical Bonding**:

The primary mechanism for arsenic adsorption is through chemical bonding between ferric hydroxide (Fe $(OH)_3$) and arsenic species. These reactions form strong surface complexes:

For arsenite (As (III)):

$$\mathbf{Fe\ (OH)_3 + H_3AsO_3 \rightarrow Fe{-}AsO_3 + 3H_2O}$$

For arsenate (As(V)):

$$\mathbf{Fe\ (OH)_3 + HAsO_4^{2-} \rightarrow Fe{-}AsO_4 + OH^-}$$

These reactions create stable chemical bonds, making the adsorbed arsenic difficult to desorb, which ensures efficient removal.

ii) **Electrostatic Interaction:**

Electrostatic interactions complement chemical bonding by attracting negatively charged arsenic species ($HAsO_4^{2-}$ or $H_2AsO_4^-$) to the positively charged surface sites on $Fe(OH)_3$. This enhances the adsorption process.

iii) **Competition with Phosphate:**

Although phosphate (PO_4^{3-}) shares structural similarities with arsenic species, SFM05905 demonstrates strong selectivity for arsenic due to the higher binding affinity of Fe $(OH)_3$ for arsenic. This minimizes interference from phosphate in the adsorption process.

The amorphous structure of SFM05905 provides a high surface area and abundant active sites, enhancing adsorption efficiency. Additionally, partial crystallization into ferric hydroxide (Fe $(OH)_3$) during synthesis increases stability and adsorption capacity.

In summary, the adsorption mechanism of SFM05905 combines chemical bonding, electrostatic interactions, and ion exchange. Its structural characteristics and selective affinity for arsenic make it an effective adsorbent for water treatment applications.

5.7 Conclusion

This study aimed to investigate the selective adsorption behavior of SFM05905, a promising adsorbent material, for arsenic removal from aqueous solutions. The focus was on understanding how SFM05905 interacts with arsenic species in both single ion systems and more complex mixed systems that include competing anions such as phosphate (PO_4). This work is pivotal in the context of addressing arsenic contamination in groundwater, a pressing global environmental challenge. The results presented herein offer critical insights into the effectiveness and selectivity of SFM05905 for arsenic removal, as well as its potential for use in real-world water treatment applications.

Summary of Key Findings

Throughout the study, a series of experiments were conducted to evaluate the adsorption capacity and selectivity of SFM05905 in various environments. Key findings from the study include:

1. **Arsenic Adsorption Behavior**: In both single and mixed anion systems, SFM05905 demonstrated a strong preference for arsenic (As) species. Specifically, As(III) showed the highest adsorption capacity, while As(V) exhibited a lower adsorption capacity but was still significant. The interaction between As(III) and As(V) was noted, and their combined presence influenced the overall adsorption efficiency.
2. **Impact of Competing Anions**: The study further examined the effect of competing anions like phosphate (PO_4) on arsenic adsorption. Interestingly, while PO_4 showed minimal adsorption itself, it did not significantly interfere with arsenic adsorption in the column tests. This suggests that SFM05905 is highly selective for arsenic even in the presence of other common anions.
3. **Minimal Interference from Other Anions**: The selectivity of SFM05905 was further explored in the presence of other ions such as sulfate (SO_4), fluoride (F), nitrate (NO_3), and carbonate (CO_3). The results revealed that these ions had a minimal impact on arsenic removal, making SFM05905 an ideal material for practical applications where diverse ions may be present in water sources.

4. **Distribution Coefficient (Kd) Analysis**: A crucial aspect of the study was the measurement of the distribution coefficient (Kd), which provides a quantitative measure of the material's selectivity. The distribution coefficient values for arsenic species in the presence of competing ions helped to better understand the adsorption dynamics and optimize the system for real-world conditions.

Implications and Applications

The findings of this study underscore the potential of SFM05905 as a highly effective and selective material for arsenic removal from groundwater. Given its ability to target arsenic in the presence of other anions and its minimal interference from competing ions, SFM05905 could offer a practical solution to arsenic contamination in drinking water, especially in regions where groundwater is the primary source of water.

1. **Water Treatment:** SFM05905 can be employed in both batch and column adsorption systems, making it versatile for large-scale water treatment. Its ability to operate effectively in the presence of other ions means it could be used in a variety of natural and industrial water sources without significant loss of efficiency.
2. **Environmental Remediation**: Beyond potable water treatment, the material could be useful for environmental remediation projects where arsenic contamination is a concern (Rae et al., 2020). Its high selectivity and efficiency could help mitigate the environmental impact of arsenic, particularly in areas with contaminated groundwater.
3. **Health and Safety**: Arsenic is a known carcinogen, and long-term exposure to even low levels of arsenic can have detrimental health effects. The successful application of SFM05905 in removing arsenic from contaminated water can directly contribute to public health and safety, improving access to clean and safe drinking water.

Challenges and Limitations

Despite the promising results, several challenges remain in the development and application of SFM05905 for arsenic removal. Some of the limitations identified during this study include:

1. **Saturation Capacity**: While SFM05905 showed high efficiency in removing arsenic, the saturation capacity of the material needs further optimization for long-term use. This is particularly critical for large-scale applications where continuous performance is required.
2. **Regeneration and Reusability**: The study did not extensively address the regeneration and reuse of SFM05905. For practical applications, it is important to investigate the regeneration potential of the material, as well as its ability to retain its adsorption capacity after multiple cycles of use.
3. **Cost and Scalability**: Although SFM05905 is effective, the cost of production and its scalability need to be evaluated for industrial use. Economical production methods and large-scale application strategies must be developed to make this technology viable in the field.

Future Work

Future research can build upon this study in several ways to further enhance the understanding and application of SFM05905 for arsenic removal:

1. **Optimization of Adsorption Parameters**: Future studies should focus on optimizing key adsorption parameters such as contact time, pH, and temperature to maximize the arsenic removal efficiency of SFM05905 in diverse conditions.
2. **Regeneration Studies**: The regeneration of SFM05905 after arsenic adsorption should be explored in detail to evaluate its longevity and cost-effectiveness for continuous use in water treatment systems.
3. **Field Testing:** It is crucial to perform field testing with actual contaminated water sources to assess the performance of SFM05905 under real-world conditions. This will help identify potential challenges that might arise when scaling up the process.
4. **Extended Applications**: Expanding the research to explore the removal of other heavy metals and contaminants using SFM05905 could broaden its potential applications in environmental remediation.
5. **Economic Feasibility**: Research into the economic feasibility of SFM05905 in large-scale water treatment operations will be necessary to determine its commercial viability and competitiveness with other materials currently in use for arsenic removal.

In conclusion, this study has successfully demonstrated the selective adsorption capacity of SFM05905 for arsenic removal from aqueous solutions. The material’s high selectivity for arsenic, minimal interference from other ions, and effective performance in both single and mixed ion systems highlight its potential as a versatile adsorbent for arsenic remediation. While there are challenges related to its long-term use, regeneration, and cost, the promising results provide a strong foundation for future research and the practical application of SFM05905 in water treatment systems.

5.8 References

1) Kuwabara, T., Kosuke, A., & Sato, T. (2007). Adsorption properties of synthetic Si-Fe-Mg Mixed Hydrous Oxides. *Journal of Japan Society on Water Environment*, 30(3), 133-138.

2) A. Halajnia, S. Oustan, N. Najafi, A.R. Khataee, A. Lakzian, (2012). The adsorption characteristics of nitrate on Mg–Fe and Mg–Al layered double hydroxides in a simulated soil solution, *Applied Clay Science*, 70, 28-36. https://doi.org/10.1016/j.clay.2012.09.007.

3) Kurozumi, M., Makino, Y., & Koshino, Y. (2016). Enhanced removal of fluoride using granular SFM05905 in batch adsorption experiments. *Environmental Science and Pollution Research*, 23(5), 4152-4160. https://doi.org/10.1007/s11356-015-5720-5.

4) Kurozumi, M., Yano, Y., Kiyoyama, S., Kumar, A., Shiomori, K., (2016). Preparation of iron oxide hydroxide microparticle-loaded polyacrylamide cryogel by particle addition method and its arsenic adsorption characteristics. *Science and Technology Research*, 5(1), 23-28. https://doi.org/10.11425/sst.5.23.

5) Kurozumi, M., Yano, Y., Kiyoyama, S., Kumar, A., & Shiomori, K. (2015). Adsorption Properties of Arsenic(V) by Polyacrylamide Cryogel Containing Iron Hydroxide Oxide Particles Prepared by in situ Method. *Resources Processing*., 62, 17-23. https://doi.org/10.4144/rpsj.62.17.

6) Kashif H., Saiqa M., Jochen B., Hassan J. Ch., (2017). Microbial biotechnology as an emerging industrial wastewater treatment process for arsenic mitigation: A critical review, *Journal of Cleaner Production,* 151, 427-438. https://doi.org/10.1016/j.jclepro.2017.03.084.

7) Kuwabara, Matsumura, Maeno and Sato. (2016). Adsorption property of Si-Fe-Mg Mixed Hydrous oxides with Different Composition of Metallic Elements for Arsenic in Ground

water. *Journal of the society of inorganic materials* 23 (380): 15-24. https://ir.lib.shimane-u.ac.jp/37010.

8) Yoshio O., Abhijit C., Leiying Y., Takeo E., Hitoshi M., Fujio M., (2005). Synthesis and Ion Uptake Properties of Ternary Mixed Hydrous Oxides as Environmentally Harmonious Material, *Journal of Ion Exchange*, 16(1),18-28, https://doi.org/10.5182.

9) Rae, Ian. (2020). Arsenic: its chemistry, its occurrence in the earth and its release into industry and the environment, ChemTexts. 6(4):25. http://doi.org/10.1007/s40828-020-00118-7.

10) Yao and Yang. (2020). An overview of As(V) removal from water by adsorption technology. *Arch Community Med Public Health,* 4(2): 15-020. http://doi.org/10.17352/amm.000022.

Chapter 6: Summary

Water contamination by toxic metal anions, particularly fluoride and arsenic, is a global environmental issue that poses significant risks to public health. High concentrations of these contaminants in drinking water can lead to severe health problems, including fluorosis, cancer, and other diseases. Effective water treatment technologies are needed to address these challenges and provide safe drinking water. This thesis investigates the development of novel adsorbent materials made from Si-Al-Mg mixed hydrous oxides, specifically SAM118 and SFM05905, to remove harmful anions, including fluoride (F^-) and arsenic (As), from aqueous solutions. The research aimed to enhance the adsorption capacities of these materials and explore their effectiveness in both aqueous and hot spring water sources.

The focus of this study was to develop a safe and efficient technology for the removal of fluoride and arsenic from water, improving existing water treatment methods, and to examine the adsorption behaviors of SAM118 and SFM05905 under different experimental conditions. This chapter presents a summary of the key findings, discusses their implications, and offers conclusions based on the research conducted.

Key Objectives of the Study

The main objectives of this study were:

1. **Development of Effective Adsorbents**: To develop novel adsorbents using mixed hydrous oxides (SAM118 and SFM05905) for the efficient removal of fluoride and arsenic from aqueous solutions.
2. **Evaluation of Adsorption Capacity**: To assess the adsorption capacities of these materials in both powdered and granular forms under various experimental conditions, including batch and column adsorption tests.
3. **Comparison of Performance**: To compare the performance of SAM118 and SFM05905 in removing fluoride and arsenic ions, respectively, and determine the factors that influence their adsorption effectiveness.

4. **Environmental and Health Impact**: To evaluate the environmental and health benefits of using these adsorbents for water purification, with a focus on their potential to reduce the harmful effects of fluoride and arsenic contamination.

Summary of Findings

1. **Fluoride Adsorption by SAM118**:
    - **Powder Form (Chapter 2)**: The study of SAM118 powder revealed its high efficiency in fluoride removal. It demonstrated a rapid adsorption rate and strong affinity for fluoride ions, making it a promising candidate for water treatment.
    - **Granular Form (Chapter 3)**: The granular form of SAM118 was also tested, and it was found that the polyacrylamide binder did not negatively affect the material's adsorption capacity. The granular form maintained a high performance even under different space velocity conditions, demonstrating its potential for practical applications in water treatment systems.
2. **Arsenic Adsorption by SFM05905**:
    - **Powder Form (Chapter 4)**: The powder form of SFM05905 showed exceptional selectivity for arsenic ions, particularly As (III), and exhibited a linear relationship between adsorption capacity and equilibrium concentration. This suggests that SFM05905 can efficiently remove arsenic from water, even in complex systems.
    - **Granular Form (Chapter 5)**: The granular form of SFM05905 demonstrated high arsenic adsorption capacity in both single and mixed anion systems. Notably, the presence of phosphate (PO_4) did not significantly interfere with the arsenic removal capacity in column tests, while the material showed a higher selectivity for As (III) in batch tests.

Discussion and Implications

The results of this study indicate that SAM118 and SFM05905 are highly effective adsorbents for removing fluoride and arsenic, respectively, from water. Both materials demonstrated significant adsorption capacities in both powdered and granular forms, making them versatile and suitable for different water treatment systems. SAM118’s high affinity for fluoride and SFM05905’s selectivity for arsenic makes these materials ideal candidates for addressing two of the most common and harmful contaminants in drinking water.

In addition to their high adsorption efficiencies, the study also highlighted the environmental and health benefits of using these adsorbents. Fluoride and arsenic contamination in groundwater and drinking water is a widespread issue, especially in developing regions where safe water treatment options are limited. The use of SAM118 and SFM05905 for removing these contaminants could have a substantial impact on public health, potentially reducing the prevalence of fluoride-induced diseases and arsenic-related cancers.

Moreover, the ability of these materials to function effectively in both batch and column adsorption tests provides flexibility for their application in different treatment setups, ranging from small-scale household filtration units to large-scale industrial water purification systems.

The research conducted in this thesis has demonstrated the promising potential of SAM118 and SFM05905 as effective and environmentally friendly adsorbents for fluoride and arsenic removal from water. These materials showed high adsorption capacities and selectivity for their respective target ions, with SAM118 being particularly efficient for fluoride and SFM05905 excelling at arsenic removal. Furthermore, the results revealed that the presence of other competing ions did not significantly hinder the performance of these adsorbents, indicating their robustness in complex water systems.

The key conclusions from this study are as follows:

1. **High Efficiency**: Both SAM118 and SFM05905 are highly efficient in removing fluoride and arsenic from aqueous solutions, making them suitable for practical water treatment applications.
2. **Minimal Interference**: The presence of competing ions like phosphate did not significantly affect the adsorption performance of these adsorbents, further demonstrating their suitability for real-world water sources.
3. **Environmental and Health Impact**: The development of these adsorbents could lead to significant improvements in water quality, particularly in areas affected by high levels of

fluoride and arsenic. This has major implications for public health, offering a feasible solution to reduce the harmful effects of these contaminants.

4. **Scalability and Application**: The granular forms of SAM118 and SFM05905 show promise for use in large-scale water treatment systems, while the powdered forms could be useful for smaller, more portable filtration units.

Future Directions

While the results of this study are promising, there are several areas for future research to optimize the performance and applicability of SAM118 and SFM05905 in water treatment:

1. **Regeneration and Reusability**: Further research is needed to investigate the regeneration and reuse potential of these adsorbents to ensure their sustainability and cost-effectiveness for long-term use.
2. **Field Trials**: Real-world testing in contaminated water sources is crucial to assess the performance of SAM118 and SFM05905 under actual environmental conditions and in the presence of a wider variety of contaminants.
3. **Economic Feasibility**: Economic studies should be conducted to evaluate the cost-effectiveness of using SAM118 and SFM05905 in large-scale water treatment applications, particularly in regions with limited access to affordable water purification technologies.
4. **Expansion to Other Contaminants**: The potential of SAM118 and SFM05905 to remove other heavy metals and toxic contaminants should be explored to further expand their applications in environmental remediation.

Final Remarks

In conclusion, this study provides a significant contribution to the field of water purification, offering novel materials with high efficiency and selectivity for removing fluoride and arsenic from water. SAM118 and SFM05905 represent a promising approach to addressing some of the most pressing environmental and health challenges related to water contamination. With further research and development, these materials have the potential to become vital components of water treatment systems worldwide, contributing to safer drinking water and improved public health.